1973

Linear stability of non-parallel flow in the entrance region of ducts

Francis Chung-ti Shen

Department: Mechanical and Aerospace Engineering

LINEAR STABILITY OF NON-PARALLEL FLOW IN THE ENTRANCE REGION OF DUCTS

By

FRANCIS CHUNG-TI SHEN, 1940-

A DISSERTATION

Presented to the Faculty of the Graduate School of the

UNIVERSITY OF MISSOURI-ROLLA

In Partial Fulfillment of the Requirements for the Degree

DOCTOR OF PHILOSOPHY

in

MECHANICAL ENGINEERING

1973

T. S. Chen
Advisor

J. R. Fawcett

Lyle G. Rhea

C. Y. Ho

A. J. Perrin

Ronald H. Howell

ABSTRACT

An investigation is made of the linear stability of the developing flow of an incompressible fluid in the entrance region of annular ducts, circular tubes, and parallel-plate channels. Small axisymmetric disturbances for annular duct and tube flows and small two-dimensional disturbances for channel flow are considered in the analysis. In formulating the stability problems, account is taken of the transverse velocity component of the mainflow. This results in the modified Orr-Sommerfeld equations, one for annular duct and tube flows and the other for channel flow. The mainflow velocity fields utilized in the stability analysis are those from the solutions of the linearized momentum equations.

The governing equation for the disturbances and the boundary conditions for each of the flow configurations constitute an eigenvalue problem. The eigenvalue problems for the annular duct and circular tube flows are solved by a fourth order Runge-Kutta integration scheme along with a differential correction iteration technique. An orthonormalization process is used to remove the "parasitic error" inherent in the numerical integration of the disturbance equations. For flow in the parallel-plate channels, the eigenvalue problem is solved by a finite difference method and the differential correction iteration scheme is employed to obtain the eigenvalues.

Neutral stability characteristics and critical Reynolds numbers at various axial locations are obtained for the developing flow in the annular ducts with radius ratios of 2.0 and 3.33, in the circular tubes, and in the parallel-plate channels, using the modified Orr-Sommerfeld equations. These stability results for the annular duct flow are also computed using the conventional Orr-Sommerfeld equation. Representative eigenfunctions are also presented for the annular duct flow. Comparisons of the results from the modified Orr-Sommerfeld equations are made with those from the conventional equations for all three flow configurations.

The main findings of the present study are: (1) laminar flow in the entrance region of annular ducts, circular tubes, and parallel-plate channels is unstable to small axisymmetric or two-dimensional disturbances; (2) the critical Reynolds number for the developing flow in the annular ducts and parallel-plate channels decreases monotonically as the axial distance increases; (3) the flow in the annular ducts becomes more stable as the ratio of the outer to inner radius increases; (4) the minimum critical Reynolds numbers for annular duct flow occur in the fully developed flow region and have the values of 9720 and 40530, respectively, for radius ratios of 2.0 and 3.33; (5) the minimum critical Reynolds number for tube flow is about 19780 and occurs in the entrance region; (6) the modified Orr-Sommerfeld

equation provides critical Reynolds numbers that differ somewhat from those obtained from the conventional equation; and (7) the effect of non-parallelism of the mainflow (that is, the effect of the mainflow transverse velocity) on the stability characteristics of the developing flow in ducts is of significance only in the range of small Reynolds numbers.

ACKNOWLEDGMENT

The author wishes to express his most sincere gratitude to his advisor, Professor T. S. Chen, for his assistance, advice, and encouragement in this work. Professor Chen suggested this thesis topic and has continually provided vital recommendations and criticisms throughout the entire course of the investigation and during the preparation of the manuscripts. Special thanks are also due to Professors Lyle G. Rhea, Anthony J. Penico, Thomas R. Faucett, Ronald H. Howell, and C. Y. Ho for their assistance.

The author is also indebted to his fellow graduate student Mr. Lung-mau Huang for many discussions concerning the computational aspects of the present investigation. The support of the computational expenses by the Mechanical Engineering Department and the Computer Center of the University of Missouri-Rolla is gratefully acknowledged.

The author expresses thanks to his wife, Linda Ling-te, for her sacrifice, patience, and encouragement throughout the course of the present investigation.

Finally, the author wishes to dedicate this dissertation to his parents, Mr. and Mrs. Wei-tung Shen, for their encouragement and support in every aspect throughout his entire graduate studies.

TABLE OF CONTENTS

TABLE OF CONTENTS (continued)

TABLE OF CONTENTS (continued)

LIST OF FIGURES

LIST OF TABLES

LIST OF TABLES (continued)

NOMENCLATURE

a_i	coefficients appearing in equation (3.31)
A	constant defined in equation (2.11); also matrix defined in equation (4.8a)
A_i	coefficients defined in equation (4.32)
B	matrix defined in equation (4.6)
B_i	coefficients defined in equation (4.35); also coefficients defined in equation (4.15)
B_J, B_Y	constants defined in equation (3.14)
c	dimensionless complex phase speed, $c=c_r+ic_i$
c*	dimensional complex phase speed, $c^*=c_r^*+ic_i^*$
C_j	series coefficients appearing in equation (2.10)
E, F_J, G_J, H_J	constants defined in equation (2.13)
E_j	functions defined in equation (4.4)
G_N	constant defined in equation (4.13)
F	function defined in equation (4.23)
g	variable defined in equation (4.39)
h	step size
J_n, Y_n	Bessel Functions of the first kind and the second kind of order n
K	radius ratio for annular duct, $K=r_2^*/r_1^*$
L	operator defined in equation (4.2)
L*	half-spacing of parallel-plate channels
L_c^*	characteristic length; $L_c^*=(K-1)r_2^*/2K$ for annular duct, $L_c^*=r_0^*$ for tube, $L_c^*=L^*$ for channel
M	radius ratio for annular duct, $M=r_1^*/r_2^*$

NOMENCLATURE (continued)

N	number of steps
O-S	Orr-Sommerfeld
$P^{(i)}$	upper triangular matrix defined in equation (4.18)
P_{ij}	elements of matrix $P^{(i)}$
r	dimensionless radial coordinate
r*	dimensional radial coordinate
$r^*_0; r^*_1, r^*_2$	dimensional radius for tube; inner radius and outer radius for annular duct
R	Reynolds number
t	dimensionless time
t*	dimensional time
$\hat{u}, \hat{v}, \hat{p}$	dimensional axial and radial velocity components and pressure
u^*, v^*, p^*	dimensional axial and radial velocity components and pressure for mainflow
u^+, v^+, p^+	time dependent dimensional disturbances for axial and radial velocity components and pressure
$\bar{u}^*, u^*_{max}$	dimensional average and maximum velocities of mainflow
u^*_c	characteristic velocity, $u^*_c = \bar{u}^*$
U,V	dimensionless mainflow velocity components in the axial and radial coordinates, $U = u^*/u^*_c$ $V = v^*/u^*_c$
U_{fd}	dimensionless fully developed axial velocity, $U_{fd} = u^*_{fd}/u^*_c$
U*	dimensionless axial difference velocity
x*	dimensional physical axial coordinate
X	dimensionless physical axial coordinate, $X = (x^*/L^*)/(u^*L^*/\nu)$

NOMENCLATURE (continued)

X^*	dimensionless stretched axial coordinate, $X^*=(\xi^*/L_c^*)/(u_c^*L_c^*/\nu)$
y	dimensionless transverse coordinate
y^*	dimensional transverse coordinate
$y_j^{(i)}$	elements of linearly independent matrix Y defined in equation (4.7)
Y	matrix defined in equation (4.7d)
Z_J, Z_Y	functions defined in equation (2.11)
α	dimensionless wave number, $\alpha=\alpha^*L_c^*$
α^*	dimensional wave number
α_j	eigenvalues of equations (2.12), (2.16), and (2.22)
β	matrix defined in equation (4.7)
β_j	elements of matrix β defined in equation (4.7)
δ	central difference operator
ε	weight function defined in equations (2.14), (2.18), and (2.24)
η	dimensionless radius defined in equation (2.8), $\eta=r^*/r_2^*$
θ	variable defined in equation (4.33)
Λ	function defined in equations (2.4) and (4.30)
μ	average operator
ν	kinematic viscosity
ξ^*	dimensional stretched coordinate
ρ	fluid density
ϕ	dimensionless amplitude of stream function defined in equation (3.11)

NOMENCLATURE (continued)

ϕ^+	dimensional amplitude of stream function defined in equation (3.10)
$\bar{\phi}_s^{(j)}$	function defined in equation (4.13)
$\tilde{\phi}$	function defined in equation (4.15)
χ	dimensionless physical axial coordinate defined in equation (2.8), $\chi=(x^*/r_2^*)/(\bar{u}^* r_2^*/\nu)$
χ^*	dimensionless stretched axial coordinate defined in equation (2.8), $\chi^*=(\xi^*/r_2^*)/(\bar{u}^* r_2^*/\nu)$
Ψ	function defined in equation (4.30)
Ψ^+	dimensional stream function of disturbance defined in equations (3.10) and (3.24)

Subscripts

c	critical condition
fd	fully developed condition
g	rapidly growing solution
gn	normalized rapidly growing solution
i	imaginary part
r	real part
s	slowly growing solution
sn	normalized slowly growing solution

Superscripts

$\bar{}$	average quantity
',","',""	derivatives with respect to r or y

I. INTRODUCTION

A. General Background

It is well known that there are two types of motions of a viscous fluid, namely, laminar and turbulent flow. In laminar flow, the fluid moves in parallel layers, one layer of fluid sliding over the other and each fluid particle following a smooth and continuous path. The fluid particles in each layer remain in an orderly sequence without passing one another. In turbulent flow, the path of any individual particle is zigzag and irregular, but on a statistical basis the over-all motion of the aggregate of fluid particles is regular and predictable. Turbulence can be generated by fluid flow past a solid surface or by the flow of layers of fluids at different velocities past or over one another.

For the problem of linear hydrodynamic stability, the question is whether the flow is stable or unstable to infinitesimally small disturbances. To achieve this goal, small disturbances are superimposed onto a given laminar flow. The undisturbed laminar flow is called the mainflow or primary flow. If the disturbances decay, the flow remains laminar and is said to be stable. If the disturbances grow, the flow is called unstable. If the disturbances neither grow nor decay, then the flow is said to be neutrally stable.

To analyze the behavior of disturbances, one can study

the timewise or spacewise stability of the mainflow. In formulating the stability problem for tube or annular duct flow with coordinates (x^*,r^*,ϕ^*), the general three-dimensional disturbance velocities are represented in the form of $u^+(x^*,r^*,\phi^*,t^*)=u(r^*)\exp[i(\alpha^*x^*+n\phi^*-\alpha^*c^*t^*)]$ where α^* is an axial wave number, c^* is phase speed and n is an azimuthal wave number (the case of axisymmetric disturbances corresponds to n=0). In general, α^* and c^* are complex numbers. If α^* is taken to be real and c^* to be complex, then the stability is solved in the timewise sense or as a temporal stability problem. If c^* is taken to be real and α^* to be complex, then a spacewise (spatial) stability problem results. The latter problem is more closely related to experimental work. The majority of the analytical work appearing in the literature deals with timewise stability problems. Gill (1965) concluded that there is no spatial growth of rotationally symmetric disturbances in a circular tube.

There are no exact solutions known to exist in the study of hydrodynamic stability problems. The solutions are, therefore, obtained by approximate methods. Of the approximate methods of solutions, there are two basic types, the asymptotic and the numerical methods. The asymptotic method is based on the condition that the parameter α^*R (where R is the Reynolds number) is large. In the past, the asymptotic method developed by Heisenberg (1924), Tollmien

(1929,1947) and Lin (1945,1967) were applied to boundary layer flow, pipe flow, and plane Poiseuille flow. In these problems, one needs to consider only one critical layer (where the phase velocity equals the mainflow velocity) in the analysis. This is due to the symmetric nature of the mainflow velocity profiles in these flows. For an annular duct, due to the lack of the symmetry of the main velocity profiles, there are two critical layers. With some minor modifications, Mott (1966) extended the asymptotic method of Lin to cover two critical layers and studied the stability characteristics of the fully developed annular duct flow.

In the numerical methods of solution, there are several different techniques which have been employed. They include the finite difference method by Thomas (1953), the method of weighted residuals by Finlyson (1966), the method of matched initial value problems by Nachtsheim (1964), the filter integration method by Kaplan (1964), and the orthonormalization method by Wazzan, Okamura, and Smith (1967,1968). A very complete review and comparison of all these methods is given by Gersting (1970).

B. A Brief Review of the Previous Work

Many investigations on the linear stability of duct flows have appeared in the literature. The fact that fully developed flow in a parallel-plate channel (i.e. the plane Poiseuille flow) is unstable for large Reynolds numbers is

well established. The fully developed flow in an annular duct has been shown to be unstable for large Reynolds numbers when subjected to small axisymmetric disturbances (Mott 1966). For flow in a circular tube, it has been found that the fully developed Hagen-Poiseuille flow is stable when subjected to either small axisymmetric disturbances (Leite 1959, Schensted 1960, Gill 1965, Corcos and Sellars 1959, Davey and Drazin 1969) or small non-axisymmetric disturbances (Lessen, Sadler and Liu 1968, Burridge 1970, Salwen and Grosch 1972, Gary and Rouleau 1972).

The stability characteristic of hydrodynamically developing flow in the entrance region of a parallel-plate channel was investigated by Chen and Sparrow (1967). They found that the developing flow is unstable at large Reynolds numbers. For the developing flow in a pipe, Huang (1973) has shown that the flow is unstable to either small axisymmetric disturbances or small non-axisymmetric disturbances at large Reynolds numbers. The instability of the developing tube flow subject to axisymmetric disturbances was also verified by Tatsumi (1952).

The stability analysis for the developing flow in ducts discussed above are based on the assumption that the main flow can be regarded locally as a parallel flow consisting only of the streamwise velocity component, with the transverse velocity component being zero. Such a model is exact for fully developed duct flows, whereas for the entrance

region flow it is an approximation. Presently, there are only a few studies on linear stability available in the literature which account for the transverse velocity component in the mainflow. These include the work of Chen, Sparrow, and Tsou (1971), Chen and Huang (1972), Barry and Ross (1970), Haaland (1972), and Ling and Reynolds (1971). However, these investigators concerned themselves with the boundary layer flows. To the best knowledge of the present author, no work has been done on the stability of the developing duct flows in which the mainflow transverse velocity is included in the analysis.

C. The Present Investigation

In the present investigation, the stability characteristics of several duct flows in which the velocity profile is developing, is investigated by the linearized method. The purpose is to determine whether small disturbances superimposed on the developing laminar flow would grow or decay with time. The fluid is assumed to be Newtonian and incompressible.

The governing equations for the disturbed flow include the continuity equation and the Navier-Stokes equations, which are non-linear, coupled partial differential equations. Thus, the stability problem is a non-linear problem. However, for small disturbances, we assume that the equations may be linearized; that is, terms that are quadratic or

higher in the disturbances and their derivatives can be neglected. In the present investigation, a modified version of the Orr-Sommerfeld equation for circular tube and annular duct flows is derived in which account is taken of the transverse velocity component in the mainflow. The corresponding equation for plane flow has been given elsewhere (see, for example, Chen, Sparrow, and Tsou, 1971).

The problems covered in this dissertation are:

(1) The stability of the developing laminar flow in the entrance region of annular ducts, subjected to axisymmetric small disturbances using both the conventional and the modified Orr-Sommerfeld equations.

(2) The stability of the developing laminar flow in the entrance region of a circular tube, subjected to axisymmetric small disturbances using the modified Orr-Sommerfeld equation.

(3) The stability of the developing laminar flow in the entrance region of a parallel-plate channel, subjected to two-dimensional small disturbances using the modified Orr-Sommerfeld equation.

The reasons that axisymmetric or two-dimensional disturbances are considered in these problems are as follows.

For problem (1), Gersting (1970) has shown that for the fully developed annular duct flow, it is sufficient to consider only axially symmetric disturbances rather than axially non-symmetric disturbances. He proved that the

"ϕ-component" of the disturbances will decay. Since in the hydrodynamic development region, the duct flow is basically a boundary layer flow, it can be expected from Squire's theorem (1933) that the axisymmetric disturbances will be more unstable than the non-axisymmetric disturbances for the developing flow.

For problem (2), Huang (1973) has shown that axisymmetric disturbances are more unstable than non-axisymmetric disturbances for the developing flow in the immediate neighborhood of the inlet of a circular tube.

For channel flow in problem (3), it has been shown as a direct result of Squire's theorem that two-dimensional disturbances are more unstable than three-dimensional disturbances.

To the best knowledge of the author, the first problem has never been investigated. This problem constitutes the main bulk of the present dissertation. In all three configurations, the timewise stability characteristics are studied using numerical methods of solution. The numerical methods used are the integration method for problem (1) and (2) and the finite difference method for problem (3). To remove the "parasitic error" inherent in the numerical integration of the disturbance equation, an orthonormalization process (Dettman 1962) was employed.

Neutral stability curves at different axial locations in the entrance region of annular ducts and circular tubes

are generated. The critical Reynolds numbers at various locations are obtained and presented for all three flow configurations. Representative results of eigenfunctions for the annular duct flow are also presented. Finally, the stability results from the non-parallel flow model are compared with those obtained from the parallel flow model for all the problems investigated.

II. THE MAINFLOW

For a fully developed flow in a duct, the velocity solution can be expressed in an exact form. However, for the developing flow in the entrance region, the velocity field, even for laminar flow, does not yield an exact solution. This is due to the nonlinearity of the inertia terms which appear in the equations of motion. Various approximate methods have been developed by different investigators to obtain the velocity solutions in the entrance region of ducts. Among them are the Karman-Pohlhausen integral method (Siegel 1953, Campbell and Slattery 1963), the method of patching of the upstream and downstream solutions at some intermediate location (Goldstein 1938, Roidt and Cess 1962, Collins and Schowalter 1962), and the linearization method by Sparrow and Lin (1964). Of these methods, the linearization method appears to be the most useful in the stability analysis, because in this method the velocity solutions can be represented in closed form.

In the linearization method of solution, the non-linear inertia terms in the axial momentum equation are linearized by introducing a stretched axial coordinate and a function which includes the pressure gradient and the residual of the inertia terms. With application of the principle of conservation of mass, this function may be eliminated from the axial momentum equation. The velocity solution then can be

written as the sum of the fully developed velocity and a difference velocity which approaches zero at large downstream distances.

To investigate the stability of the flow in the entrance region of an annular duct, a circular tube, and a parallel-plate channel, it is necessary to obtain the mainflow expression for each flow configuration. The mainflows for these three configurations will be considered separately in the following sections. The mainflows are assumed to be steady, laminar, Newtonian, and incompressible.

A. Annular Ducts

For the conditions of incompressible flow and axial symmetry, the continuity and x*-momentum equations are

$$\frac{\partial (r^*u^*)}{\partial x^*} + \frac{\partial (r^*v^*)}{\partial r^*} = 0 \tag{2.1}$$

$$u^*\frac{\partial u^*}{\partial x^*} + v^*\frac{\partial u^*}{\partial r^*} = -\frac{1}{\rho}\frac{dp^*}{dx^*} + \frac{\nu}{r^*}\frac{\partial}{\partial r^*}\left(r^*\frac{\partial u^*}{\partial r^*}\right) \tag{2.2}$$

where x* is the axial coordinate, r* is the radial coordinate, u* and v* are the velocity components in the x* and r* directions, ρ is the density and ν is the kinematic viscosity. In writing (2.2), use is made of the boundary layer assumptions $p^*=p^*(x^*)$ and $\partial^2 u^*/\partial x^{*2} << \partial/\partial r^*(r^*\partial u^*/\partial r^*)$. Equations (2.1) and (2.2) are to be solved subject to the no-slip condition and the inlet condition.

$$u^*=v^*=0 \quad \text{at} \quad r^*=r^*_1 \quad \text{and} \quad r^*=r^*_2$$
$$u^*=u^*_0 \quad \text{at} \quad x^*=0 \tag{2.3}$$

where r^*_1 and r^*_2 are, respectively, the inner radius and outer radius of the duct. In addition, u^*_0 is assumed to be uniform (i.e., $u^*_0=\bar{u}^*$) across the entrance section at $x^*=0$.

Due to the nonlinearity of the inertia terms there exists a difficulty in solving for flow development from equations (2.1) and (2.2). Sparrow and Lin (1964) introduced the following linearized form for (2.2)

$$\varepsilon(x^*)\bar{u}^* \frac{\partial u^*}{\partial x^*} = \Lambda(x^*) + \frac{\nu}{r^*}\frac{\partial}{\partial r^*}\left(r^*\frac{\partial u^*}{\partial r^*}\right) \tag{2.4}$$

in which $\varepsilon(x^*)$ is a yet undetermined function of x^* which weights the average velocity $\bar{u}^*$, while $\Lambda(x^*)$ is a second undetermined function which includes the pressure gradient dp^*/dx^* and the residual of the inertia terms. The function $\Lambda(x^*)$ may be eliminated from (2.4) by integrating it over the cross-section

$$\int_{r^*_1}^{r^*_2} \varepsilon(x^*)\bar{u}^* \frac{\partial u^*}{\partial x^*} r^* dr^* = \int_{r^*_1}^{r^*_2} \Lambda(x^*) r^* dr^* + \int_{r^*_1}^{r^*_2} \nu \frac{\partial}{\partial r^*}\left(r^*\frac{\partial u^*}{\partial r^*}\right) dr^* \tag{2.5}$$

Using the law of mass conservation

$$\frac{\partial}{\partial x^*}\left[\int_{r^*_1}^{r^*_2} 2\pi r^* u^* dr^*\right] = 0 \tag{2.6}$$

the left-hand side of (2.5) is identically equal to zero. This results in

$$\Lambda(x^*) = - \frac{\nu}{(r_2^{*2}-r_1^{*2})/2} \left[r_2^* \left(\frac{\partial u^*}{\partial r^*}\right)\Big|_{r_2^*} - r_1^* \left(\frac{\partial u^*}{\partial r^*}\right)\Big|_{r_1^*} \right] . \quad (2.7)$$

It is also convenient at this point to introduce the dimensionless variables

$$\chi=(x^*/r_2^*)/(\bar{u}^* r_2^*/\nu), \quad U=u^*/\bar{u}^*, \quad \eta=r^*/r_2^*, \quad M=1/K=r_1^*/r_2^* \quad (2.8a)$$

and also a stretched axial coordinate ξ^* defined as

$$dx^*=\varepsilon d\xi^*, \quad \chi^*=(\xi^*/r_2^*)/(\bar{u}^* r_2^*/\nu) \quad (2.8b)$$

With these dimensionless variables and the use of (2.7), equation (2.4) becomes

$$\eta \frac{\partial U}{\partial \chi^*} = -\frac{2\eta}{1-M^2}\left[\left(\frac{\partial U}{\partial \eta}\right)\Big|_1 - M\left(\frac{\partial U}{\partial \eta}\right)\Big|_M \right] + \frac{\partial}{\partial \eta}\left(\eta \frac{\partial U}{\partial \eta}\right) \quad (2.9)$$

The introduction of the stretched axial coordinate ξ^* temporarily puts aside the need to determine the weight function ε. The flow development may now be solved from (2.9) as a function of χ^* and η. To complete the solution, it is necessary to relate ξ^* to the physical coordinate x^*; this will be carried out later.

Let the velocity solution $U(\chi^*,\eta)$ be the sum of the fully developed velocity $U_{fd}(\eta)$ and a difference velocity $U^*(\chi^*,\eta)$ which approaches zero for large values of χ^*.

$$U(\chi^*,\eta) = U_{fd}(\eta) + U^*(\chi^*,\eta) \tag{2.10a}$$

The solution as obtained by Sparrow and Lin (1964) is

$$U = \frac{2[1-\eta^2+2A\ \ell n(\eta)]}{1+M^2-2A} + \sum_{j=1}^{\infty} C_j[-\frac{Z_Y(1)}{Z_J(1)} Z_J(\eta) + Z_Y(\eta)]\exp(-\alpha_j^2\chi^*) \tag{2.10b}$$

where

$$A = \frac{M^2-1}{2\ \ell n(M)} \tag{2.11a}$$

$$Z_J(\eta) = J_0(\alpha_j\eta) + \frac{2[MJ_1(\alpha_jM)-J_1(\alpha_j)]}{\alpha_j(1-M^2)} \tag{2.11b}$$

$$Z_Y(\eta) = Y_0(\alpha_j\eta) + \frac{2[MY_1(\alpha_jM)-Y_1(\alpha_j)]}{\alpha_j(1-M^2)} \tag{2.11c}$$

The J and Y functions are Bessel Functions of the first kind and second kind. The eigenvalues α_j are the roots of

$$Z_J(M)Z_Y(1)-Z_J(1)Z_Y(M) = 0 \tag{2.12}$$

The first 30 eigenvalues α_j along with $\alpha_j(1-M)$ for the parametric values M=1/2 and 1/3.33 are listed in Table 1. The expression for the series coefficients C_j is derived as (see Appendix A)

$$C_j = \frac{2(F_1-2AF_2)}{(1+M^2-2A)[F_3(1)-F_3(M)]} \tag{2.13a}$$

where

$$F_1 = -[Z_Y(1)/Z_J(1)]G_J + G_Y + 0.25(1-M^4)E \qquad (2.13b)$$

$$F_2 = -[Z_Y(1)/Z_J(1)]H_J + H_Y + 0.25[M^2-2M^2\ell n(M)-1]E \qquad (2.13c)$$

$$F_3(\eta) = 0.5[Z_Y(1)/Z_J(1)]^2\eta^2[J_0^2(\alpha_j\eta)+J_1^2(\alpha_j\eta)] + 0.5\eta^2[Y_0^2(\alpha_j\eta) + Y_1^2(\alpha_j\eta)] + 0.5\eta^2E^2 -[Z_Y(1)/Z_J(1)]\eta^2[J_0(\alpha_j\eta)Y_0(\alpha_j\eta) + J_1(\alpha_j\eta)Y_1(\alpha_j\eta)] + (2E/\alpha_j)\{\eta^2Y_1(\alpha_j\eta) - [Z_Y(1)/Z_J(1)]\eta J_1(\alpha_j\eta)\} \qquad (2.13d)$$

$$\alpha_j^3G_J = (\alpha_j^2-4)J_1(\alpha_j) - (\alpha_j^2M^2-4)MJ_1(M\alpha_j) + 2\alpha_jJ_0(\alpha_j) - 2\alpha_jM^2J_0(M\alpha_j) \qquad (2.13e)$$

$$\alpha^2H_J = -\alpha_jMJ_1(M\alpha_j)\ \ell n(M) + J_0(\alpha_j) - J_0(M\alpha_j) \qquad (2.13f)$$

$$\alpha_j(1-M^2)E = 2\{-[Z_Y(1)/Z_J(1)][MJ_1(M\alpha_j)-J_1(\alpha_j)] + MY_1(M\alpha_j) - Y_1(\alpha_j)\} \qquad (2.13g)$$

The terms G_Y and H_Y are obtained from G_J and H_J by replacing J by Y. In the velocity solution (2.10b), the first term corresponds to the fully developed velocity U_{fd}, while the series corresponds to the difference velocity U*. The flow

is essentially fully developed at $\chi^*/[1-(r_1^*/r_2^*)]^2=0.10$. The stretched axial coordinate ξ^* (or χ^*) is related to the physical axial coordinate x^* (or χ) by the relation

$$\chi = \int_0^{\chi^*} \varepsilon(\chi^*)d\chi^* \text{ or } x^* = \int_0^{\xi^*} \varepsilon(\xi^*)d\xi^* \tag{2.14a}$$

where the weight function ε is given by

$$\varepsilon(\chi^*) = \frac{\int_M^1 \eta(2U-1.5U^2)(\partial U^*/\partial\chi^*)d\eta}{(\partial U/\partial\eta)_1 - M(\partial U/\partial\eta)_M + \int_M^1 \eta(\partial U/\partial\eta)^2 d\eta} \tag{2.14b}$$

The numerical results for χ^*, ε and χ are given in Table B-1, Appendix B.

Equations (2.10b), (2.14a), and (2.14b) fully specify the velocity development expressed as $U=u^*/\bar{u}^*$ as a function of χ and η. As χ^* or χ approaches infinity, (2.10b) reduces to the velocity solution for the fully developed flow.

B. Circular Tubes

The mainflow velocity solution for the developing flow in a circular tube can also be obtained by the linearization method. For uniform inlet velocity, it is given by Sparrow, Lin, and Lundgren (1964) as

$$U = u^*/\bar{u}^* = 2(1-\eta^2) + \sum_{j=1}^{\infty}\{4[J_0(\alpha_j\eta)/J_0(\alpha_j)-1]/\alpha_j^2\}\exp(-\alpha_j^2 X^*) \tag{2.15}$$

in which the eigenvalues α_j are the roots of

$$J_1(\alpha_j) = 0.5\alpha_j J_0(\alpha_j) \tag{2.16}$$

where J_0 and J_1 are Bessel Functions of the first kind.

In (2.15), the dimensionless variables are

$$\eta = r^*/r_0^* \ , \quad X = (x^*/r_0^*)/(\bar{u}^* r_0^*/\nu) \ , \quad X^* = (\xi^*/r_0^*)/(\bar{u}^* r_0^*/\nu)$$

$$U = u^*/\bar{u}^* \tag{2.17}$$

in which r^* is the radial coordinate, r_0^* is the tube radius, and $\bar{u}^*$ is the average velocity.

The first 30 eigenvalues α_j are listed in Table 2. In the velocity solution (2.15), the first term corresponds to the fully developed velocity U_{fd}, while the series term corresponds to the difference velocity U^*. The flow is essentially fully developed at $X^*=0.20$. The stretched axial coordinate ξ^* (or X^*) is related to the physical axial coordinate x^* (or X) by the relation

$$X = \int_0^{X^*} \varepsilon(X^*)dX^* \quad \text{or} \quad x^* = \int_0^{\xi^*} \varepsilon(\xi^*)d\xi^* \tag{2.18a}$$

where the weight function ε is given by

$$\varepsilon(X^*) = \frac{\int_0^1 (2U-1.5U^2)(\partial U/\partial X^*)\eta d\eta}{(\partial U/\partial \eta)_1 + \int_0^1 (\partial U/\partial \eta)^2 \eta d\eta} \tag{2.18b}$$

The numerical results of X^*, ε and X are given in Table B-2, Appendix B.

Equations (2.15), (2.18a), and (2.18b) give a complete velocity solution U as a function of X and η.

Table 1

Eigenvalues for Annular Duct Flow

j	$M=r_1^*/r_2^*=1/2.0$ α_j	$\alpha_j(1-M)$	$M=r_1^*/r_2^*=1/3.33$ α_j	$\alpha_j(1-M)$
1	12.51052	6.25526	8.86562	6.20327
2	17.98511	8.99256	12.86147	8.99918
3	25.10464	12.55233	17.90129	12.52553
4	30.90770	15.45385	22.09186	15.45767
5	37.68036	18.84018	26.90041	18.82221
6	43.62122	21.81061	31.17526	21.81332
7	50.25142	25.12571	35.88995	25.11218
8	56.26845	28.13423	40.21199	28.13632
9	62.82059	31.41030	44.87565	31.39948
10	68.88603	34.44302	49.22788	34.44473
11	75.38881	37.69441	53.85938	37.68539
12	81.48778	40.74389	58.23260	40.74533
13	87.95653	43.97827	62.84200	43.97053
14	94.07997	47.03999	67.23063	47.04125
15	100.52393	50.26197	71.82394	50.25519
16	106.66603	53.33302	76.22444	53.33419
17	113.09108	56.54504	80.80538	56.53950
18	119.24809	59.62405	85.21520	59.62505
19	125.65810	62.82905	89.78652	62.82360
20	131.82712	65.91356	94.20391	65.91445
21	138.22491	69.11247	98.76744	69.10755
22	144.40390	72.20196	103.19108	72.20277
23	150.79160	75.39580	107.74817	75.39136
24	156.97900	78.48950	112.17704	78.49024
25	163.35844	81.67922	116.72875	81.67507
26	169.55282	84.77641	121.16214	84.77711
27	175.92518	87.96259	125.70920	87.95869
28	182.12568	91.06284	130.14652	91.06348
29	188.49178	94.24589	134.68958	94.24226
30	194.69757	97.34879	139.13029	97.34942

Table 2

Eigenvalues for Parallel-Plate Channel and Circular Tube Flows

	Parallel-Plate Channel	Circular Tube
j	α_j	α_j
1	4.49341	5.13562
2	7.72525	8.41724
3	10.90412	11.61984
4	14.06619	14.79595
5	17.22075	17.95982
6	20.37129	21.11700
7	23.51944	24.27011
8	26.66605	27.42057
9	29.81160	30.56920
10	32.95638	33.71652
11	36.10062	36.86286
12	39.24443	40.00845
13	42.38791	43.15345
14	45.53113	46.29800
15	48.67413	49.44216
16	51.81697	52.58602
17	54.95967	55.72963
18	58.10225	58.87302
19	61.24472	62.01622
20	64.38712	65.15927
21	67.52943	68.30219
22	70.67168	71.44499
23	73.81387	74.58769
24	76.95602	77.73030
25	80.09813	80.87283
26	83.24019	84.01529
27	86.38222	87.15768
28	89.52422	90.30003
29	92.66618	93.44232
30	95.80814	96.58456

C. Parallel-Plate Channels

The mainflow velocity solution for the developing flow in a parallel-plate channel with uniform inlet velocity can also be obtained from the boundary layer equations

$$\frac{\partial u^*}{\partial x^*} + \frac{\partial v^*}{\partial y^*} = 0 \tag{2.19}$$

$$u^*\frac{\partial u^*}{\partial x^*} + v^*\frac{\partial u^*}{\partial y^*} = -\frac{1}{\rho}\frac{dp^*}{dx^*} + \nu\frac{\partial^2 u^*}{\partial y^{*2}} \tag{2.20}$$

by the linearization method. Equations (2.19) and (2.20) are the continuity and x*-momentum equations, respectively. The solution is given by Sparrow, Lin, and Lundgren (1964) as

$$U = u^*/\bar{u}^* = 1.5(1-y^2) + \sum_{j=1}^{\infty} (2/\alpha_j^2)\{[\cos(\alpha_j y)/\cos(\alpha_j)]-1\}\exp(-\alpha_j^2 X^*) \tag{2.21}$$

in which the eigenvalues α_j are the roots of

$$\tan(\alpha_j) = \alpha_j \tag{2.22}$$

In (2.21) the dimensionless variables are defined as

$$y = y^*/L^* \ , \quad X = (x^*/L^*)/(\bar{u}^*L^*/\nu) \ , \quad X^* = (\xi^*/L^*)/(\bar{u}^*L^*/\nu) \ ,$$

$$U = u^*/\bar{u}^* \tag{2.23}$$

in which L* is the half-spacing between the plates, y* is the transverse coordinate as measured from the centerline of the channel, x* is the axial coordinate as measured from the

entrance, and $\bar{u}^*$ is the average velocity.

The first 30 eigenvalues α_j are listed in Table 2. In the velocity solution (2.21), the first term corresponds to the fully developed velocity U_{fd}, while the series corresponds to the difference velocity U*. Obviously, U* will be of significance only in the entrance region and will approach zero at large downstream distances. At X*=0.20, the flow is essentially fully developed. The stretched axial coordinate ξ^* (or X*) is related to the physical axial coordinate x* (or X) by the relation

$$X = \int_0^{X^*} \varepsilon(X^*)\,dX^* \quad \text{or} \quad x^* = \int_0^{\xi^*} \varepsilon(\xi^*)\,d\xi^* \tag{2.24a}$$

where the weight function ε is given by

$$\varepsilon(X^*) = \frac{\int_0^1 (2U-1.5U^2)(\partial U/\partial X^*)\,dy}{(\partial U/\partial y)_1 + \int_0^1 (\partial U/\partial y)^2\,dy} \tag{2.24b}$$

The numerical results of X*, ε, and X are given in Table B-3, Appendix B.

Equations (2.21) and (2.24) together constitute a complete velocity solution U as a function of X and y.

III. FORMULATION OF THE STABILITY PROBLEM

A. The Modified Orr-Sommerfeld Equations

The linear stability equations in terms of the amplitude function ϕ, in which the mainflow transverse velocity component is included, are derived in this section. They are referred to as the modified Orr-Sommerfeld equations.

1. Annular Ducts

The modified Orr-Sommerfeld equation for the annular duct flow is derived in this section. The continuity equation and the Navier-Stokes equations for axisymmetric flow are

$$\frac{\partial \hat{u}}{\partial x^*} + \frac{\partial \hat{v}}{\partial r^*} + \frac{\hat{v}}{r^*} = 0 \tag{3.1}$$

$$\frac{\partial \hat{u}}{\partial t^*} + \hat{u}\frac{\partial \hat{u}}{\partial x^*} + \hat{v}\frac{\partial \hat{u}}{\partial r^*} = -\frac{1}{\rho}\frac{\partial \hat{p}}{\partial x^*} + \nu\left[\frac{\partial^2 \hat{u}}{\partial x^{*2}} + \frac{1}{r^*}\frac{\partial \hat{u}}{\partial r^*} + \frac{\partial^2 \hat{u}}{\partial r^{*2}}\right] \tag{3.2}$$

$$\frac{\partial \hat{v}}{\partial t^*} + \hat{u}\frac{\partial \hat{v}}{\partial x^*} + \hat{v}\frac{\partial \hat{v}}{\partial r^*} = -\frac{1}{\rho}\frac{\partial \hat{p}}{\partial r^*} + \nu\left[\frac{\partial^2 \hat{v}}{\partial x^{*2}} + \frac{1}{r^*}\frac{\partial \hat{v}}{\partial r^*} - \frac{\hat{v}}{r^{*2}} + \frac{\partial^2 \hat{v}}{\partial r^{*2}}\right] \tag{3.3}$$

where t^* is time; $\hat{p}$ is static pressure; x^* and r^* denote, respectively, the axial and radial coordinates; and $\hat{u}$, and $\hat{v}$ denote the velocity components, respectively, in the x^* and r^* directions. If u^*, v^*, p^* denote mainflow quantities and u^+, v^+, p^+ are the corresponding disturbances, then

$$\hat{u}(r^*,x^*,t^*) = u^*(r^*,x^*) + u^+(r^*,x^*,t^*) \qquad (3.4a)$$

$$\hat{v}(r^*,x^*,t^*) = v^*(r^*,x^*) + v^+(r^*,x^*,t^*) \qquad (3.4b)$$

$$\hat{p}(r^*,x^*,t^*) = p^*(r^*,x^*) + p^+(r^*,x^*,t^*) \qquad (3.4c)$$

Substitution of (3.4) into equations (3.1) through (3.3), followed by subtraction of the mainflow and neglect of the squares of the disturbance quantities, gives

$$\frac{\partial u^+}{\partial x^*} + \frac{\partial v^+}{\partial r^*} + \frac{v^+}{r^*} = 0 \qquad (3.5)$$

$$\frac{\partial u^+}{\partial t^*} + u^*\frac{\partial u^+}{\partial x^*} + u^+\frac{\partial u^*}{\partial x^*} + v^*\frac{\partial u^+}{\partial r^*} + v^+\frac{\partial u^*}{\partial r^*} = -\frac{1}{\rho}\frac{\partial p^+}{\partial x^*}$$

$$+ \nu\left[\frac{\partial^2 u^+}{\partial x^{*2}} + \frac{\partial^2 u^+}{\partial r^{*2}} + \frac{1}{r^*}\frac{\partial u^+}{\partial r^*}\right] \qquad (3.6)$$

$$\frac{\partial v^+}{\partial t^*} + u^*\frac{\partial v^+}{\partial x^*} + u^+\frac{\partial v^*}{\partial x^*} + v^*\frac{\partial v^+}{\partial r^*} + v^+\frac{\partial v^*}{\partial r^*} = -\frac{1}{\rho}\frac{\partial p^+}{\partial r^*}$$

$$+ \nu\left[\frac{\partial^2 v^+}{\partial x^{*2}} + \frac{\partial^2 v^+}{\partial r^{*2}} + \frac{1}{r^*}\frac{\partial v^+}{\partial r^*} - \frac{v^+}{r^{*2}}\right] \qquad (3.7)$$

The pressure term p^+ may be eliminated from (3.6) and (3.7) by cross differentiation and subtraction. The resulting equation is then simplified by using the continuity equation and the boundary layer assumptions

$$\frac{\partial v^*}{\partial x^*} << \frac{\partial u^*}{\partial r^*}, \quad \frac{\partial^2 v^*}{\partial x^{*2}} << \frac{\partial^2 v^*}{\partial r^{*2}}, \quad \text{and} \quad \frac{\partial^2 u^*}{\partial x^{*2}} << \frac{\partial^2 u^*}{\partial r^{*2}} .$$

After simplification, the resulting equation is

$$\frac{\partial^2 u^+}{\partial t^* \partial r^*} - \frac{\partial^2 v^+}{\partial t^* \partial x^*} + u^*\left(\frac{\partial^2 u^+}{\partial x^* \partial r^*} - \frac{\partial^2 v^+}{\partial x^{*2}}\right) + v^*\left(\frac{\partial^2 u^+}{\partial r^{*2}} - \frac{\partial^2 v^+}{\partial x^* \partial r^*}\right.$$

$$\left. + \frac{1}{r^*}\frac{\partial v^+}{\partial x^*} - \frac{1}{r^*}\frac{\partial u^+}{\partial r^*}\right) - u^+\left(\frac{\partial^2 v^*}{\partial r^{*2}} + \frac{1}{r^*}\frac{\partial v^*}{\partial r^*} - \frac{v^*}{r^{*2}}\right) + v^+\left(\frac{\partial^2 u^*}{\partial r^{*2}}\right.$$

$$\left. - \frac{1}{r^*}\frac{\partial u^*}{\partial r^*}\right) = \nu\left\{\frac{\partial}{\partial r^*}\left[\frac{\partial^2 u^+}{\partial x^{*2}} + \frac{1}{r^*}\frac{\partial}{\partial r^*}\left(r^*\frac{\partial u^+}{\partial r^*}\right)\right] - \frac{\partial}{\partial x^*}\left[\frac{\partial^2 v^+}{\partial x^{*2}}\right.\right.$$

$$\left.\left. + \frac{1}{r^*}\frac{\partial}{\partial r^*}\left(r^*\frac{\partial v^+}{\partial r^*}\right) - \frac{v^+}{r^{*2}}\right]\right\} \qquad (3.8)$$

When this equation is compared with the corresponding equation from the derivation of the conventional Orr-Sommerfeld equation for parallel flow, the terms involving v* and its derivatives are seen as the additional terms.

The disturbance velocities are related to the stream function of the disturbance ψ^+ by the relations

$$u^+ = \frac{1}{r^*}\frac{\partial \psi^+}{\partial r^*}, \quad v^+ = -\frac{1}{r^*}\frac{\partial \psi^+}{\partial x^*} \qquad (3.9)$$

where ψ^+ satisfies the continuity equation (3.5) and is assumed to be of the form

$$\psi^+(x^*,r^*,t^*) = \phi^+(r^*)\ \exp[i\alpha^*(x^*-c^*t^*)] \qquad (3.10)$$

In (3.10) ϕ^+ is the amplitude function of stream function, $c^* = c_r^* + ic_i^*$ is the complex wave velocity, and α^* is the

wave number. If c_i^* is less than zero, the disturbance will decay and the flow is stable; if c_i^* is greater than zero, the disturbance will grow and the flow is unstable. For the neutral stability c_i^* is equal to zero. Upon substitution of u^+ and v^+ from (3.9) to (3.8), there will result a fourth order differential equation for the disturbance amplitude $\phi^+(r^*)$ in dimensional form.

Next, one introduces the following dimensionless variables

$$r=r^*/L_c^* \ , \quad U=u^*/u_c^* \ , \quad V=v^*/u_c^* \ , \quad c=c^*/u_c^* \ , \quad \alpha=\alpha^* L_c^* \ ,$$

$$t=t^*/(u_c^*/L_c^*) \ , \quad R=u_c^* L_c^*/\nu \ , \quad \phi=\phi^+/(u_c^* L_c^{*2}) \tag{3.11}$$

where L_c^* is the characteristic length and u_c^* is the characteristic velocity. For the annular duct flow, the u_c^* and L_c^* are taken to be $u_c^*=\bar{u}^*$, $L_c^*=(K-1)r_2^*/2K$, $K=1/M=r_2^*/r_1^*$, with r_1^* and r_2^* denoting, respectively, the inner radius and outer radius. In dimensionless form, one arrives at the following modified Orr-Sommerfeld equation

$$\phi'''' - 2\phi'''/r + 3\phi''/r^2 - 3\phi'/r^3 + \alpha^2(-2\phi'' + 2\phi'/r + \alpha^2\phi)$$

$$+ i\alpha R\{(c-U)(\phi''-\phi'/r-\alpha^2\phi) + [\partial^2 U/\partial r^2-(\partial U/\partial r)/r]\phi\} + R\{[-\phi'''$$

$$+3\phi''/r-\phi'(4/r^2-\alpha^2)-(2\alpha^2/r)\phi]V + \phi'(\partial V/\partial r)/r + \phi'(\partial^2 V/\partial r^2)\}= 0$$

(3.12)

where the primes denote differentiation with respect to r. When this equation is compared with the conventional

Orr-Sommerfeld equation, the terms involving V and its partial derivatives are seen as the additional terms. That is, these additional terms are zero under the parallel flow assumption.

The terms $\partial U/\partial r$, $\partial^2 U/\partial r^2$, V, $\partial V/\partial r$, and $\partial^2 V/\partial r^2$ will now be evaluated from the mainflow solution of Chapter II. From the mainflow solution, equation (2.10b), and with application of the continuity equation, one obtains

$$\partial U/\partial r = [(K-1)/2K]\{2(-2\eta+2A/\eta)/(1+M^2-2A) + \sum_{j=1}^{\infty} C_j\alpha_j[\{Z_Y(1)/Z_J(1)\}J_1(\alpha_j\eta)-Y_1(\alpha_j\eta)]\exp(-\alpha_j^2\chi^*)\} \quad (3.13a)$$

$$\partial^2 U/\partial r^2 = [(K-1)/2K]^2\{-4(1+A/\eta^2)/(1+M^2-2A) + \sum_{j=1}^{\infty} C_j\alpha_j[\{Z_Y(1)/Z_J(1)\}\{-J_1(\alpha_j\eta)/\eta+\alpha_j J_0(\alpha_j\eta)\} - \{-Y_1(\alpha_j\eta)/\eta + \alpha_j Y_0(\alpha_j\eta)\}]\exp(-\alpha_j^2\chi^*)\} \quad (3.13b)$$

$$V = [(K-1)/(2K\varepsilon R)] \sum_{j=1}^{\infty} C_j\alpha_j\{-[Z_Y(1)/Z_J(1)]\{[J_1(\alpha_j\eta)-MJ_1(\alpha_j M)/\eta] + B_J\alpha_j(\eta^2-M^2)/2\eta\} + \{[Y_1(\alpha_j\eta)-MY_1(\alpha_j M)/\eta] + B_Y\alpha_j(\eta^2-M^2)/2\eta\}\}\exp(-\alpha_j^2\chi^*) \quad (3.13c)$$

$$\partial V/\partial r = \{[(K-1)/(2K)]^2/(\varepsilon R)\}\sum_{j=1}^{\infty} C_j\alpha_j\{-[Z_Y(1)/Z_J(1)]\{-J_1(\alpha_j\eta)/\eta$$

$$+\alpha_j J_0(\alpha_j\eta)+MJ_1(\alpha_j M)/\eta^2+B_J\alpha_j[1+(M^2/\eta^2)]/2\}$$

$$+\{-Y_1(\alpha_j\eta)/\eta+\alpha_j Y_0(\alpha_j\eta)+MY_1(\alpha_j M)/\eta^2$$

$$+B_Y\alpha_j[1+(M^2/\eta^2)]/2\}\}\exp(-\alpha_j^2\chi^*) \qquad (3.13d)$$

$$\partial^2 V/\partial r^2 = \{[(K-1)/(2K)]^3/(\varepsilon R)\}\sum_{j=1}^{\infty} C_j\alpha_j\{-[Z_Y(1)/Z_J(1)]$$

$$\{\alpha_j J_0(\alpha_j\eta)/\eta-\alpha_j J_1(\alpha_j\eta)-[2MJ_1(\alpha_j M)+B_J\alpha_j M^2]/\eta^3\}$$

$$+\{\alpha_j Y_0(\alpha_j\eta)/\eta-\alpha_j Y_1(\alpha_j\eta)-[2MY_1(\alpha_j M)+B_Y\alpha_j M^2]/\eta^3\}\}$$

$$\exp(-\alpha_j^2\chi^*) \qquad (3.13e)$$

where

$$B_J = 2[MJ_1(\alpha_j M)-J_1(\alpha_j)]/[\alpha_j(1-M^2)]$$

$$B_Y = 2[MY_1(\alpha_j M)-Y_1(\alpha_j)]/[\alpha_j(1-M^2)] \qquad (3.14)$$

Note that $\eta=r(K-1)/2K$ and that the relationships

$$dJ_0(\alpha_j\eta)/d\eta = -\alpha_j J_1(\alpha_j\eta)$$

$$dJ_1(\alpha_j\eta)/d\eta = -J_1(\alpha_j\eta)/\eta + \alpha_j J_0(\alpha_j\eta)$$

have been used in the derivation of equations (3.13a) through (3.13d).

2. Circular Tubes

The modified Orr-Sommerfeld equation for the tube flow is the same as for the annular duct flow and is given by equation (3.12). However, in this case, the tube radius r_0^* is used as the characteristic length L_c^*. The mainflow U is given by equation (2.15).

Use of equation (2.15) along with the continuity equation yields the mainflow velocities and their partial derivatives appearing in the disturbance equation as

$$\partial U/\partial r = -4r - 4\sum_{j=1}^{\infty}\{J_1(\alpha_j r)/[\alpha_j J_0(\alpha_j)]\}\exp(-\alpha_j^2 X^*) \qquad (3.15a)$$

$$\partial^2 U/\partial r^2 = -4 + 4\sum_{j=1}^{\infty}\{J_1(\alpha_j r)/[\alpha_j r J_0(\alpha_j)] - J_0(\alpha_j r)/J_0(\alpha_j)\}$$

$$\exp(-\alpha_j^2 X^*) \qquad (3.15b)$$

$$V = \{-2/(\varepsilon R)\}\sum_{j=1}^{\infty}\{r - 2J_0(\alpha_j r)/[\alpha_j J_0(\alpha_j)]\}\exp(-\alpha_j^2 X^*) \qquad (3.15c)$$

$$\partial V/\partial r = \{-2/(\varepsilon R)\}\sum_{j=1}^{\infty}\{1 + 2J_1(\alpha_j r)/J_0(\alpha_j)\}\exp(-\alpha_j^2 X^*) \qquad (3.15d)$$

$$\partial^2 V/\partial r^2 = \{-4/(\varepsilon R)\}\sum_{j=1}^{\infty}\{-J_1(\alpha_j r)/[r J_0(\alpha_j)]$$

$$+\alpha_j J_0(\alpha_j r)/J_0(\alpha_j)\}\exp(-\alpha_j^2 X^*) \qquad (3.15e)$$

3. Parallel-Plate Channels

The modified Orr-Sommerfeld equation for plane flow has been derived by Chen, Sparrow, and Tsou (1971). For convenience, the highlights of their work will be given. The starting point of the analysis is the Navier-Stokes equations for incompressible, two-dimensional, time-dependent fluid motion. Consider a parallel-plate flow with velocity components $\hat{u}$ and $\hat{v}$ in the streamwise and transverse directions (x^* and y^*, respectively) and with static pressure distribution $\hat{p}$. If u^*, v^*, p^* denote mainflow quantities and u^+, v^+, p^+ the corresponding disturbances, then

$$\begin{aligned} \hat{u}(x^*,y^*,t^*) &= u^*(x^*,y^*) + u^+(x^*,y^*,t^*) \ , \\ \hat{v}(x^*,y^*,t^*) &= v^*(x^*,y^*) + v^+(x^*,y^*,t^*) \ , \\ \hat{p}(x^*,y^*,t^*) &= p^*(x^*,y^*) + p^+(x^*,y^*,t^*) \ . \end{aligned} \tag{3.16}$$

The continuity equation and the Navier-Stokes equations for two-dimensional plane flow are

$$\frac{\partial \hat{u}}{\partial x^*} + \frac{\partial \hat{v}}{\partial y^*} = 0 \tag{3.17}$$

$$\frac{\partial \hat{u}}{\partial t^*} + \hat{u}\frac{\partial \hat{u}}{\partial x^*} + \hat{v}\frac{\partial \hat{u}}{\partial y^*} = -\frac{1}{\rho}\frac{\partial \hat{p}}{\partial x^*} + \nu\left(\frac{\partial^2 \hat{u}}{\partial x^{*2}} + \frac{\partial^2 \hat{u}}{\partial y^{*2}}\right) \tag{3.18}$$

$$\frac{\partial \hat{v}}{\partial t^*} + \hat{u}\frac{\partial \hat{v}}{\partial x^*} + \hat{v}\frac{\partial \hat{v}}{\partial y^*} = -\frac{1}{\rho}\frac{\partial \hat{p}}{\partial y^*} + \nu\left(\frac{\partial^2 \hat{v}}{\partial x^{*2}} + \frac{\partial^2 \hat{v}}{\partial y^{*2}}\right) \tag{3.19}$$

Substitution of (3.16) into equations (3.18) and (3.19), followed by subtraction of the mainflow and linearization of the disturbance quantities, gives

$$\frac{\partial u^+}{\partial t^*} + u^*\frac{\partial u^+}{\partial x^*} + u^+\frac{\partial u^*}{\partial x^*} + v^*\frac{\partial u^+}{\partial y^*} + v^+\frac{\partial u^*}{\partial y^*} = -\frac{1}{\rho}\frac{\partial p^+}{\partial x^*} + \nu\left(\frac{\partial^2 u^+}{\partial x^{*2}} + \frac{\partial^2 u^+}{\partial y^{*2}}\right) \tag{3.20}$$

$$\frac{\partial v^+}{\partial t^*} + u^*\frac{\partial v^+}{\partial x^*} + u^+\frac{\partial v^*}{\partial x^*} + v^*\frac{\partial v^+}{\partial y^*} + v^+\frac{\partial v^*}{\partial y^*} = -\frac{1}{\rho}\frac{\partial p^+}{\partial y^*} + \nu\left(\frac{\partial^2 v^+}{\partial x^{*2}} + \frac{\partial^2 v^+}{\partial y^{*2}}\right) \tag{3.21}$$

Equations (3.20) and (3.21) keep all of the terms involving $\partial u^+/\partial x^*$, v^+, $\partial v^+/\partial x^*$, and $\partial v^+/\partial y^*$ that are normally neglected in the derivation of the conventional Orr-Sommerfeld equation. The pressure p^+ may now be eliminated from equations (3.20) and (3.21) by cross differentiation and subtraction. The resulting equation is then simplified by using the continuity equation for mainflow and the conditions $\partial^2 u^*/\partial x^{*2} << \partial^2 u^*/\partial y^{*2}$ and $\partial^2 v^*/\partial x^{*2} << \partial^2 v^*/\partial y^{*2}$. This results in

$$\frac{\partial^2 u^+}{\partial y^*\partial t^*} - \frac{\partial^2 v^+}{\partial x^*\partial t^*} + u^*\left(\frac{\partial^2 u^+}{\partial y^*\partial t^*} - \frac{\partial^2 v^+}{\partial x^{*2}}\right) + v^*\left(\frac{\partial^2 u^+}{\partial y^{*2}} - \frac{\partial^2 v^+}{\partial x^*\partial y^*}\right)$$

$$+ v^+\frac{\partial^2 u^*}{\partial y^{*2}} - u^+\frac{\partial^2 v^*}{\partial y^{*2}} = \nu\left\{\frac{\partial}{\partial y^*}\left(\frac{\partial^2 u^+}{\partial x^{*2}} + \frac{\partial^2 u^+}{\partial y^{*2}}\right) - \frac{\partial}{\partial x^*}\left(\frac{\partial^2 v^+}{\partial x^{*2}} + \frac{\partial^2 v^+}{\partial y^{*2}}\right)\right\} \tag{3.22}$$

Compared with the corresponding equation from the derivation

of the conventional Orr-Sommerfeld equation, equation (3.22) contains additional terms $v^*\partial^2 u^+/\partial y^{*2}$, $v^*\partial^2 v^+/\partial x^*\partial y^*$, and $u^+\partial^2 u^*/\partial y^{*2}$.

The disturbance velocities are related to the stream function of the disturbance Ψ^+ by the relations

$$u^+ = \partial\Psi^+/\partial y^* \ , \qquad v^+ = -\partial\Psi^+/\partial x^* \tag{3.23}$$

where Ψ^+ satisfies the continuity equation and is assumed to be of the form

$$\Psi^+(x^*,y^*,t^*) = \phi^+(y^*)\ \exp\{i\alpha^*(x^*-c^*t^*)\} \tag{3.24}$$

Upon substitution of u^+ and v^+ and (3.24) into (3.22), there results a fourth order differential equation for the disturbance amplitude $\phi^+(y^*)$. With the introduction of the following dimensionless variables,

$$y=y^*/L^* \ , \quad U=u^*/\bar{u}^* \ , \quad V=v^*/\bar{u}^* \ , \quad c=c^*/\bar{u}^* \ , \quad \alpha=\alpha^*L^* \ ,$$

$$t=t^*/(L^*/\bar{u}^*) \ , \quad R=\bar{u}^*L^*/\nu \ , \quad \phi=\phi^+/(L^{*2}\bar{u}^*) \tag{3.25}$$

one obtains the modified Orr-Sommerfeld equation

$$\phi''''-2\alpha^2\phi''+\alpha^4\phi+i\alpha R\{(c-U)(\phi''-\alpha^2\phi)+(\partial^2U/\partial y^2)\phi$$

$$+(i/\alpha)[V(\phi'''-\alpha^2\phi')-(\partial^2V/\partial y^2)\phi]\} = 0 \tag{3.26}$$

in which the primes denote differentiation with respect to y. For parallel flow, $V=\partial^2V/\partial y^2=0$, and equation (3.26) reduces to the conventional Orr-Sommerfeld equation.

The terms $\partial^2 U/\partial y^2$, V, and $\partial^2 V/\partial y^2$ can be readily evaluated from the mainflow solution (2.19) and the continuity equation. They are given by

$$\partial^2 U/\partial y^2 = -3 - 2 \sum_{j=1}^{\infty} \{\cos(\alpha_j y)/\cos(\alpha_j)\} \exp(-\alpha_j^2 X^*) \qquad (3.27a)$$

$$V = (2/\varepsilon R) \sum_{j=1}^{\infty} \{\sin(\alpha_j y)/[\alpha_j \cos(\alpha_j)] - y\} \exp(-\alpha_j^2 X^*) \qquad (3.27b)$$

$$\partial^2 V/\partial y^2 = -(2/\varepsilon R) \sum_{j=1}^{\infty} \{\alpha_j \sin(\alpha_j y)/\cos(\alpha_j)\} \exp(-\alpha_j^2 X^*) \qquad (3.27c)$$

B. The Boundary Conditions

The disturbances are subject to physical constraints at the bounding walls (or at the bounding wall and center) of the ducts. These constraints give rise to boundary conditions for different flow configurations are discussed separately in the following sub-sections.

1. Annular Ducts

The four boundary conditions for equation (3.12) for annular duct flow are obtained by requiring that the disturbance velocities u^+ and v^+ be zero at the inner and outer walls. In terms of $\phi(r)$, they can be expressed as

$$\phi\left(\frac{2}{K-1}\right) = \phi'\left(\frac{2}{K-1}\right) = 0 \quad , \quad \phi\left(\frac{2K}{K-1}\right) = \phi'\left(\frac{2K}{K-1}\right) = 0 \qquad (3.28)$$

2. Circular Tubes

For axisymmetric disturbances in a circular tube flow, the disturbance velocities at the tube wall vanish. That is

$$\phi(1) = \phi'(1) = 0 \tag{3.29a}$$

The other two boundary conditions are that the disturbance velocities must be axisymmetric and finite at the center of the tube. This gives

$$\lim_{r\to 0} (\phi/r) = 0 , \quad \lim_{r\to 0} (\phi'/r) = \text{finite} \tag{3.29b}$$

3. Parallel-Plate Channels

The boundary conditions for equation (3.26) are derived from the condition that the disturbance velocities vanish at the channel walls. In terms of $\phi(y)$, one has

$$\phi(1) = \phi'(1) = 0 \tag{3.30a}$$

$$\phi(-1) = \phi'(-1) = 0 \tag{3.30b}$$

However, for the present problem, the velocity profiles are symmetric with respect to the centerline of the channel. Therefore, it is more convenient to consider only half of the channel in the stability calculations. The boundary conditions (3.30b) corresponding to the bottom wall can be replaced by those at the centerline of the channel. Since the mainflow is an even function of $y=y^*/L^*$, the solution

for $\phi(y)$ can be decomposed into even and odd modes, of which the even mode $\phi(y)$ has been found to lead to a more unstable flow. For the even mode, the boundary conditions at the bottom wall are replaced with those at the centerline

$$\phi'(0) = \phi'''(0) = 0 \qquad (3.30c)$$

C. The Eigenvalue Problems

The mathematical systems consisting of equations (3.12) and (3.28) for the annular duct flow, equations (3.12) and (3.29) for the tube flow, and equations (3.26) and (3.30) for the channel flow form the linear stability problems of interest. Since each system consists of a homogeneous fourth order linear differential equation and four boundary conditions, each is an eigenvalue problem. The general solution $\phi(r)$ (note that for the parallel-plate channels the notation $\phi(y)$ is used instead) is of form

$$\phi(r) = a_1\phi_1(r) + a_2\phi_2(r) + a_3\phi_3(r) + a_4\phi_4(r) \qquad (3.31)$$

where $\phi_1(r)$, $\phi_2(r)$, $\phi_3(r)$, and $\phi_4(r)$ are the four independent solutions of the fourth order equation and a_1, a_2, a_3, a_4 are the constants to be determined by applying the four boundary conditions for $\phi(r)$. This will result in four homogeneous algebraic equations for a_1, a_2, a_3, and a_4. A non-trivial solution to these equations exists if and only if the determinant of the coefficient matrix is zero; that is

$|D(\alpha,R,c_r,c_i)| = 0$, which leads to a secular equation

$$f(\alpha,R,c_r,c_i) = 0 \tag{3.32}$$

which gives a relationship among α, R, c_r , and c_i.

In order to obtain a non-trivial solution for ϕ, it is necessary to impose a normalizing condition. Since this normalization fixes only the scale of the solution, any choice will suffice (for example, $a_1=1$). The eigenvalue problem then represents ten real boundary conditions on the eight first-order real system, equation (3.12) or (3.26). Therefore, two of the four real parameters α, R, c_r , and c_i have to be eigenvalues. By assigning any two of the four parameters, the other two can be found as the eigenvalues.

The eigenvalue problems were solved numerically using two different numerical methods, a direct numerical integration scheme and a finite difference scheme. The eigenvalues were then obtained by an iteration scheme. The details of the numerical methods used will be presented in Chapter IV.

IV. NUMERICAL METHODS OF SOLUTION

A. General Discussion

There are several methods which can be employed in the numerical solution of differential equations. These methods can be classified into two categories; that is, algebraic and differential. In the algebraic methods, the original differential eigenvalue problem is replaced with an algebraic eigenvalue problem. These include a finite difference method and the method of weighted residuals. In the differential methods, the differential system is integrated directly, using, for example, the filter technique (Kaplan 1964) or the orthonormalization method (Dettman 1962) to remove the "parasitic error". A very complete review and comparison of all these methods is given by Gersting (1970).

In the integration process of a differential system that has general solution with vastly different growth rates, the rapidly growing solution introduces a portion of its solution into the more slowly growing solution. If the rapidly growing solution dominates the slowly growing solution, then the linear independence of the two solutions for the initial value problem is lost. In order to preserve the linear independence, an orthonormalization is used after each step of integration. That is, after each step of integration the old basis is replaced by a new orthonormal basis. This process repeats after each integration process. The Gram-Schmidt process (Dettman 1962) has been used for

performing the orthonormalization process.

In his work, Gersting introduced an additional method known as the method of near-orthonormalized integration. This method differs from the orthonormalization method in that the orthonormalization is not carried at every step of integration. Gersting pointed out that "Since it is not expected that orthonormalization will be required at each mesh point, a criterion for deciding whether or not orthonormalization is required at a particular mesh point is needed". The "angle criterion" was used in his work. He also pointed out that the number of orthonormalizations increases as the Reynolds number becomes large. For the plane Poiseuille flow at a Reynolds number of 2500 and using 101 mesh points in the region of interest, he used 90 orthonormalizations. For the tube and annular duct flow problems considered, the Reynolds numbers for the instability of flow are in the order of 10^4 and orthonormalization is required at almost every mesh point. Thus, the complete orthonormalization method was used for these flow configurations in conjunction with the Runge-Kutta integration scheme in this investigation. A computer program was written for the orthonormalization method which worked better for the present problems than the near-orthonormalization program of Gersting.

For the parallel-plate channel flow, a finite difference method is used which closely follows the work of Chen (1966) and Chen, Sparrow, and Tsou (1971).

B. The Orthonormalization Method

To solve the eigenvalue problem by a direct numerical integration scheme, one needs to transform the eigenvalue problem into an initial value problem. Due to the nature of the stability problems involved in the present investigation, in which instability of flow occurs at very high Reynolds numbers, the differential equations for ϕ become very singular at these high Reynolds numbers. This gives rise to "parasitic error" during the numerical integration of the equation. To keep the sets of numerical solutions for ϕ independent, this "parasitic error" has to be removed during the integration process. Finally, the eigenvalues can be determined by an iteration scheme. These numerical aspects of the problem are discussed in this section.

1. Transformation of the Eigenvalue Problem into an Initial Value Problem

In order to apply the numerical procedure to be discussed, it is more convenient to transform the differential equation (3.12) into the form

$$\phi'''' + L(\phi,\phi',\phi'',\phi''') = 0 \qquad (4.1)$$

where

$$L(\phi,\phi',\phi'',\phi''') = -2\phi'''/r + 3\phi''/r^2 - 3\phi'/r^3 + \alpha^2(-2\phi'' + 2\phi'/r + \alpha^2\phi) + i\alpha R\{(c-U)(\phi''-\phi'/r-\alpha^2\phi) + [\partial^2U/\partial r^2 - (\partial U/\partial r)/r]\phi\} + R\{[-\phi'''+3\phi''/r-(4/r^2-\alpha^2)\phi'-(2\alpha^2/r)\phi]V + (\partial V/\partial r)(\phi'/r)+(\partial^2V/\partial r^2)\phi'\} \quad (4.2)$$

The boundary conditions for annular duct flow and for circular tube flow are given, respectively, by equations (3.28) and (3.29).

The first step of the transformation is to transform the differential eigenvalue problem to a boundary value problem. As explained in Section C, Chapter III, any two of the four parameters α, R, c_r , and c_i can be assigned and the other two found as eigenvalues. By assigning the values for the parameters and then selecting values for the eigenvalues, the eigenvalue problem is transformed into a boundary value problem. However, the eigenvalues are yet to be determined in this problem. Therefore two things must be done in order to use this direct integration method. First, an estimate of the eigenvalues is to be made. Secondly, an iteration scheme must be available to obtain the eigenvalues which approach close to the exact eigenvalues within a prescribed convergence criterion. These two things can be accomplished and will be discussed in Sub-sections 5 and 6.

In the analysis to follow, we shall use the annular duct flow as an example, because it applies to the tube flow as well. The only difference in the analysis between these two flows appears in the boundary conditions.

Let

$$\begin{aligned} y_1(r) &= \phi(r) \\ y_2(r) &= \phi'(r) \\ y_3(r) &= \phi''(r) \\ y_4(r) &= \phi'''(r) \end{aligned} \tag{4.3}$$

then the governing system (4.1) becomes

$$\begin{aligned} y_1'(r) &= y_2(r) \\ y_2'(r) &= y_3(r) \\ y_3'(r) &= y_4(r) \\ y_4'(r) &= -L(\phi,\phi',\phi'',\phi''') \\ &= E_1 y_1 + E_2 y_2 + E_3 y_3 + E_4 y_4 \end{aligned} \tag{4.4a}$$

where

$$\begin{aligned} E_1 &= -\alpha^4 + i\alpha R[(c-U)\alpha^2+\partial^2 U/\partial r^2-(\partial U/\partial r)/r] + 2\alpha^2 RV/r \\ E_2 &= 3/r^3 - 2\alpha^2/r + i\alpha R(c-U)/r + R[(4/r^2-\alpha^2)V \\ &\quad +(\partial V/\partial r)/r+\partial^2 V/\partial r^2] \\ E_3 &= -3/r^2 -2\alpha^2 - i\alpha R(c-U) - 3RV/r \\ E_4 &= 2/r + RV \end{aligned}$$

The boundary conditions (3.28) become

$$y_1(r=r_1=2/(K-1)) = y_2(r=r_1=2/(K-1)) = 0 \tag{4.4b}$$

$$y_1(r=r_2=2K/(K-1)) = y_2(r=r_2=2K/(K-1)) = 0 \tag{4.4c}$$

In matrix form, equation (4.4a) may be written as

$$\begin{bmatrix} y_1' \\ y_2' \\ y_3' \\ y_4' \end{bmatrix} = \begin{bmatrix} 0 & 1 & 0 & 0 \\ 0 & 0 & 1 & 0 \\ 0 & 0 & 0 & 1 \\ E_1 & E_2 & E_3 & E_4 \end{bmatrix} \begin{bmatrix} y_1 \\ y_2 \\ y_3 \\ y_4 \end{bmatrix} \tag{4.5a}$$

and the boundary conditions (4.4b) and (4.4c), respectively, as

$$\begin{bmatrix} 1 & 0 & 0 & 0 \\ 0 & 1 & 0 & 0 \end{bmatrix} \begin{bmatrix} y_1(r_1) \\ y_2(r_1) \\ y_3(r_1) \\ y_4(r_1) \end{bmatrix} = \begin{bmatrix} 0 \\ 0 \end{bmatrix} \tag{4.5b}$$

and

$$\begin{bmatrix} 1 & 0 & 0 & 0 \\ 0 & 1 & 0 & 0 \end{bmatrix} \begin{bmatrix} y_1(r_2) \\ y_2(r_2) \\ y_3(r_2) \\ y_4(r_2) \end{bmatrix} = \begin{bmatrix} 0 \\ 0 \end{bmatrix} \tag{4.5c}$$

In a compact form, equations (4.5a) through (4.5c) are expressible as

$$y'(r) = Ay(r) \tag{4.6a}$$

and

$$By(r_1) = 0 \tag{4.6b}$$

$$By(r_2) = 0 \tag{4.6c}$$

where

$$y' = \begin{Bmatrix} y_1' \\ y_2' \\ y_3' \\ y_4' \end{Bmatrix}, \quad y = \begin{Bmatrix} y_1 \\ y_2 \\ y_3 \\ y_4 \end{Bmatrix}, \quad A = \begin{Bmatrix} 0 & 1 & 0 & 0 \\ 0 & 0 & 1 & 0 \\ 0 & 0 & 0 & 1 \\ E_1 & E_2 & E_3 & E_4 \end{Bmatrix} \tag{4.6d}$$

$$B = \begin{Bmatrix} 1 & 0 & 0 & 0 \\ 0 & 1 & 0 & 0 \end{Bmatrix} \tag{4.6e}$$

The operator L is linear and the boundary conditions are also linear. The boundary value problem (4.6) can, therefore, be solved directly in terms of a set of initial value problems.

To numerically integrate a fourth order differential equation for ϕ by the initial value technique, one needs to specify the initial values of ϕ, ϕ', ϕ'', and ϕ''' at the starting point. Since $\phi(r_1)$ and $\phi'(r_1)$ are known (boundary conditions), the values $\phi''(r_1)$ and $\phi'''(r_1)$ have to be specified. This can be done by assigning $\phi''(r_1)=0$ and $\phi'''(r_1)=1$, and $\phi''(r_1)=1$ and $\phi'''(r_1)=0$, which gives rise to two independent solutions ϕ_1 and ϕ_2 for ϕ. Let $y^{(1)}$ and $y^{(2)}$ be the corresponding two independent solutions. Then

$$y(r) = \beta_1 y^{(1)}(r) + \beta_2 y^{(2)}(r) \tag{4.7a}$$

$$\text{or} \quad \begin{Bmatrix} y_1(r) \\ y_2(r) \\ y_3(r) \\ y_4(r) \end{Bmatrix} = \beta_1 \begin{Bmatrix} y_1^{(1)}(r) \\ y_2^{(1)}(r) \\ y_3^{(1)}(r) \\ y_4^{(1)}(r) \end{Bmatrix} + \beta_2 \begin{Bmatrix} y_1^{(2)}(r) \\ y_2^{(2)}(r) \\ y_3^{(2)}(r) \\ y_4^{(2)}(r) \end{Bmatrix} \tag{4.7b}$$

In matrix form, this gives

$$y(r) = Y(r)\ \beta \tag{4.7c}$$

where

$$y(r) = \begin{bmatrix} y_1(r) \\ y_2(r) \\ y_3(r) \\ y_4(r) \end{bmatrix}, \qquad Y(r) = \begin{bmatrix} y_1^{(1)}(r) & y_1^{(2)}(r) \\ y_2^{(1)}(r) & y_2^{(2)}(r) \\ y_3^{(1)}(r) & y_3^{(2)}(r) \\ y_4^{(1)}(r) & y_4^{(2)}(r) \end{bmatrix} \tag{4.7d}$$

and β is a constant matrix

$$\beta = \begin{bmatrix} \beta_1 \\ \beta_2 \end{bmatrix} \tag{4.7e}$$

In order to assure that $y(r)$ in (4.7c) is a solution to (4.6a), the matrices $Y(r)$ and β in (4.7c) must be chosen such that

$$Y'(r) = A\ Y(r) \tag{4.8a}$$

with the initial condition

$$B\ Y(r_1) = 0 \tag{4.8b}$$

Equations (4.8a) and (4.8b) determine the two initial value problems, one for each column of $Y(r)$. With the boundary condition

$$B\ y(r_2) = B\ Y(r_2)\ \beta = 0 \tag{4.9a}$$

the constants β_1 and β_2 can then be determined, as (4.9a) can be written as

$$\begin{bmatrix} 1 & 0 & 0 & 0 \\ 0 & 1 & 0 & 0 \end{bmatrix} \begin{bmatrix} y_1^{(1)}(r_2) & y_1^{(2)}(r_2) \\ y_2^{(1)}(r_2) & y_2^{(2)}(r_2) \\ y_3^{(1)}(r_2) & y_3^{(2)}(r_2) \\ y_4^{(1)}(r_2) & y_4^{(2)}(r_2) \end{bmatrix} \begin{bmatrix} \beta_1 \\ \beta_2 \end{bmatrix} = 0 \qquad (4.9b)$$

or

$$\begin{bmatrix} y_1^{(1)}(r_2) & y_1^{(2)}(r_2) \\ y_2^{(1)}(r_2) & y_2^{(2)}(r_2) \end{bmatrix} \begin{bmatrix} \beta_1 \\ \beta_2 \end{bmatrix} = 0 \qquad (4.9c)$$

Thus, there exists a non-trivial solution for β_1 and β_2 if and only if the determinant of (4.9c) vanishes, that is,

$$\begin{vmatrix} y_1^{(1)}(r_2) & y_1^{(2)}(r_2) \\ y_2^{(1)}(r_2) & y_2^{(2)}(r_2) \end{vmatrix} = 0 \qquad (4.10)$$

The analysis presented above is an exact algorithm. However, in the actual computation it has a so called parasitic error in the numerical integration of the disturbance equation. The Runge-Kutta integration scheme was employed in the present study. The problem of the parasitic error will be examined next.

2. The Parasitic Error

As pointed out earlier, in a differential system that has general solutions with vastly different growth rates, there exists a parasitic error during the course of the numerical integration process. The error introduced by portions of the rapidly growing solution into the more slowly growing solution is called the parasitic error. When the parasitic error develops, the slowly growing solution is dominated by the rapidly growing solution and the linear independence of the solutions of the initial value problem is lost. The following technique is used to remove the parasitic error.

In the solution of the modified or conventional Orr-Sommerfeld equation by a numerical method, it has been found that one of the initial value problems produces only a slowly growing solution and the other produces only a rapidly growing solution, rather than each solution having a combination of the slowly growing solution and the rapidly growing solution. Let ϕ_s be the slowly growing solution and ϕ_g the rapidly growing solution. By the definition of parasitic error, the slowly growing solution is being influenced by the rapidly growing solution, but ϕ_g cannot be affected by the parasitic error.

Let the integration interval be divided into N equal subintervals and let integers in brackets 0,1,2,...,N be the end points of these subintervals. Then, the initial

conditions (4.8b) for the initial value problems assume the form

$$\begin{bmatrix} 1 & 0 & 0 & 0 \\ 0 & 1 & 0 & 0 \end{bmatrix} \begin{bmatrix} \phi_s[0] & \phi_g[0] \\ \phi_s'[0] & \phi_g'[0] \\ \phi_s''[0] & \phi_g''[0] \\ \phi_s'''[0] & \phi_g'''[0] \end{bmatrix} = \begin{bmatrix} 0 & 0 \\ 0 & 0 \end{bmatrix} \tag{4.11}$$

and the condition (4.10) from which eigenvalues are determined becomes

$$\begin{vmatrix} \phi_s[N] & \phi_g[N] \\ \phi_s'[N] & \phi_g'[N] \end{vmatrix} = 0 \tag{4.12}$$

where [0] and [N] are the left-side end point and right-side end point, respectively. The terms $\phi_s[N]$, $\phi_s'[N]$, $\phi_g[N]$, and $\phi_g'[N]$ are from the exact algorithm.

Let $\bar{\phi}_s[i]$ and $\bar{\phi}_g[i]$ be the numerical approximations to the exact solutions $\phi_s[i]$ and $\phi_g[i]$ at the ith point. Since $\phi_g[i]$ is not affected by the parasitic error, we have

$$\bar{\phi}_g^{(j)}[i] = \phi_g^{(j)}[i] \qquad j=0,1,2,3; \quad i=0,1,2,\ldots,N \tag{4.13a}$$

where the superscript (j) denotes the order of differentiation. But for the slowly growing solution $\bar{\phi}_s$, it contains a parasitic error from the rapidly growing solution at every integration step. After an integration step from the point

[0] to point [1], $\bar{\phi}_s^{(j)}[1]$ becomes

$$\bar{\phi}_s^{(j)}[1] = \phi_s^{(j)}[1] + G_1 \phi_g^{(j)}[1] \tag{4.13b}$$

where G_1 is a constant. If the parasitic error is not removed and the integration is carried on to the point [N], then the term $G_N \phi_g^{(j)}[N]$ will finally dominated $\phi_s^{(j)}[N]$; that is

$$\bar{\phi}_s^{(j)}[N] = \phi_s^{(j)}[N] + G_N \phi_g^{(j)}[N] \simeq G_N \phi_g^{(j)}[N] \tag{4.13c}$$

and equation (4.12) therefore becomes

$$\begin{vmatrix} \bar{\phi}_s[N] & \phi_g[N] \\ \bar{\phi}_s'[N] & \phi_g'[N] \end{vmatrix} = \begin{vmatrix} G_N \phi_g[N] & \phi_g[N] \\ G_N \phi_g'[N] & \phi_g'[N] \end{vmatrix} = 0 \tag{4.14}$$

Equation (4.14) is identically zero for any choice of eigenvalues , so the parasitic error has to be removed or the condition (4.12) will not be satisfied.

To remove the parasitic error from the integrated solution $\bar{\phi}_s$, an auxiliary solution $\tilde{\phi}_s$ is chosen such that ϕ_g is not contained in $\tilde{\phi}_s$. Let

$$\tilde{\phi}_s^{(j)}[i] = \bar{\phi}_s^{(j)}[i] - B_i \phi_g^{(j)}[i] \tag{4.15a}$$

To remove ϕ_g from (4.15a), $\tilde{\phi}_s$ is made orthogonal to ϕ_g , that is

$$< \tilde{\phi}_s^{(j)}[i] \ , \ \tilde{\phi}_g^{(j)}[i] > = 0$$

or

$$< \bar{\phi}_s^{(j)}[i] \ , \ \phi_g^{(j)}[i] > - B_i < \phi_g^{(j)}[i] \ , \ \phi_g^{(j)}[i] > = 0$$

Thus

$$B_i = \frac{< \bar{\phi}_s^{(j)}[i] \ , \ \phi_g^{(j)}[i] >}{< \phi_g^{(j)}[i] \ , \ \phi_g^{(j)}[i] >}$$

and (4.15a) becomes

$$\tilde{\phi}_s^{(j)}[i] = \bar{\phi}_s^{(j)}[i] - \frac{< \bar{\phi}_s^{(j)}[i] \ , \ \phi_g^{(j)}[i] >}{< \phi_g^{(j)}[i] \ , \ \phi_g^{(j)}[i] >} \phi_g^{(j)}[i] \qquad (4.15b)$$

A normalization of equations (4.13a) and (4.15b) yield

$$\phi_{gn}^{(j)}[i] = \frac{\phi_g^{(j)}[i]}{|| \ \phi^{(j)}[i] \ ||} \qquad (4.16a)$$

and

$$\tilde{\phi}_{sn}^{(j)}[i] = \frac{\bar{\phi}_s^{(j)}[i] - \frac{< \bar{\phi}_s^{(j)}[i] \ , \ \phi_g^{(j)}[i] >}{< \phi_g^{(j)}[i] \ , \ \phi_g^{(j)}[i] >} \phi_g^{(j)}[i]}{\left|\left| \ \bar{\phi}_s^{(j)}[i] - \frac{< \bar{\phi}_s^{(j)}[i] \ , \ \phi_g^{(j)}[i] >}{\phi^{(j)}[i] \quad \phi^{(j)}[i]} \phi^{(j)}[i] \right|\right|}$$

After each integration, a Gram-Schmidt orthonormalization process is performed, and with the use of (4.16) the parasitic error can then be removed. The Gram-Schmidt orthonormalization process is discussed next.

3. The Gram-Schmidt Orthonormalization Process

The Gram-Schmidt orthonormalization process is given by Dettman (1962). The linearly independent vector $y^{(1)}(r_i)$ and $y^{(2)}(r_i)$ in (4.7a) are related to their respective orthonormal sets $x^{(1)}(r_i)$ and $x^{(2)}(r_i)$ defined by

$$x^{(1)}(r_i) = \begin{Bmatrix} x_1^{(1)}(r_i) \\ x_2^{(1)}(r_i) \\ x_3^{(1)}(r_i) \\ x_4^{(1)}(r_i) \end{Bmatrix} \quad , \qquad x^{(2)}(r_i) = \begin{Bmatrix} x_1^{(2)}(r_i) \\ x_2^{(2)}(r_i) \\ x_3^{(2)}(r_i) \\ x_4^{(2)}(r_i) \end{Bmatrix}$$

through the relation

$$x^{(1)} = \frac{y^{(1)}}{\| y^{(1)} \|} \tag{4.17a}$$

and

$$x^{(2)} = \frac{y^{(2)} - \langle x^{(1)}, y^{(2)} \rangle x^{(1)}}{\| y^{(2)} - \langle x^{(1)}, y^{(2)} \rangle x^{(1)} \|} \tag{4.17b}$$

If the relationship between $y(r_i)$ and $x(r_i)$ is expressed through a constant matrix $P^{(i)}$ by

$$x(r_i) = y(r_i)\ P^{(i)} \tag{4.18a}$$

where

$$x(r_i)=\{x^{(1)}(r_i)\quad x^{(2)}(r_i)\}\ ,\quad y(r_i)=\{y^{(1)}(r_i)\quad y^{(2)}(r_i)\}\ ,$$

$$P^{(i)} = \begin{bmatrix} P_{11} & P_{12} \\ 0 & P_{22} \end{bmatrix} \tag{4.18b}$$

a comparison among equations (4.17a), (4.17b), and (4.18) gives

$$P_{11} = \frac{1}{||\ y^{(1)}\ ||} \tag{4.19a}$$

$$P_{22} = \frac{1}{W_{22}} = \frac{1}{||\ y^{(2)} - \langle x^{(1)}\ ,\ y^{(2)}\rangle\ x^{(1)}\ ||} \tag{4.19b}$$

and

$$P_{12} = -\ \frac{\langle x^{(1)}\ ,\ y^{(2)}\rangle}{W_{22}}\ P_{11} \tag{4.19c}$$

By comparing (4.16a) with (4.17a) and (4.16b) with (4.17b) it is clear that

$$x^{(1)}(r_i) = \begin{pmatrix} \phi_{gn}[i] \\ \phi'_{gn}[i] \\ \phi''_{gn}[i] \\ \phi'''_{gn}[i] \end{pmatrix}, \qquad x^{(2)}(r_i) = \begin{pmatrix} \tilde{\phi}_{sn}[i] \\ \tilde{\phi}'_{sn}[i] \\ \tilde{\phi}''_{sn}[i] \\ \tilde{\phi}'''_{sn}[i] \end{pmatrix}, \tag{4.20a}$$

$$y^{(1)}(r_i) = \begin{pmatrix} \phi_{g}[i] \\ \phi'_{g}[i] \\ \phi''_{g}[i] \\ \phi'''_{g}[i] \end{pmatrix}, \qquad y^{(2)}(r_i) = \begin{pmatrix} \bar{\phi}_{s}[i] \\ \bar{\phi}'_{s}[i] \\ \bar{\phi}''_{s}[i] \\ \bar{\phi}'''_{s}[i] \end{pmatrix}. \tag{4.20b}$$

Substituting these results into equations (4.19a), (4.19b), and (4.19c), one obtains

$$P_{11} = \frac{1}{[(\phi_g)^2+(\phi'_g)^2+(\phi''_g)^2+(\phi'''_g)^2]^{1/2}} \tag{4.21a}$$

$$B_i = \langle x^{(1)}, y^{(2)} \rangle$$

$$= (\phi_{gn}\phi_g+\phi'_{gn}\phi'_g+\phi''_{gn}\phi''_g+\phi'''_{gn}\phi'''_g)^{1/2} \tag{4.21b}$$

$$W_{22} = ||y^{(2)}-B_i x^{(1)}||$$

$$= [(\bar{\phi}_s-B_i\phi_{gn})^2+(\bar{\phi}'_s-B_i\phi'_{gn})^2+(\bar{\phi}''_s-B_i\phi''_{gn})^2+(\bar{\phi}'''_s-B_i\phi'''_{gn})^2]^{1/2}$$

(4.21c)

$$P_{22} = 1/W_{22} \tag{4.21d}$$

$$P_{12} = -\langle x^{(1)}, y^{(2)} \rangle P_{11}/W_{22} = -B_i P_{11}/W_{22} \tag{4.21e}$$

With $P^{(i)}$ determined, equation (4.18) relates $x(r_i)$ to $y(r_i)$. This completes the orthonormalization process at each step of the integration.

4. The Runge-Kutta Method

This numerical integration scheme was employed in the present study. The highlights of this method is described here. Consider a fourth order differential equation

$$y'''' = f(x,y,y',y'',y''') \tag{4.22a}$$

which is to be integrated with the initial conditions

$$y_0^{(\nu)} = y^{(\nu)}(x_0) \qquad (\nu=0,1,2,3) \tag{4.22b}$$

at the point $x=x_0$. The approximate values of y, y', y", and y"' at the next point one step ahead, $x_1=x_0+h$, are given by the following expressions (Collatz, 1966)

x	y	$hy'=v_1$
x_0	y_0	v_{10}
$x_0+h/2$	$y_0+v_{10}/2+v_{20}/4+v_{30}/8+k_1/16$	$v_{10}+v_{20}+3v_{30}/4+k_1/2$
$x_0+h/2$	$y_0+v_{10}/2+v_{20}/4+v_{30}/8+k_1/16$	$v_{10}+v_{20}\ 3v_{30}/4+k_1/2$
x_0+h	$y_0+v_{10}+v_{20}+v_{30}+k_3$	$v_{10}+2v_{20}+3v_{30}+4k_3$
$x_1=x_0+h$	$y_1=y_0+v_{10}+v_{20}+v_{30}+k$	$v_{11}=v_{10}+2v_{20}+3v_{30}+k'$

$h^2y''/2=v_2$	$h^3y'''/6=v_3$	$k_\nu=(h^4/24)\ f(x,y,y',y'',y''')$
v_{20}	v_{30}	k_1
$v_{20}+3v_{30}/2+3k_1/2$	$v_{30}+2k_1$	k_2
$v_{20}+3v_{30}/2+3k_1/2$	$v_{30}+2k_2$	k_3
$v_{20}+3v_{30}+6k_3$	$v_{30}+4k_3$	k_4
$v_{21}=v_{20}+3v_{30}+k''$	$v_{31}=v_{30}+k'''$	

where

$$k = (8k_1+4k_2+4k_3-k_4)/15 ,$$

$$k' = (9k_1+6k_2+6k_3-k_4)/5 ,$$

$$k'' = 2(k_1+k_2+k_3) ,$$

$$k''' = 2(k_1+2k_2+2k_3+k_4)/3 .$$

The integration process is continued from one end of the region to the other.

5. The Differential Correction Iteration Scheme

To obtain the eigenvalues of the stability problem, one needs an iteration scheme. Of the various schemes available, the differential correction iteration scheme was found to be very efficient and used in the present study. Let $F=F_r+iF_i$ be a complex function of the two real variables x_1 and x_2. Then, one can write

$$dF_r(x_1,x_2) = \frac{\partial F_r(x_1,x_2)}{\partial x_1} dx_1 + \frac{\partial F_r(x_1,x_2)}{\partial x_2} dx_2 \qquad (4.23a)$$

$$dF_i(x_1,x_2) = \frac{\partial F_i(x_1,x_2)}{\partial x_1} dx_1 + \frac{\partial F_i(x_1,x_2)}{\partial x_2} dx_2 \qquad (4.23b)$$

Replacing the differential operators by the forward difference operator Δ, equations (4.23a) and (4.23b) become

$$\Delta F_r(x_1,x_2) = \left.\frac{\Delta F_r(x_1,x_2)}{\Delta x_1}\right|_{x_2} \Delta x_1 + \left.\frac{\Delta F_r(x_1,x_2)}{\Delta x_2}\right|_{x_1} \Delta x_2 \qquad (4.24a)$$

$$\Delta F_i(x_1,x_2) = \left.\frac{\Delta F_i(x_1,x_2)}{\Delta x_1}\right|_{x_2} \Delta x_1 + \left.\frac{\Delta F_i(x_1,x_2)}{\Delta x_2}\right|_{x_1} \Delta x_2 \qquad (4.24b)$$

If one applies (4.24) to the problem under consideration, it is seen that x_1 and x_2 are the eigenvalues and F is the determinantal value of (4.10). Let ζ_1 and ζ_2 be the eigenvalues that satisfy $F(\zeta_1,\zeta_2)=0$, and x_1 and x_2 be the first estimate for the eigenvalues such that $F(x_1,x_2) \neq 0$. Then the iteration scheme is performed in the following manner.

(a) Chosse the values of x_1 and x_2, perform the orthonormalization process and compute the determinantal values $F_{r1}(x_1,x_2)$ and $F_{i1}(x_1,x_2)$.

(b) Perturb x_1 and x_2 such that $x_{1p}=x_1(1+\varepsilon_1)$ and

$x_{2p}=x_2(1+\varepsilon_2)$, where ε_1 and ε_2 are small numbers. Compute $F_{r2}(x_{1p},x_2)$, $F_{i2}(x_{1p},x_2)$, $F_{r3}(x_1,x_{2p})$, and $F_{i3}(x_1,x_{2p})$.

Steps (a) and (b) provide three determinantal values corresponding to three sets of estimated eigenvalues in the vicinity of ζ_1 and ζ_2.

(c) Apply steps (a) and (b) to equation (4.24). Since the values of $F_r(x_1+\Delta x_1,x_2+\Delta x_2)$ and $F_i(x_1+\Delta x_1,x_2+\Delta x_2)$ at the new trial point are approximated to be zero, this yields

$$F_r = 0 = F_{r1} + \frac{F_{r2}-F_{r1}}{x_1\varepsilon_1}\Delta x_1 + \frac{F_{r3}-F_{r1}}{x_2\varepsilon_2}\Delta x_2 \qquad (4.25a)$$

$$F_i = 0 = F_{i1} + \frac{F_{i2}-F_{i1}}{x_1\varepsilon_1}\Delta x_1 + \frac{F_{i3}-F_{i1}}{x_2\varepsilon_2}\Delta x_2 \qquad (4.25b)$$

Solve equation (4.25) for Δx_1 and Δx_2.

(d) The new estimated values of x_1 and x_2 for step (a), i.e., x_{1n} and x_{2n}, are then given by

$$x_{1n} = x_1 + \Delta x_1 , \quad x_{2n} = x_2 + \Delta x_2$$

(e) Repeat the process until the determinantal values $F_r(\zeta_1,\zeta_2)$ and $F_i(\zeta_1,\zeta_2)$ are vanishingly small (within the set criterion). This gives the desired eigenvalues ζ_1 and ζ_2.

This iterative scheme requires three passes through the integration for each iteration. However, this disadvantage

is offset by the use of partial derivatives in the iteration, resulting in a more rapid convergence for the iteration.

6. Method to Obtain Eigenvalues

The eigenvalue problem is solved as follows. An estimate of the eigenvalues is first made. Equation (4.8a) is then integrated, using the initial condition (4.8b) at $r=r_1$, up to $r=r_2$ and the determinant (4.10) evaluated. If the determinant is equal to zero, then the chosen eigenvalues are the correct eigenvalues of the problem. The condition that the determinant (4.10) be equal to zero is the core of the iteration scheme for finding the eigenvalues of the original system (3.12) or (4.1) with the boundary conditions (3.28). Once the eigenvalues have been found, equation (4.9) may be used to determine a relationship between β_1 and β_2; one of the β's may be assigned an abritary value of, say, 1. This fixes the amplitude of the eigenfunction

$$y(r) = \beta_1 y^{(1)}(r) + \beta_2 y^{(2)}(r).$$

In summary, the procedure for solving the system (3.12) and (3.28) or (4.8) and (4.10) consists of the following steps:

a) Assign any two of the parameters α, R, c_r, and c_i; for example, assign α and c_i.

b) Choose an initial estimate for the eigenvalues, the two of the α, R, c_r, and c_i not selected in step a) that is, R and c_r.

c) Integrate the initial value problem consisting of

equations (4.8a) and (4.8b) from $r=r_1$ to $r=r_2$.

d) Compute the value of the determinant (4.10).

e) If the value of the determinant is not zero, adjust the initial estimate for the eigenvalues (R and c_r) systematically and repeat the process in steps c) and d). The differential correction iteration scheme is used to refine the estimate of the eigenvalues. This scheme was described in Section 5 of this chapter.

f) If the value of the determinant is zero, then the eigenvalue problem is solved. These eigenvalues R and c_r along with the assigned values of α and c_i are then used to compute the eigenfunction. This is done by choosing an arbitrary value of one of the β's, e.g., $\beta_{1r}=1$, and using (4.9c) to determine β_{1i}, β_{2r}, and β_{2i}. The eigenfunctions y(r) are then computed with (4.7a).

7. Generation of the Neutral Stability Curves

Mott (1966) has obtained the neutral stability results for the fully developed flow in annular ducts. In his work, Mott used the maximum velocity u^*_{max}, as the characteristic velocity. However, in the entrance region flow, the average velocity $\bar{u}^*$ was chosen as the characteristic velocity. This choice was made because the u^*_{max} depends on χ^*, while $\bar{u}^*$ contains no χ^*-dependent quantities. With the neutral stability results available for the fully developed flow ($\chi^*=\infty$), the eigenvalues at a smaller χ^* value can be

obtained by the iteration scheme, using those values at $\chi^*=\infty$ as the initial estimates.

Once a point on the stability curve at this smaller value is obtained, the neutral stability curve can be generated. This is done as follows. One can increase or decrease α, using R and c_r from that point as the initial estimates to find the new values of R and c_r for which $c_i=0$, and so on. This choice is usually done in the nose area (i.e. in the neighborhood of the critical point where R is a minimum). One can also find α and c_r for given values of R and $c_i=0$. This latter approach is quite efficient in mapping out the upper branch of the neutral curve, where the change in α with respect to R is slow. After the neutral curve for this smaller χ^* is obtained, the neutral curve for the next smaller χ^* is obtained by repeating the same process, and so on. The critical Reynolds numbers $(R)_c$ (that is, the minimum Reynolds number on the neutral curve) for each value of χ^* can be readily obtained by examining the neutral curves along the nose region.

For the tube flow, Huang (1973) has obtained a set of results of $(R)_c$ at various axial locations X* under the parallel flow assumption, that is, the results are from the solution of the conventional Orr-Sommerfeld equation. These results were used as the initial estimates of the eigenvalues in the stability calculations for the non-parallel tube flow using the modified Orr-Sommerfeld equation.

The neutral stability curves and the critical Reynolds numbers from both parallel and non-parallel flow assumptions for annular ducts and circular tubes are presented in Chapter V.

8. Eigenfunctions

Once the eigenvalues have been obtained with sufficient accuracy, the eigenfunctions can be obtained by the Gram-Schmidt orthonormalization process described in Section 3 of this chapter.

If $Q(r_i) = [Q^{(1)}(r_i), Q^{(2)}(r_i)]$ is a set of the two independent solutions of the initial value problem after the integration, then by the Gram-Schmidt process, it is related to the orthonormal set $Z(r_i)$ by

$$Z(r_i) = Q(r_i)P^{(i)} \tag{4.26}$$

where $P^{(i)}$ is a constant matrix given by (4.18a) and the two independent solutions $Q^{(1)}(r_i)$ and $Q^{(2)}(r_i)$ are given by (4.20b).

The eigenfunction $y(r_m)$ is obtained from

$$y(r_m) = \beta_1 Z^{(1)}(r_m) + \beta_2 Z^{(2)}(r_m) \tag{4.27a}$$

where $Z^{(1)}(r_m)$ and $Z^{(2)}(r_m)$ are given by (4.20a), and $r_m = r_2$, the outer radius, is the last point. In matrix form, this equation can be written as

$$y(r_m) = Z(r_m)\beta^{(m)} \tag{4.27b}$$

where $\beta^{(m)}$, the constant matrix (see equation (4.9a)), is to be found from

$$BZ(r_m)\beta^{(m)} = 0 \tag{4.27c}$$

in which B is given by (4.6e). Note that one of the β's is to be specified, for example, $\text{real}(\beta_1)=\beta_{1r}=1$. The superscript on $\beta^{(i)}$ indicates the matrix at the mesh point r_i.

The eigenfunction at the point next to the last point $r=r_m=r_2$ may be obtained by the backward substitution (Conte, 1966) as follows. Combining equations (4.27b) and (4.26) yields

$$y(r_m)=Z(r_m)\beta^{(m)}=Q(r_m)P^{(m)}\beta^{(m)}=Q(r_m)\beta^{(m-1)} \tag{4.28a}$$

where $\beta^{(m-1)}=P^{(m)}\beta^{(m)}$. Similarly, at the next point r_{m-1}, one obtains

$$y(r_{m-1})=Z(r_{m-1})\beta^{(m-1)}=Q(r_{m-1})\beta^{(m-2)} \tag{4.28b}$$

with $\beta^{(m-2)}=P^{(m-1)}\beta^{(m-1)}$, and so on.

In general,

$$y(r_j) = Q(r_j)\beta^{(j-1)} \quad ; \; j=m,m-1,\ldots,1 \tag{4.29a}$$

where

$$\beta^{(j-1)} = P^{(j)}\beta^{(j)} \quad ; \; j=m,m-1,\ldots,1 \tag{4.29b}$$

Thus, the entire procedure for finding the eigenfunction consists of two processes. First, a forward integration (Runge-Kutta integration) is performed during which $Q(r_j)$ is retained at each point and $P^{(j)}$ is retained at each point of orthonormalization. Second, a backward calculation is made, using (4.29) to calculate the constants $\beta^{(j)}$ and the eigenfunction $y(r)$.

The representative eigenfunctions for the developing flow in the annular ducts are presented in Chapter V.

C. The Finite Difference Method

This method was employed in the stability calculations for the parallel-plate channel. The method has proven accuracy and was conveniently available (Chen 1966).

In the finite difference method, the differential equation and the boundary conditions are transformed into a system of linear algebraic equations. The flow field is subdivided into N equal subintervals with (N+1) discrete points. The differential operator is then replaced by a suitable difference operator, e.g. the forward difference operator, the backward difference operator or the central difference operator. A further transformation is carried out to reduce the relatively large truncation error. The boundary conditions are included in the transformation. This gives a system of (N+1) algebraic equations. For a non-trivial solution to exist, an algebraic eigenvalue

problem with a secular equation in the form of (3.32), i.e., $f(R,\alpha,c_r,c_i)=0$, must be solved. An iteration scheme is then applied to determine the eigenvalues. The details of this method can be found, for example, in Chen (1966). Its highlights will be given here.

1. Formulation of the Finite Difference Equations

The expressions in equations (3.27a), (3.27b), and (3.27c) can be put in the form

$$\partial^2 U/\partial y^2 = \Lambda \tag{4.30a}$$

$$V = \Omega/R \tag{4.30b}$$

$$\partial^2 V/\partial y^2 = \Psi/R \tag{4.30c}$$

where

$$\Lambda = -3 - 2\sum_{j=1}^{\infty}\{\cos(\alpha_j y)/\cos(\alpha_j)\}\exp(-\alpha_j^2 X^*) \tag{4.31a}$$

$$\Omega = (2/\varepsilon)\sum_{j=1}^{\infty}\{\sin(\alpha_j y)/[\alpha_j\cos(\alpha_j)]\}\exp(-\alpha_j^2 X^*) \tag{4.31b}$$

$$\Psi = -(2/\varepsilon)\sum_{j=1}^{\infty}\{\alpha_j\sin(\alpha_j y)/\cos(\alpha_j)\}\exp(-\alpha_j^2 X^*) \tag{4.31c}$$

With equations (4.30) and (4.31), the modified Orr-Sommerfeld equation (3.26) can be written in the form

$$D^4\phi + A_1 D^3\phi + A_2 D^2\phi + A_3 D\phi + A_4\phi = 0 \tag{4.32a}$$

where

$$A_1 = -\Omega\ , \tag{4.32b}$$

$$A_2 = \alpha R(U-c)/i - 2\alpha^2 \ , \tag{4.32c}$$

$$A_3 = \alpha^2\Omega + \Psi = -\alpha^2 A_1 - A_1'' \ , \tag{4.32d}$$

$$A_4 = \alpha^4 - \alpha R[\alpha^2(U-c)+\Lambda]/i \tag{4.32e}$$

For a conventional Orr-Sommerfeld equation without the third derivative, the equation can be solved directly by using the transformation of Thomas (1953). This is because, without the third derivative, the truncation error is relatively small. However, the third derivative does appear in the modified Orr-Sommerfeld equation, and it must be removed first. Fu (1967) has introduced the transformation

$$\phi(y) = \theta(y) \exp\left[-\int_0^y (A_1/4)\, dy\right] \tag{4.33}$$

for changing the variable $\phi(y)$ to $\theta(y)$. With (4.33), equation (4.32a) is transformed into (Chen, Sparrow, and Tsou, 1971)

$$D^4\theta + B_1 D^2\theta + B_2 D\theta + B_3\theta = 0 \tag{4.34}$$

in which

$$B_1 = A_2 - 3A_1^2/8 - 3A_1'/2 \ , \tag{4.35a}$$

$$B_2 = A_3 - A_1 A_2/2 + A_1^3/8 - A_1'' \ , \tag{4.35b}$$

$$B_3 = A_4 - A_1 A_3/4 + A_1^2 A_2/16 - 3A_1^4/256 + 3A_1^2 A_1'/32 + 3(A_1')^2/16 - A_1'''/4 - A_1' A_2/4 \tag{4.35c}$$

and

$$A_1' = \partial A_1/\partial y = -(2/\varepsilon) \sum_{j=1}^{\infty} \{\cos(\alpha_j y)/\cos(\alpha_j) - 1\} \exp(-\alpha_j^2 X^*) \tag{4.36a}$$

$$A_1'' = \partial^2 A_1/\partial y^2 = (2/\varepsilon) \sum_{j=1}^{\infty} \alpha_j \{\sin(\alpha_j y)/\cos(\alpha_j)\} \exp(-\alpha_j^2 X^*) \tag{4.36b}$$

$$A_1''' = \partial^3 A_1/\partial y^3 = (2/\varepsilon) \sum_{j=1}^{\infty} \alpha_j^2 \{\cos(\alpha_j y)/\cos(\alpha_j)\} \exp(-\alpha_j^2 X^*) \tag{4.36c}$$

The boundary conditions (3.30a) and (3.30c), when expressed in terms of $\theta(y)$, become

$$\theta(1) = \theta'(1) = 0 \tag{4.37a}$$

$$\theta'(0) = \theta'''(0) = 0 \tag{4.37b}$$

Since equation (4.34) does not contain the third derivative, Thomas's transform can be employed to formulate the difference equations.

The matrix transformation for a function $g(y)$ and its derivatives in finite difference form with the order of accuracy to $\theta(\delta^3)$, is

$$\begin{Bmatrix} g \\ hDg \\ h^2D^2g \\ h^3D^3g \\ h^4D^4g \end{Bmatrix} = \begin{bmatrix} 1 & 0 & 0 & 0 & 0 \\ 0 & 1 & 0 & 0 & 0 \\ 0 & 0 & 1 & 0 & 0 \\ 0 & 0 & 0 & 1 & 0 \\ 0 & 0 & 0 & 0 & 1 \end{bmatrix} \begin{Bmatrix} g \\ \mu\delta g \\ \delta^2 g \\ \mu\delta^3 g \\ \delta^4 g \end{Bmatrix} + \begin{Bmatrix} 0 \\ O(\delta^3) \\ O(\delta^4) \\ O(\delta^5) \\ O(\delta^6) \end{Bmatrix} \tag{4.38a}$$

where

$$\begin{bmatrix} g \\ \mu\delta g \\ \delta^2 g \\ \mu\delta^3 g \\ \delta^4 g \end{bmatrix} = \begin{bmatrix} 0 & 0 & 1 & 0 & 0 \\ 0 & -1/2 & 0 & 1/2 & 0 \\ 0 & 1 & -2 & 1 & 0 \\ -1/2 & 1 & 0 & -1 & 1/2 \\ 1 & -4 & 6 & -4 & 1 \end{bmatrix} \begin{bmatrix} g(y-2h) \\ g(y-h) \\ g(y) \\ g(y+h) \\ g(y+2h) \end{bmatrix} \qquad (4.38b)$$

with δ and μ denoting the central difference operator and the average operator, respectively.

Thomas (1953) introduced the transformation

$$g(y) = [1-h^2D^2/6+h^4D^4/90]\theta(y) \qquad (4.39)$$

to relate $g(y)$ to $\theta(y)$. It can be shown from finite differences (Hildebrand, 1956) that

$$\begin{bmatrix} \theta \\ hD\theta \\ h^2D^2\theta \\ h^3D^3\theta \\ h^4D^4\theta \end{bmatrix} = \begin{bmatrix} 1 & 0 & 1/6 & 0 & 1/360 \\ 0 & 1 & 0 & 0 & 0 \\ 0 & 0 & 1 & 0 & 1/12 \\ 0 & 0 & 0 & 1 & 0 \\ 0 & 0 & 0 & 0 & 1 \end{bmatrix} \begin{bmatrix} g \\ \mu\delta g \\ \delta^2 g \\ \mu\delta^3 g \\ \delta^4 g \end{bmatrix} + \begin{bmatrix} O(h^8) \\ O(h^5) \\ O(h^8) \\ O(h^5) \\ O(h^8) \end{bmatrix} \qquad (4.40)$$

Substituting (4.38b) into (4.40) yields

$$\begin{bmatrix} \theta \\ hD\theta \\ h^2D^2\theta \\ h^3D^3\theta \\ h^4D^4\theta \end{bmatrix} = \begin{bmatrix} 1/360 & 7/45 & 41/60 & 7/45 & 1/360 \\ 0 & -1/2 & 0 & 1/2 & 0 \\ 1/12 & 2/3 & -3/2 & 2/3 & 1/12 \\ -1/2 & 1 & 0 & -1 & 1/2 \\ 1 & -4 & 6 & -4 & 1 \end{bmatrix} \begin{bmatrix} g(y-2h) \\ g(y-h) \\ g(y) \\ g(y+h) \\ g(y+2h) \end{bmatrix} + \begin{bmatrix} O(h^8) \\ O(h^5) \\ O(h^8) \\ O(h^5) \\ O(h^8) \end{bmatrix}$$

(4.41)

Thus, it is seen that the values of $\theta(y)$ and its derivatives at a point are related to the values of $g(y-2h)$, $g(y-h)$, $g(y)$, $g(y+h)$, and $g(y+2h)$ at five discrete points.

2. Formulation of the Algebraic Equations

Equation (4.34) can be expressed in matrix form as

$$[M]\{g\} = (D^4+B_1D^2+B_2D+B_3)\theta = 0 \tag{4.42}$$

Substituting (4.41) into (4.42) gives

$$[M]\{g\} = a_1g(y-2h)+a_2g(y-h)+a_3g(y)+a_4g(y+h)+a_1g(y+2h) \tag{4.43}$$

where

$$\begin{aligned} h^2a_1 &= 1/h^2+B_1/12+B_2h^2/360 \\ h^2a_2 &= -4/h^2+2B_1/3-B_2h/2+7B_3h^2/45 \\ h^2a_3 &= 6/h^2-3B_1/2+41B_3h^2/60 \\ h^2a_4 &= -4/h^2+2B_1/3+B_2h/2+7B_3h^2/45 \end{aligned} \tag{4.44}$$

The independent variable y takes on the values 0, h, 2h,..., (N-1)h, and Nh=1.

In order to evaluate the quantities on the right-hand side of (4.43) at the boundaries y=0 (centerline) and y=1 (upper wall), it is necessary to know the values of g at two points which are outside of each of the boundaries; i.e., $g(-h)$, $g(-2h)$ and $g((N+1)h)$, $g((N+2)h)$. These values are

obtained by applying the boundary cinditions in conjunction with (4.41). Application of (4.37b) gives

$$g(-h) = g(h) \tag{4.45a}$$

$$g(-2h) = g(2h) \tag{4.45b}$$

and the use of (4.37a) yields

$$g((N+1)h) = g((N-1)h) \tag{4.46a}$$

$$g((N+2)h) = -g((N-2)h) - 112g((N-1)h) - 246g(Nh) \tag{4.46b}$$

Equations (4.43), (4.45a), (4.45b), (4.46a), and (4.46b) provide complete information for writing (N+1) simultaneous, complex, algebraic equations given by the relation

$$\left[M(R,\alpha,c)\right]\{g\} = 0 \tag{4.47}$$

Since these equations are linear and homogenous, there exists a non-trivial solution if and only if the determinant of the coefficient matrix is zero, that is,

$$\mathrm{Det}\left[M(R,\alpha,c)\right] = 0 \tag{4.48}$$

The eigenvalue problem is now reduced to the solution of the determinantal equation (4.48), which consists of finding the eigenvalues (any two of the four variables R, α, c_r , c_i) for given values of the two parameters (the two of R, α, c_r , c_i not selected as eigenvalues). When the elements of the coefficient matrix $[M]$ are written out, it is of form

$$(M) = \begin{Bmatrix} a_3 & a_2+a_4 & 2a_1 & & & & & \\ a_2 & a_1+a_3 & a_4 & a_1 & & & & \\ a_1 & a_2 & a_3 & a_4 & a_1 & & 0 & \\ & \cdot & \cdot & \cdot & \cdot & \cdot & & \\ & & \cdot & \cdot & \cdot & \cdot & \cdot & \\ & 0 & & a_1 & a_2 & a_3 & a_4 & a_1 \\ & & & & a_1 & a_2 & a_1+a_3 & a_4 \\ & & & & & 0 & (a_4+a_2-112a_1) & (a_3-246a_1) \end{Bmatrix}$$

(4.49)

In computing the neutral stability results for non-parallel flow in the parallel-plate channel, the initial estimates of the eigenvalues were taken from the results of Chen (1966) for the parallel flow assumption. With the use of the differential correction iteration scheme described in the previous Section B, the eigenvalues can be determined. The relationship between the critical Reynolds number $(R)_c$ and the axial location X was obtained in a manner similar to that previously discussed in the annular duct flow. In order to compare the results from the parallel flow and non-parallel flow models under the same conditions, the number of steps used for each of the X* values was the same as that used by Chen. These two sets of results will be compared in the next chapter.

D. Effect of Step Size on Eigenvalues

In order to obtain accurate numerical results, the effect of the step size on the accuracy of the eigenvalues needs to be considered. Strictly speaking, the exact values of the eigenvalues are obtainable only when the number of steps N is increased to infinity. This is not feasible in any numerical procedure. However, one chooses the number of steps large enough to achieve accuracies that are sufficient for practical purpose.

The effect of the step size on the accuracy of the eigenvalues was checked for the numerical solution as applied to the annular duct flow. The accuracies of the eigenvalues for the tube and channel flows were checked, respectively, by Huang (1973) and Chen (1966). In Table 3 are shown the representative variations of the eigenvalues (c_r,R) or (c_r,c_i) for given values of $(\alpha,c_i=0)$ or (α,R) with the number of steps used in the stability calculations. The results are for annular duct flow with $K=r_2^*/r_1^*=2.0$ and 3.33 at axial locations $\chi^*=0.008$, 0.004, 0.0015, 0.001 and 0.0025, respectively. It can be seen from the table that as the number of steps is increased, the eigenvalues converge to certain limiting values. To maintain the accuracy of the numerical results, as χ^* decreases, it was found that for a given K value, the number of steps must be increased (i.e., the step size must be decreased). The actual number of steps used in the stability calculations for annular duct flow at different axial locations are listed in Table 4.

Table 3

The Effect of Number of Steps on the Accuracy of Eigenvalues, Annular Duct Flow

K	χ*	N	α	R	c_r	c_i
2.0	0.008	100	0.95	11169	0.301944	0
2.0	0.008	150	0.95	11249	0.301779	0
2.0	0.008	200	0.95	11259	0.301769	0
2.0	0.004	100	1.218513	20000	0.285351	0
2.0	0.004	150	1.205245	20000	0.285922	0
2.0	0.004	200	1.203887	20000	0.286045	0
2.0	0.0015	100	0.95	42877	0.218792	0
2.0	0.0015	150	0.95	44865	0.217953	0
2.0	0.0015	200	0.95	45227	0.217858	0
2.0	0.001	100	1.685	19324	0.299829	0
2.0	0.001	150	1.685	21893	0.295085	0
2.0	0.001	200	1.685	22396	0.294353	0
2.0	0.001	300	1.685	22550	0.294171	0
2.0	0.001	100	1.685	22550	0.290707	0.2761D-2
2.0	0.001	200	1.685	22550	0.293986	0.9127D-4
2.0	0.001	300	1.685	22550	0.294171	0.1032D-6
3.33	0.0025	200	1.560	42780	0.241254	0
3.33	0.0025	250	1.560	43466	0.240764	0
3.33	0.0025	300	1.560	43681	0.240626	0

*D-x = 10^{-x}

Table 4

Number of Steps Used in the Calculations at Various Axial Locations, Annular Duct Flow

K	χ*	N	K	χ*	N
2.0	∞	100	3.33	∞	150
2.0	0.016	150	3.33	0.016	150
2.0	0.008	150	3.33	0.008	200
2.0	0.004	150	3.33	0.004	250
2.0	0.003	150	3.33	0.0025	300
2.0	0.002	200			
2.0	0.0015	200			
2.0	0.001	200			

V. NEUTRAL STABILITY RESULTS AND DISCUSSION

The stability problems of the axisymmetric or two-dimensional disturbances for the duct flows were formulated in Chapter III and their numerical methods of solutions were presented in Chapter IV. In this chapter, representative neutral stability results from the solutions of the modified and conventional Orr-Sommerfeld systems are presented for the following three flow configurations.

(1) Developing laminar flow in the entrance region of annular ducts.

(2) Developing laminar flow in the entrance region of a circular tube.

(3) Developing laminar flow in the entrance region of a parallel-plate channel.

The stability results include neutral stability curves, axial variation of the critical Reynolds number, and representative eigenfunctions. Some results for the fully developed flow in annular duct flow and parallel-plate channel flow are also included. Finally, comparisons between the results from the modified and the conventional Orr-Sommerfeld equations are made for each of the three flow problems. The numerical results are tabulated in Appendices C, D, and E. All the numerical results were obtained with an IBM 360/50 digital computer.

A. Annular Duct Flow

1. Neutral Stability Curves

The neutral stability results for annular duct flow are tabulated in Tables C-1 through C-9, Appendix C, for χ^* ranging from 0.001 to ∞. In the tables, the wave number α is based on the characteristic length $L_c^*=(K-1)r_2^*/2K$, and the Reynolds number R is based on L_c^* and the average velocity $\bar{u}^*$. Also included in the tables are the dimensionless velocity of wave propagation c_r and the number of steps N used in the stability calculations.

The representative neutral stability curves from the solutions of the modified and conventional Orr-Sommerfeld equations with radius ratio of K=2.0 are shown in Figure 1 for three axial locations (in terms of the dimensionless stretched axial coordinate) at χ^*=0.0015, 0.0040, and ∞. The curve for $\chi^*=\infty$ represents the results for the fully developed flow. Those representative neutral stability curves for K=3.33 are shown in Figure 2 for three values of χ^*=0.0025, 0.008, and ∞. The solid and dashed lines in the figures represent, respectively, the results from the modified and conventional Orr-Sommerfeld equations.

It is seen from Figures 1 and 2 that the neutral stability curves shift to the left as χ^* increases; that is, the flow becomes more unstable as the axial distance increases from the duct inlet. In addition, the curves

obtained from the modified Orr-Sommerfeld equation are seen to lie slightly to the left of those obtained from the conventional Orr-Sommerfeld equation for K=2.0, Figure 1. That is, the modified Orr-Sommerfeld equation predicts critical Reynolds numbers which are somewhat lower for all locations of the stretched axial coordinate examined. However, for the case of K=3.33, Figure 2, the results for the modified Orr-Sommerfeld equation lie slightly to the right of those obtained from the conventional Orr-Sommerfeld equation, indicating that the critical Reynolds numbers are somewhat higher for all axial locations examined. Thus, inclusion of the transverse velocity component in the mainflow changes the stability characteristics of the flow to a certain extent. Its effect is most pronounced in the region near the nose of the neutral stability curves.

In Figure 3, the neutral stability curves from the modified Orr-Sommerfeld equation for both K=2.0 and K=3.33 at three locations are brought together. It is seen from the figure that the group of curves for the radius ratio K=3.33 lie to the right of those for K=2.0, indicating that the flow is more unstable for K=2.0 than for K=3.33. This fact applies to flow both in the entrance region and in the fully developed flow region.

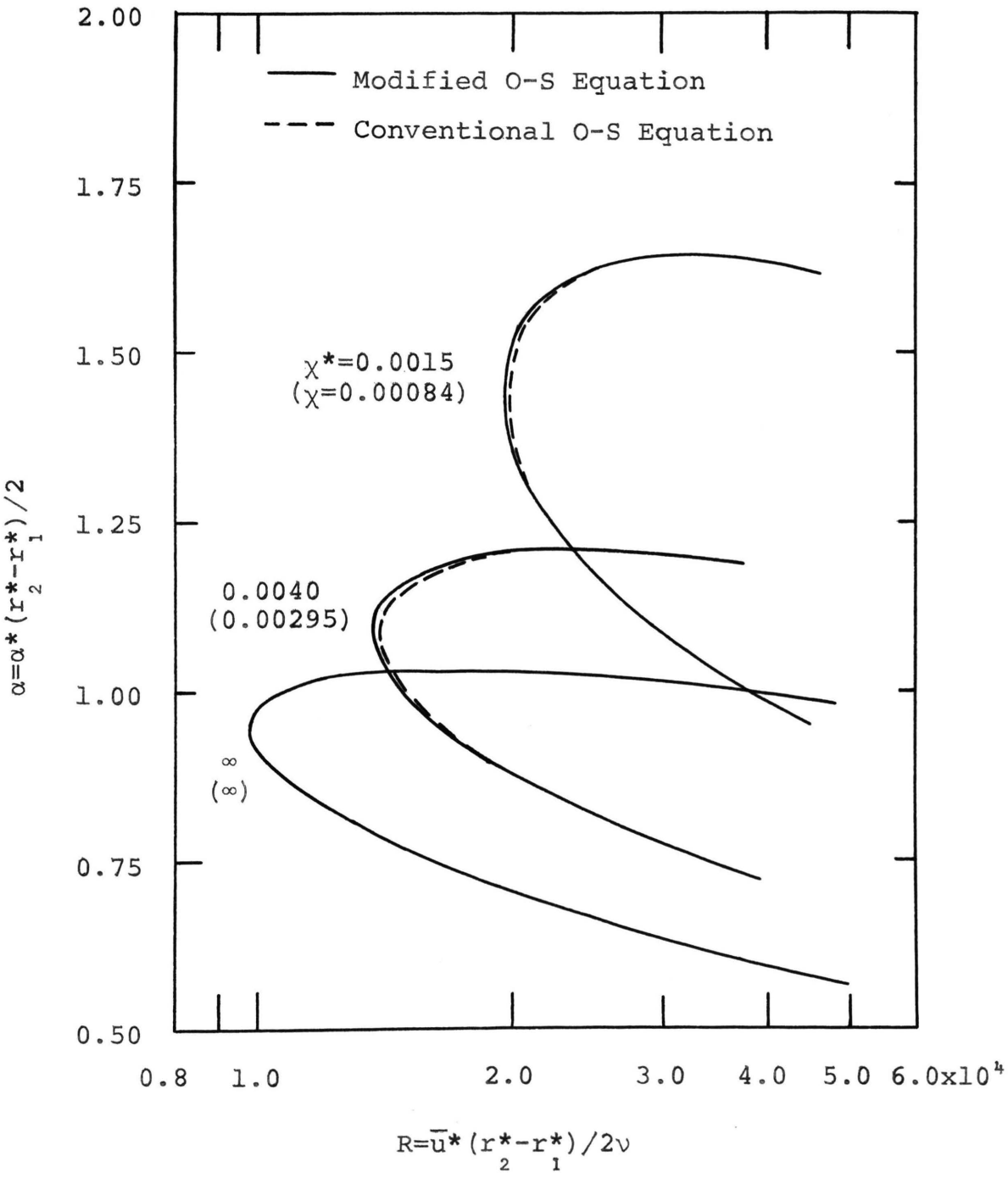

Figure 1. Representative Neutral Stability Curves for Annular Duct Flow, K=2.0.

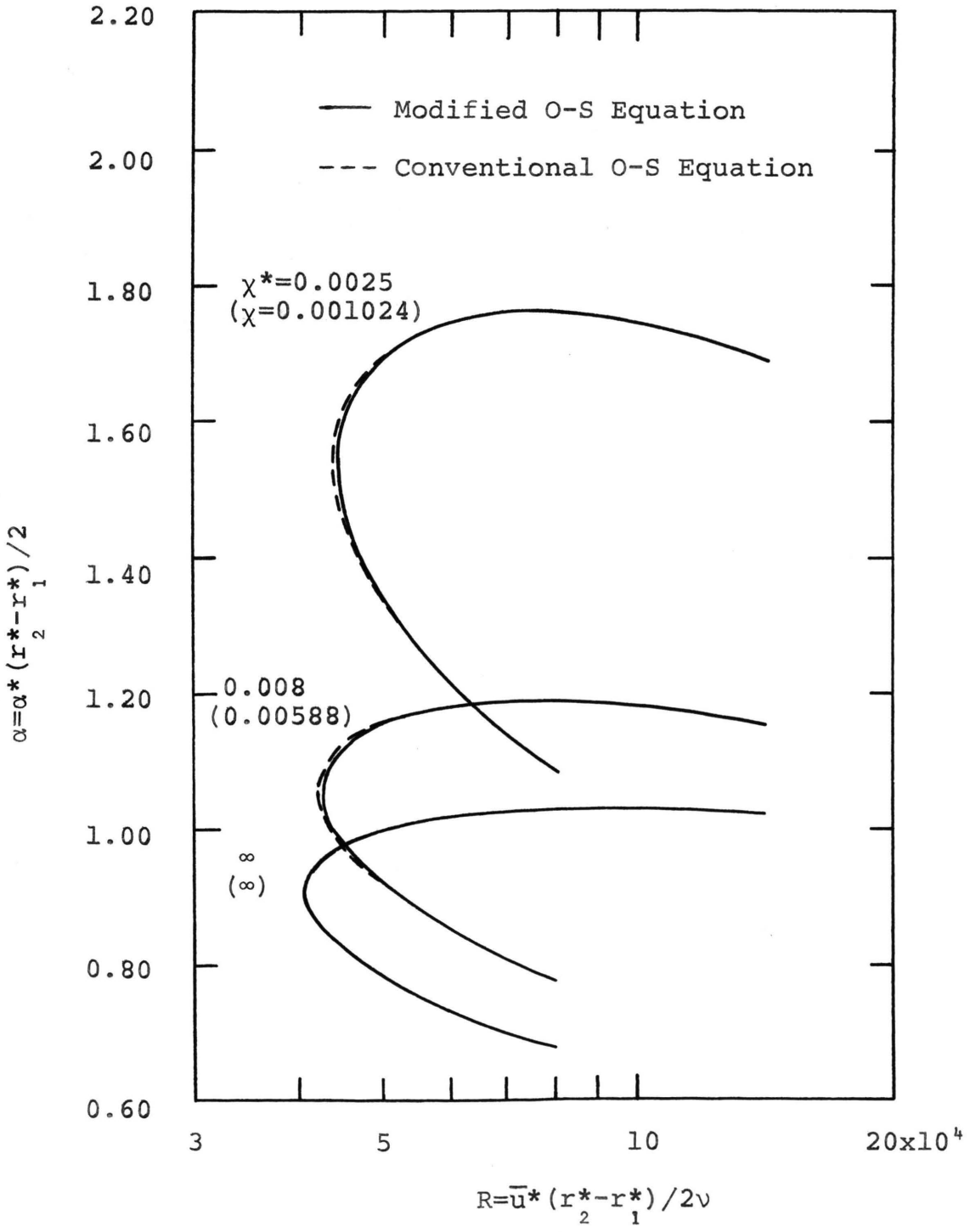

Figure 2. Representative Neutral Stability Curves for Annular Duct Flow, K=3.33.

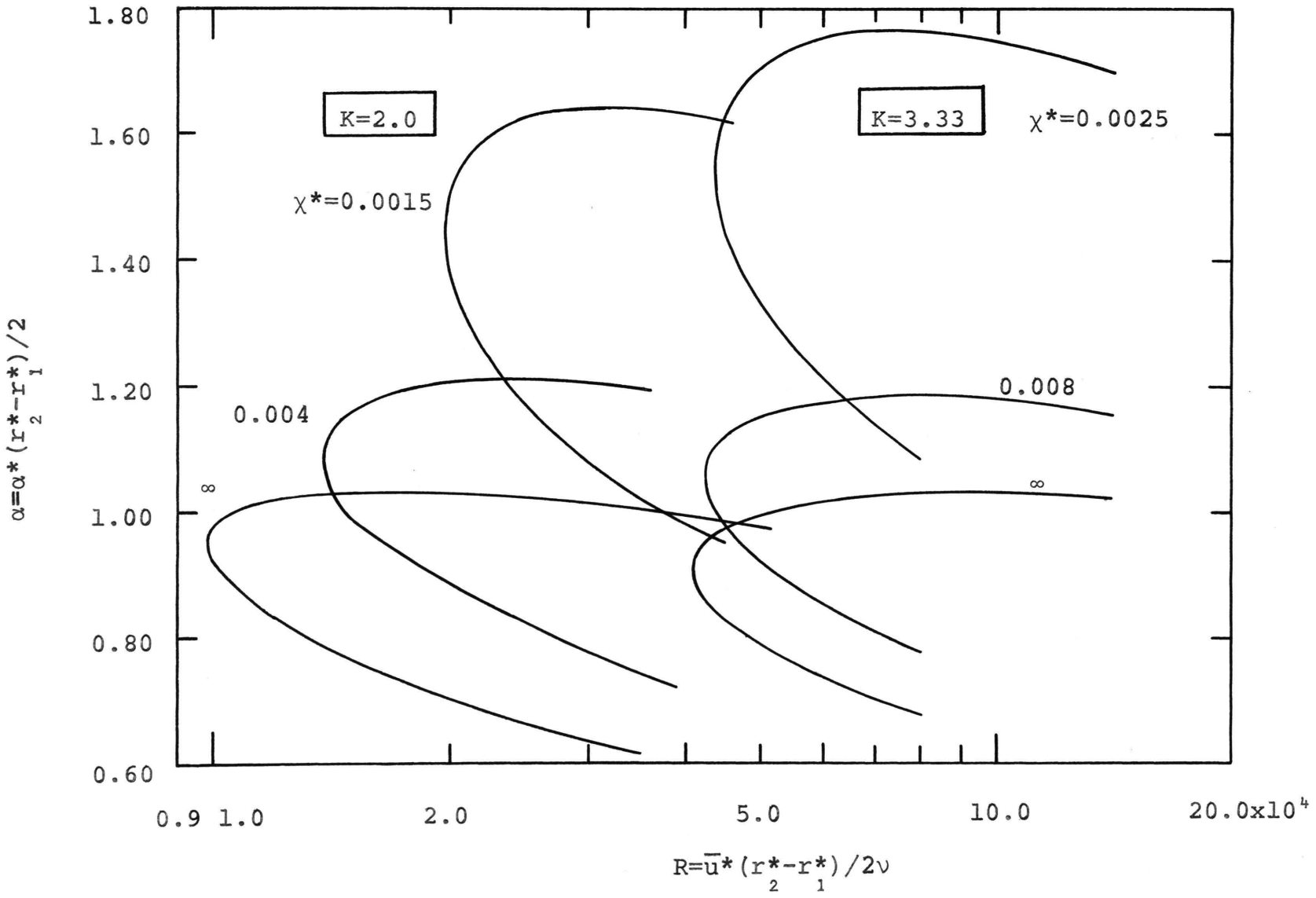

Figure 3. A Comparison of the Neutral Stability Curves Between K=2.0 and K=3.33 for Annular Duct Flow, Modified Orr-Sommerfeld Equation.

2. Axial Variation of Stability Characteristics

The neutral stability results at the critical point, $(\alpha)_c$, $(R)_c$, and $(c_r)_c$, for both the modified and conventional Orr-Sommerfeld equations are tabulated in Table C-10, Appendix C, for K=2.0 at axial locations χ^*=0.0010, 0.0015, 0.002, 0.003, 0.004, 0.008, 0.016, and ∞, for K=3.33 at χ^*=0.0025, 0.004, 0.008, 0.016, and ∞. These results are illustrated in Figure 4, in which the dimensionless physical axial coordinate X has been used as the abscissa. The coordinates X and X* are respectively related to χ and χ^* by the relations

$$X = \frac{x^*/\{(r_2^*-r_1^*)/2\}}{\bar{u}^*(r_2^*-r_1^*)/2\nu} = \{2K/(K-1)\}^2\chi$$

$$X^* = \frac{\xi^*/\{(r_2^*-r_1^*)/2\}}{\bar{u}^*(r_2^*-r_1^*)/2\nu} = \{2K/(K-1)\}^2\chi^*$$

The solid and dashed lines represent the results from the modified and conventional Orr-Sommerfeld equations, respectively. The curves for K=1.0 correspond to flow in a parallel-plate channel. This will be discussed later.

An inspection of Figure 4 reveals that the critical Reynolds numbers $(R)_c$ for K=3.33 are much higher than those for K=2.0 in the entire region of the annular duct. In addition, the critical Reynolds number for K=2.0 decreases

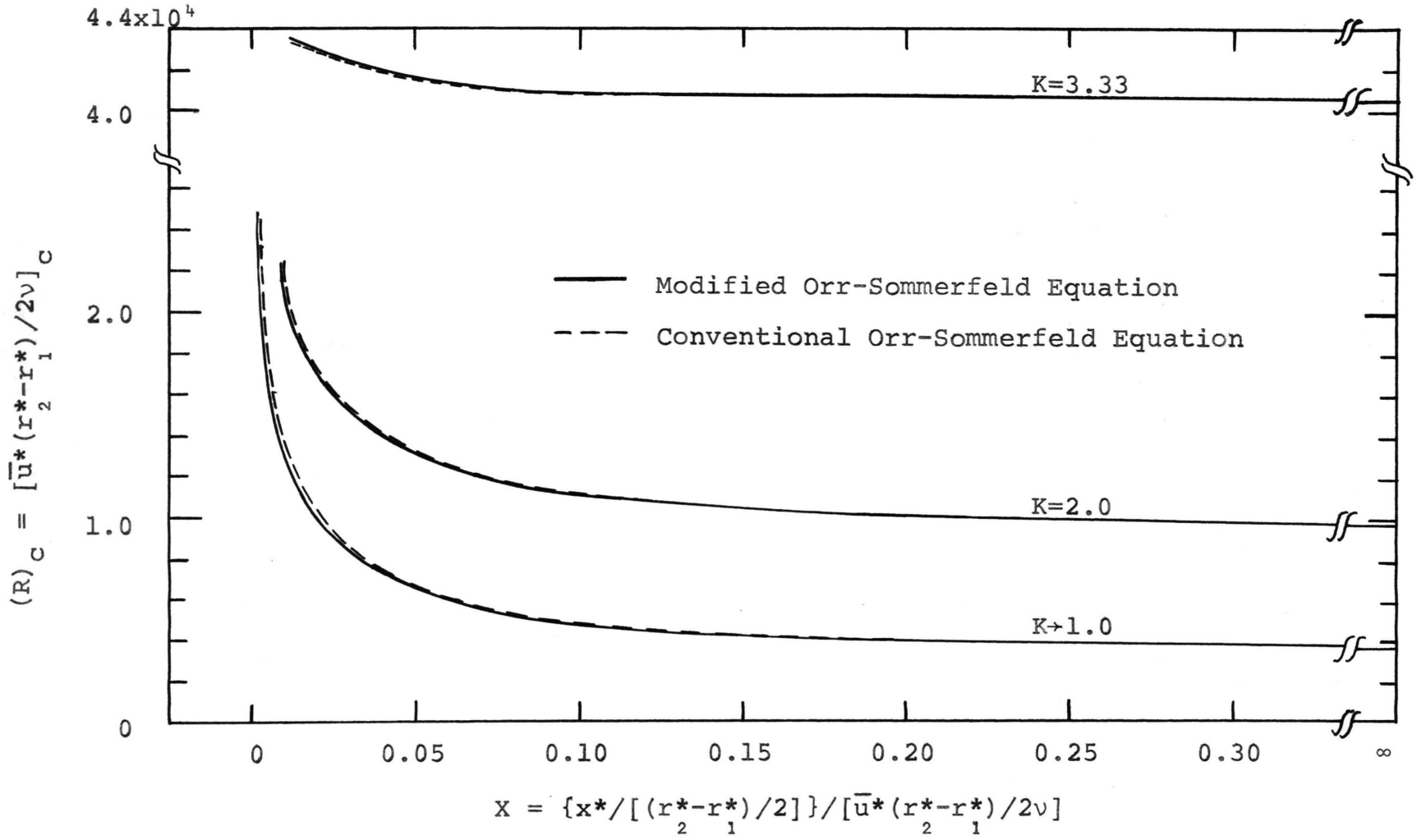

Figure 4. Axial Variation of the Critical Reynolds Number for Annular Duct Flow.

much more rapidly than for K=3.33 in the range of small X values increases. That is, the lower the value of the ratio of outer radius to inner radius, the more rapid the Reynolds number decreases in the region near the duct entrance (for example, in the region between X=0 and X=0.10). It can also be noted from the figure that the differences between the critical Reynolds numbers from solutions of the modified and conventional Orr-Sommerfeld equations are very small. At a fixed axial location, this difference is negative for K=2.0; that is, the critical Reynolds number from the modified Orr-Sommerfeld equation is less than that from the conventional Orr-Sommerfeld equation. The reverse is true for the case of K=3.33.

3. The Eigenfunctions

In Chapter IV, the technique used in obtaining the eigenfunctions was discussed. Representative numerical results of the eigenfunctions for annular duct flow are presented in this section.

The eigenfunction ϕ and its first derivative with respect to r, ϕ', for K=2.0 at the axial location $\chi^*=0.008$ ($\chi=0.00786$) with $\alpha=0.9744$, R=11137, $c_r=0.30545$, $c_i=0$, and for K=3.33 at the axial location $\chi^*=0.008$ ($\chi=0.00589$) with $\alpha=1.057$, R=42223, $c_r=0.22200$, $c_i=0$ are plotted in Figure 5 and Figure 6, respectively. These results are from the modified Orr-Sommerfeld equation and are shown as solid lines. The eigenfunctions were computed by assigning the

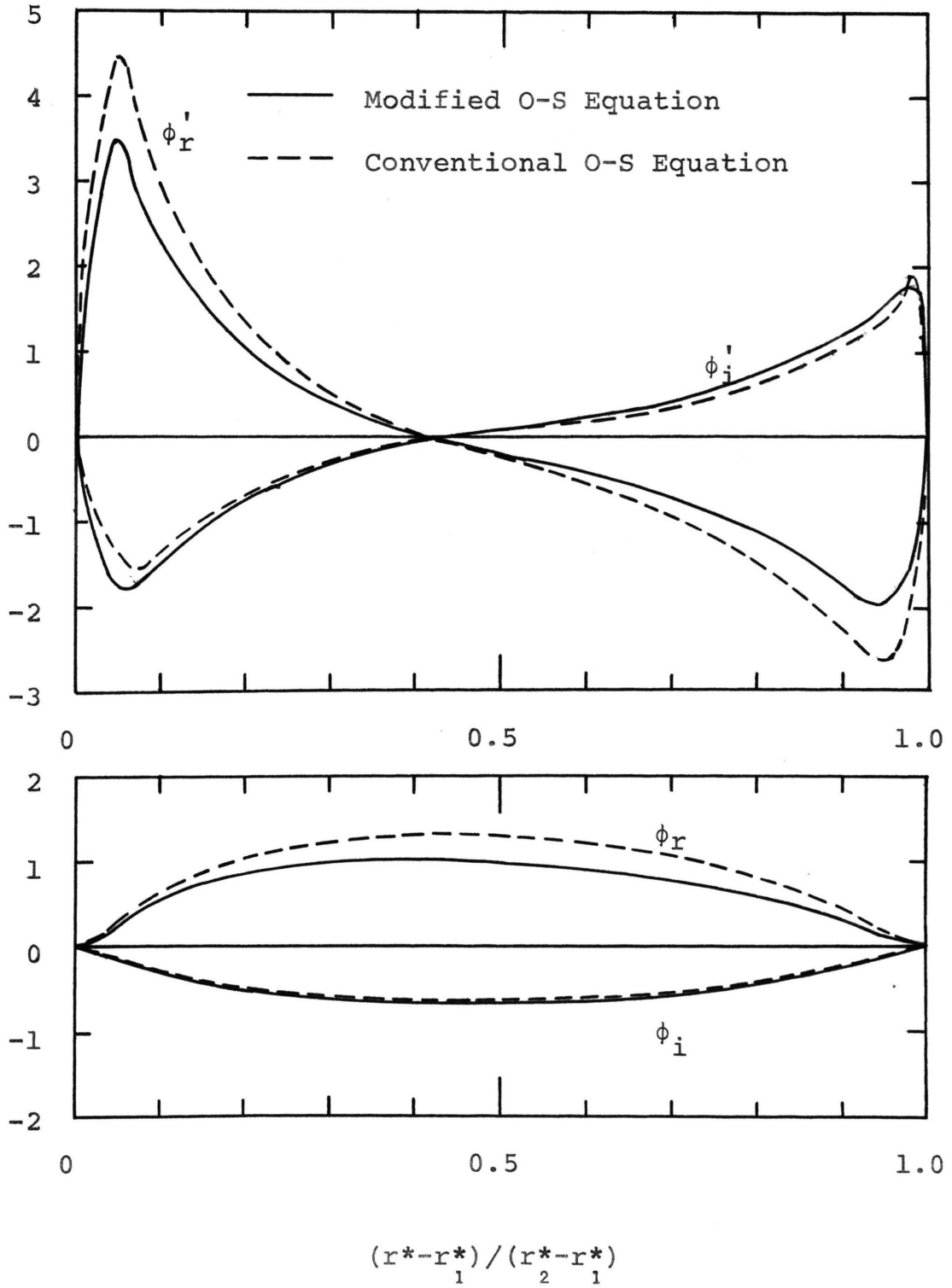

Figure 5. Representative Eigenfunctions for Annular Duct Flow, $\chi^*=0.008$, K=2.0.

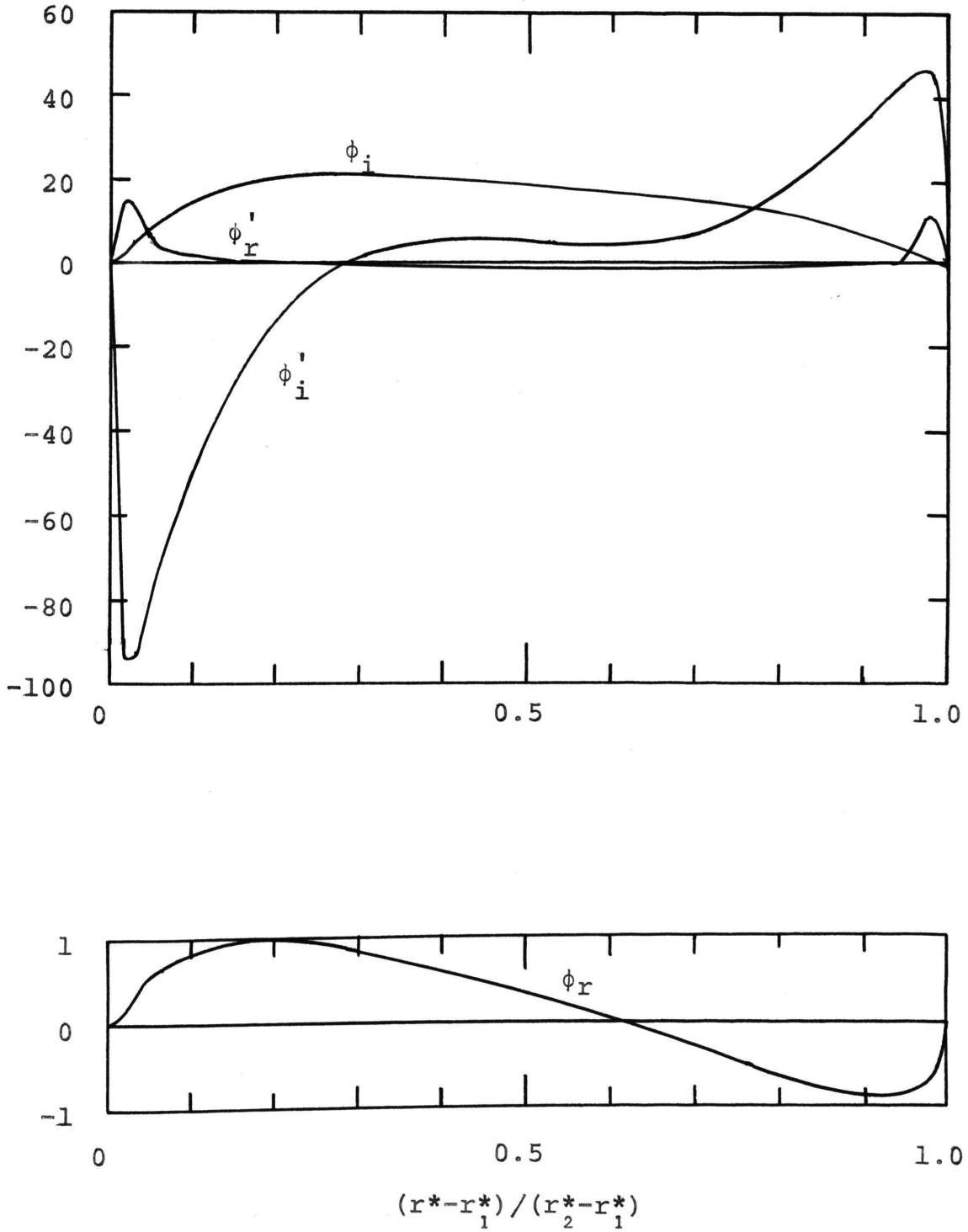

Figure 6. Representative Eigenfunctions for Annular Duct Flow, $\chi^*=0.008$, K=3.33.

real part of the coefficient β_1 in equation (4.7a) the normalizing value of 1.0 and calculating the imaginary part of β_1 and the real and imaginary parts of β_2, such that the boundary conditions, equation (3.28), at the inner wall and outer wall of the annular duct are satisfied.

The eigenfunctions from the solution of the conventional Orr-Sommerfeld equation were also computed. They correspond to α=0.9745, R=11134, c_r=0.30551, and c_i=0 for K=2.0 and α=1.0540, R=42189, c_r=0.22187, and c_i=0 for K=3.33. The curves for K=2.0 are shown in Figure 5 as dashed lines. It can be seen from the figure that there is only a slight change in magnitude between the two sets of results. The results from the conventional equation are essentially identical to those from the modified equation and are, therefore, not included in Figure 6.

It is to be noted that the results shown in Figures 5 and 6 are normalized by the maximum value of ϕ_r, the real part of ϕ.

B. Circular Tube Flow

The neutral stability results for the tube flow at various axial locations are tabulated in Tables D-1 and D-2, Appendix D. In the tables, the wave number α is based on the radius of the tube r_0^* and the Reynolds number R is based on r_0^* and the average velocity $\bar{u}^*$. Also included in the tables are the dimensionless velocity of wave propagation c_r and the number of steps N used in the stability calculations.

The neutral stability curves are shown in Figure 7 for three axial locations X*=0.003, 0.006, and 0.010 for both the modified and conventional Orr-Sommerfeld equations. It is to be noted that the dimensionless stretched axial coordinate X* is defined as $(\xi^*/r_0^*)/(\bar{u}^* r_0^*/\nu)$. Since there is no instability for the fully developed tube flow, there is no neutral curve for X*=∞. The curves with the solid lines are the results obtained from the modified Orr-Sommerfeld equation and those with the dashed lines are the results from the conventional Orr-Sommerfeld equation. The latter results are taken from Huang (1973) and are included in the figure for comparisons.

It is seen from Figure 7 that the neutral curves obtained from the modified Orr-Sommerfeld equation cross and lie slightly to the left of those from the conventional Orr-Sommerfeld equation. That is, the modified Orr-Sommerfeld equation yields critical Reynolds numbers that are somewhat lower. Thus, the effect of the mainflow transverse velocity, as accounted for in the modified equation, causes a shift in the neutral curves toward a larger wave number. The largest deviation occurs in the upper branch of the neutral curves.

The critical Reynolds numbers $(R)_c$ at various axial locations X*=0.002, 0.003, 0.005, 0.006, 0.007, 0.009, and 0.010 are tabulated in Table D-3, Appendix D. The results from the conventional Orr-Sommerfeld equation are from Huang

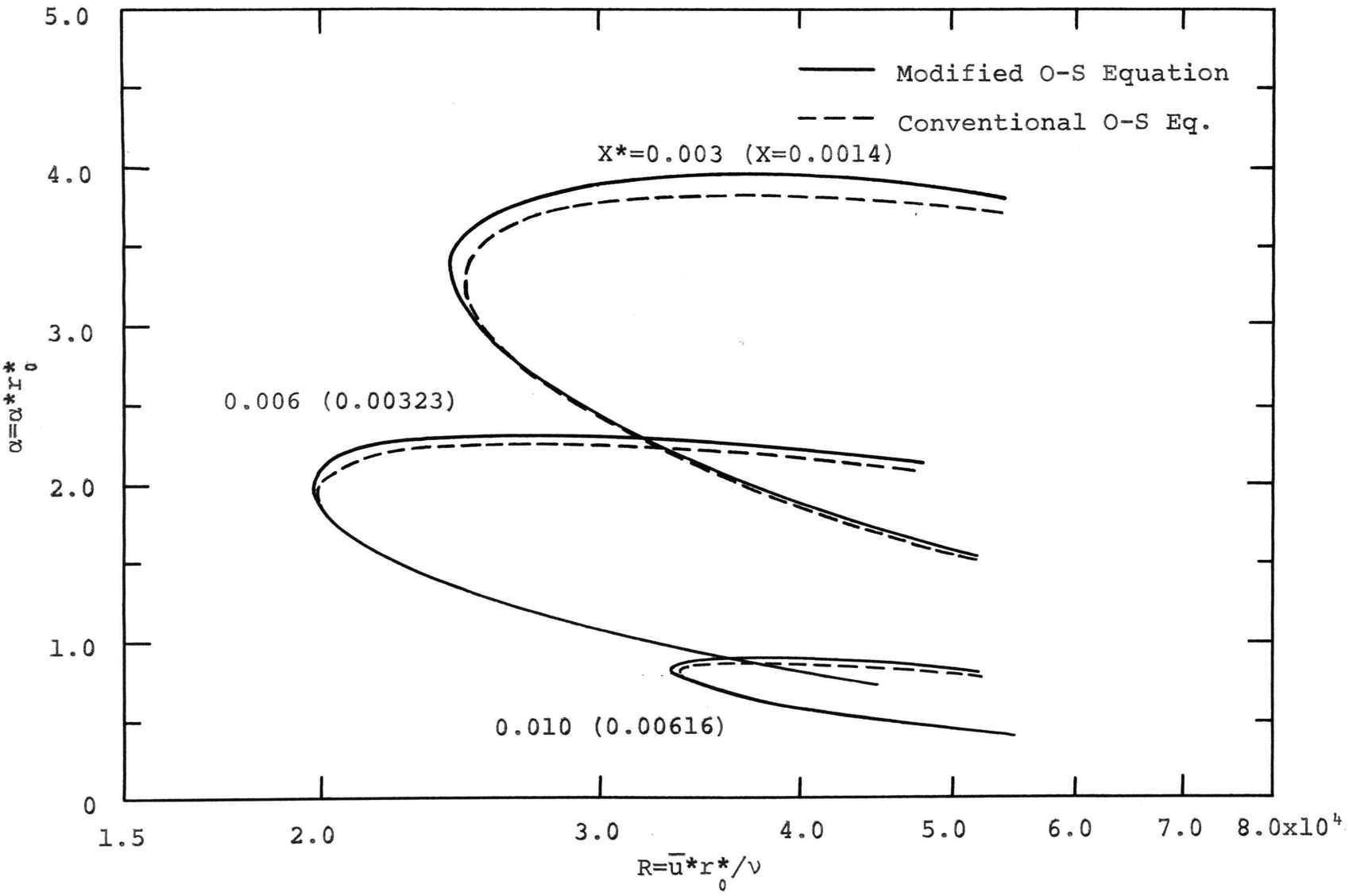

Figure 7. Representative Neutral Stability Curves for Circular Tube Flow.

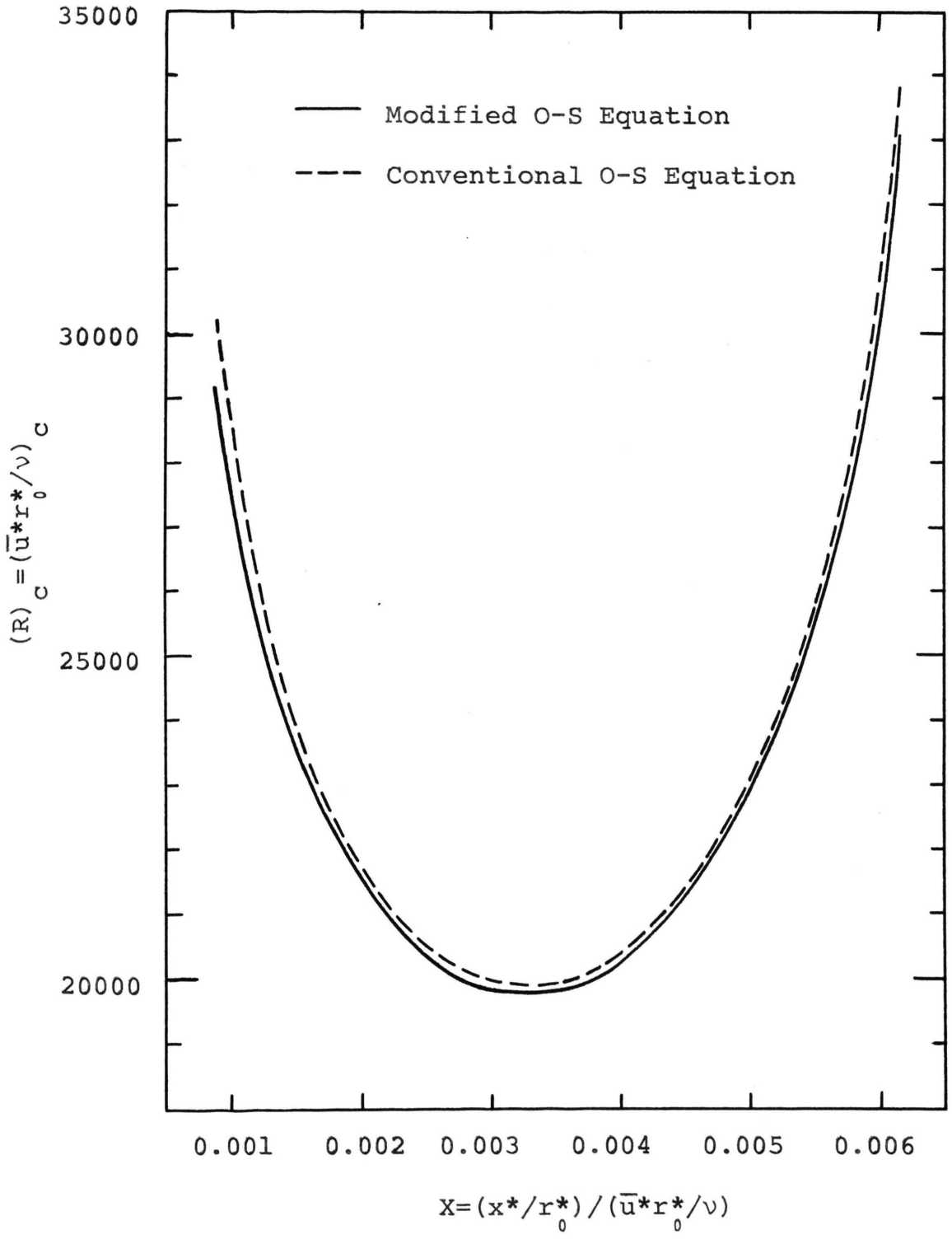

Figure 8. Axial Variation of the Critical Reynolds Number for Circular Tube Flow.

(1973). A comparison of the axial variation of the critical Reynolds number $(R)_c$ among the three sets of results is also made in Figure 8. In the abscissa of the figure, the dimensionless physical axial coordinate X is used. The solid and dashed lines represent results from the modified and conventional Orr-Sommerfeld equations, respectively.

An inspection of Figure 8 reveals that the critical Reynolds number decreases as X increases from the inlet and then increases as X increases further. It is also evident from the figure that the modified Orr-Sommerfeld equation gives critical Reynolds numbers that are smaller in the entire region of the tube. The minimum critical Reynolds numbers occur at X=0.00323 and are $(R)_c$=19780 and 19900, respectively, from the modified and conventional equations.

C. Parallel-Plate Channel Flow

The neutral stability results for the channel flow as computed from the modified Orr-Sommerfeld equation are tabulated in Table E-1, Appendix E for axial locations 0.005, 0.006, 0.008, 0.0100, 0.015, 0.02, 0.03, 0.04, 0.06, 0.08, 0.10, 0.15, 0.20, 0.30, and ∞. In the table, the wave number α is based on the half-spacing of the channel L* and the Reynolds number is based on L* and the average velocity $\bar{u}^*$. The critical stability results for the same range of X*

values are tabulated in Table E-2, Appendix E. Table E-2 includes results from solutions of the modified and conventional Orr-Sommerfeld equations. The results from the conventional equation are taken from Chen (1966).

The curves for $K \to 1.0$ in Figure 4 illustrate the variation of the critical Reynolds number $(R)_c$ with axial location X for the channel flow. It is to be noted that the characteristic length L^* for the channels is equivalent to $(r_2^* - r_1^*)/2$ for the annular ducts. Thus, the coordinates R and X in Figure 4 apply to the channel flow as well. An inspection of the curves for the parallel-plate channel flow, i.e., the curves for $K \to 1.0$, shows, as in the annular duct flow with K=2.0 and K=3.33, that there is a small difference in the critical Reynolds numbers between the two sets of results from the modified and conventional stability equations. The inclusion of the mainflow transverse velocity results in a somewhat lower critical Reynolds number.

VI. CONCLUSIONS

The present investigation deals with the linear stability of non-parallel, developing laminar flow in the entrance region of ducts. The problems covered include flow in annular ducts, circular tubes, and parallel-plate channels. The mainflow velocity fields employed in the stability analyses correspond to those obtained from the solution of the linearized momentum equations. Axisymmetric disturbances for annular duct and tube flows and two-dimensional disturbances for channel flow are considered in the analysis. By using the linear perturbation theory of hydrodynamic stability and taking into account the non-parallelism of the mainflow, the modified Orr-Sommerfeld equations for tube and channel flows were derived. The governing disturbance equation and the corresponding boundary conditions for each of the flow configurations constitute an eigenvalue problem.

The eigenvalue problems for flow in annular ducts and circular tubes were solved by a direct numerical, fourth order Runge-Kutta integration scheme along with an iteration technique. An orthonormalization process was used to remove the "parasitic error" which arises during the numerical integration of the disturbance equation. The differential correction method was used as the iteration scheme to find the eigenvalues. For the parallel-plate channels, the

eigenvalue problem was solved by a finite difference method, using an existing computer program.

In the stability calculations for flow in annular ducts, circular tubes, and parallel-plate channels, the mainflow was considered to be both parallel and non-parallel. That is, both the conventional and modified Orr-Sommerfeld equations were used in the analyses. For the developing annular duct flow, the neutral stability curves at various axial locations, the axial variation of the critical Reynolds number, and the eigenfunctions were obtained and presented for both the parallel and non-parallel flow models. For flow in the entrance region of circular tubes, neutral stability characteristics for the non-parallel flow model were examined. Representative neutral stability curves and axial variation of the critical Reynolds number were presented and compared with those based on the parallel flow model. The neutral stability results and axial variation of the critical Reynolds number for the developing channel flow were obtained from the non-parallel flow model and compared with those obtained from the parallel flow model.

From the present investigation, the following conclusions are drawn.

For annular duct flow, it is found that:

(1) The developing flow in the entrance region is unstable to axisymmetric small disturbances.

(2) The flow becomes more stable as the ratio of outer

radius to inner radius, K, increases. In addition, the critical Reynolds number decreases less rapidly in the region adjacent to the inlet as K increases.

(3) The critical Reynolds number (based on the characteristic length $L_c^*=(K-1)r_2^*/2K$ and the average velocity $\bar{u}^*$) decreases monotonically with an increase in the axial distance from the entrance and reaches a minimum value in the fully developed flow region.

(4) The minimum critical Reynolds numbers for K=2.0 and K=3.33 are 9720 and 40530, respectively.

(5) The modified Orr-Sommerfeld equation (i.e., the non-parallel flow model) gives critical Reynolds numbers that are somewhat smaller than those obtained from the conventional equation (i.e., the parallel flow model) for K=2.0 in the entire region. For K=3.33, the situation is reversed.

(6) The difference in the critical Reynolds numbers between the non-parallel and parallel flow models is small. Thus, the parallel flow assumption for the stability analysis in the entrance region of annular ducts is resonably acceptable.

For circular tube flow, it is found that:

(1) The flow in the entrance region is unstable to axisymmetric small disturbances.

(2) The critical Reynolds number decreases with an increase in the axial distance from the entrance, reaches a minimum value, and then increases monotonically to infinity as the axial distance increases farther downstream to the

fully developed flow region.

(3) For the non-parallel flow model, the minimum critical Reynolds number of 19780 (based on the tube radius and the average velocity) occurs at an axial location of X=0.00323.

(4) The non-parallel flow model based on the modified Orr-Sommerfeld equation yields critical Reynolds numbers that are somewhat smaller than those obtained from the parallel flow model based on the conventional equation for the entire region.

For parallel-plate channel flow, it is found that:

(1) The flow in the entrance region is unstable to two-dimensional small disturbances.

(2) The critical Reynolds number decreases monotonically with an increase in the axial distance from the entrance and reaches a minimum value in the fully developed flow region.

(3) The minimum critical Reynolds number of 3850 (based on the half-spacing between the plates and the average velocity) occurs in the fully developed flow region.

(4) The critical Reynolds numbers for the non-parallel flow model based on the modified Orr-Sommerfeld equation are somewhat smaller than those for the parallel flow model based on the conventional equation.

VII. REFERENCES

Barry, M.D.J. and Ross, M.A.S. 1970 The Flat Plate Boundary Layer. Part 2. The Effect of Increasing Thickness on Stability. Jour. Fluid Mech. 43, 813.

Burridge, D.M. 1970 The Stability of Poiseuille Pipe Flow to Non-Axisymmetric Disturbances, Geophysical Fluid Dynamic Institute, Techanical Report No.34, Florida State University.

Campbell, W.D. and Slattery, J.C. 1963 Flow in the Entrance of a Tube. Trans. ASME, Jour. Basic Eng. 85, 41.

Chen, T.S. 1966 Hydrodynamic Stability of Developing Flow in a Parallel-Plate Channel. Ph.D. Thesis, Department of Mechanical Engineering, University of Minnesota.

Chen, T.S. and Huang, L.M. 1972 Hydrodynamic Stability of Boundary Layers with Surface Suction. AIAA Jour. 10, 1366.

Chen, T.S. and Sparrow, E.M. 1967 Stability of the Developing Laminar Flow in a Parallel-Plate Channel. Jour. Fluid Mech. 30, 209.

Chen, T.S., Sparrow, E.M. and Tsou, F.K. 1971 The Effect of Mainflow Transverse Velocities in Linear Stability Theory. Jour. Fluid Mech. 50, 741.

Collatz, L. 1966 The Numerical Treatment of Differential Equations. Springer-Verlag New York Inc. Page 70.

Collins, M. and Schowalter, W.R. 1962 Laminar Flow in the Inlet Region of a Straight Channel. Phys. Fluids 5, 1122.

Conte, S.D. 1966 The Numerical Solution of Linear Boundary Value Problems. SIAM Review, 8, 309.

Corcos, G.M. and Sellars, J.R. 1959 On the Stability of Fully Developed Flow in a Pipe. Jour. Fluid Mech. 5, 97.

Davey, A. and Drazin, P.G. 1969 The Stability of Poiseuille Flow in a Pipe. Jour. Fluid Mech. 36, 209.

Dettman, J.W. 1962 Mathematical Methods in Physics and Engineering. McGraw-Hill Book Co., Inc. New York. Page 31.

Finlyson, B.A. and Scriven, L.E. 1966 The Method of Weighted Residuals - a Review. Appl. Mech. Rev. 19, 735.

Fu, T.S. 1967 Viscous Instability of Asymmetric Parallel Flows in Channels. Ph.D. Thesis, Department of Aeronautics and Engineering Mechanics, University of Minnesota.

Garg, V.K. and Rouleau, W.T. 1972 Linear Spatial Stability of Pipe Poiseuille Flow. Jour. Fluid Mech. 54, 113.

Gersting, Jr. J.M. 1970 The Hydrodynamic Stability of Two Axisymmetric Annular Flows. Ph.D. Thesis, Arizona State University.

Gill, A.E. 1965 On the Behaviour of Small Disturbances to Poiseuille Flow in a Circular Pipe. Jour. Fluid Mech. 21, 145.

Goldstein, S. 1938 Modern Developments in Fluid Dynamics, Clarendon Press, Oxford, England.

Graebel, W.P. 1970 The Stability of Pipe Flow, Part 1, Asymptotic Analysis for Small Wave Numbers. Jour. Fluid Mech. 43, 270.

Haaland, S.E. 1972 Contributions to Linear Stability Theory of Nearly Parallel Flows. Ph.D. Thesis, Fluid Mechanics Division, University of Minnesota.

Heisenberg, W. 1924 Uber Stabilitat and Turbulenz von Flussigkeitsstromen. Ann. Phys. 74, 577.

Hildebrand, F.B. 1956 Introduction to Numerical Analysis. McGraw-Hill Book Co., Inc. New York.

Huang, L.M. 1973 Stability of the Developing Laminar Flow in a Circular Tube. Ph.D. Thesis, University of Missouri-Rolla.

Leite, K.J. 1959 An Experimental Investigation of the Stability of Poiseuille Flow. Jour. Fluid Mech. 5, 81.

Lessen, M., Sadler, S.G. and Liu, T.Y. 1968 Stability of Pipe Poiseuille Flow. Phys. Fluids, 11, 1404.

Lin, C.C. 1945 On the Stability of Two-Dimensional Parallel Flows. Quart. Appl. Math. 3, 117, 213, 277.

Lin, C.C. 1967 The Theory of Hydrodynamic Stability. Cambridge University Press, Cambridge, England.

Ling, C.H. and Reynolds, W.C. 1971 The Effect of Non-Parallelism on the Stability of Shear Flows. Report FM-8, Department of Mechanical Engineering, Stanford University.

Liu, T.Y. 1968 An Analytical Investigation of the Stability of Hagen-Poiseuille Flow Subjected to Three-Dimensional Infinitesimal Disturbances. Ph.D. Thesis, The University of Rochester.

Mott, J.E. 1966 Stability of Viscous Parallel Flows in Annular Channels. Ph.D. Thesis. University of Minnesota.

Nachtsheim, P.R. 1964 An Initial Value Method for the Numerical Treatment of the Orr-Sommerfeld Equation for the Case of Plane Poiseuille Flow. NASA TN D-2414.

Roidt, M. and Cess, R.D. 1962 An Approximate Analysis of Laminar Magnetohydrodynamic Flow in the Entrance Region of a Flat Duct. Trans. ASME, Jour. Appl. Mech. 84, 171.

Salwen, H. and Grosch, C.E. 1972 The Stability of Poiseuille Flow in a Pipe of Circular Cross-Section. Jour. Fluid Mech. 54, 93.

Schensted, I.V. 1960 University of Michigan Engineering College Techanical Report (see Gill, A.E. 1965).

Siegel, R. 1953 The Effect of Heating on Boundary Layer Transition for Liquid Flow in a Tube. Sc.D. Thesis, Massachusetts Institute of Technology.

Sparrow, E.M., Lin, S.H. and Lundgren, T.S. 1964 Flow Development in the Hydrodynamic Entrance Region of Tubes and Ducts. Phys. Fluids 7, 338.

Sparrow, E.M. and Lin, S.H. 1964 The Developing Laminar Flow and Pressure Drop in the Entrance Region of Annular Ducts. Trans. ASME, Jour. Basic Eng. 86, 827.

Tatsumi, T. 1952 Stability of the Laminar Inlet Flow prior to the Formation of Poiseuille Regime. II, Jour. Phys. Soc. Japan 7, 619.

Thomas, L.H. 1953 The Stability of Plane Poiseuille Flow. Phys. Rev. 91, 780.

Tollmien, W. 1929 Uber die Entstehung der Turbulenz. Nachr. Ges. Wiss. Gottingen, Math. - Phys. Klasse, 21.

Tollmien, W. 1947 Asymptotische Integration der Storungsdifferentialgleichung ebener Laminar Stromungen bei hohen Reynoldsschen Zahlen. Z. Angew. Math. Mech. 25-27, 33, 70.

Wazzan, A.R., Okamura, T.T. and Smith, A.M.O. 1967 Stability of Laminar Boundary Layers at Separation. Phys. Fluids 10, 2540.

Wazzan, A.R., Okamura, T.T. and Smith, A.M.O. 1968 The Stability of Water Flow over Heated and Cooled Flat Plates. Trans. ASME, Jour. Heat Transfer 90, 109.

VIII. APPENDICES

Appendix A

Derivation of the Series Coefficients C_j of Equation (2.13a)

From the text, it has been established that the velocity solution for U is obtained from equation (2.9), namely,

$$\eta\frac{\partial U}{\partial \chi^*} = -\frac{2\eta}{1-M^2}\left[\left(\frac{\partial U}{\partial \eta}\right)\Big|_1 - M\left(\frac{\partial U}{\partial \eta}\right)\Big|_M\right] + \frac{\partial}{\partial \eta}\left(\eta\frac{\partial U}{\partial \eta}\right) \qquad (2.9)$$

as the sum of the fully developed profile $U_{fd}(\eta)$ and a difference velocity $U^*(\chi^*,\eta)$; that is from (2.10a)

$$U(\chi^*,\eta) = U_{fd}(\eta) + U^*(\chi^*,\eta) \qquad (2.10a)$$

where

$$U_{fd} = \frac{2[1-\eta^2+2A\ \ell n(\eta)]}{1+M^2-2A}, \qquad A = \frac{M^2-1}{2\ \ell n(M)} \qquad (A.1)$$

The solution for the difference velocity $U^*(\chi^*,\eta)$ is expressible in the form

$$U^*(\chi^*,\eta) = \sum_{j=1}^{\infty} k_j g_j(\eta)\ \exp(-\alpha_j^2\chi^*) \qquad (A.2)$$

where α_j^2 is a constant arising from the separation of variables.

By introducing (A.2) into (2.9) and noting that $U^*(\chi^*,\eta)$ satisfies (2.9), it is found that the function g_j must

satisfy the equation

$$(\eta g_j')' + \alpha_j^2 \eta g_j = \frac{2}{1-M^2} [g_j'(1) - M g_j'(M)] \tag{A.3a}$$

and the boundary conditions

$$g_j(M) = g_j(1) = 0 \tag{A.3b}$$

In equation (A.3a), the primes denote differentiation with respect to η. Since (A.3a) is a homogeneous equation with homogeneous boundary conditions, (A.3b), it follows that the α_j may be identified as eigenvalues and g_j as the corresponding eigenfunctions.

A solution for g_j may be constructed as

$$g_j = a_1 Z_J(\eta) + a_2 Z_Y(\eta) \tag{A.4a}$$

wherein

$$Z_J(\eta) = J_0(\alpha_j \eta) + \frac{2[M J_1(\alpha_j M) - J_1(\alpha_j)]}{\alpha_j (1-M^2)} \tag{A.4b}$$

$$Z_Y(\eta) = Y_0(\alpha_j \eta) + \frac{2[M Y_1(\alpha_j M) - Y_1(\alpha_j)]}{\alpha_j (1-M^2)} \tag{A.4c}$$

and the J and Y are Bessel Functions of the first and second kind, respectively. Application of the homogeneous boundary conditions (A.3b) to this solution leads to an algebraic equation for determining the eigenvalues α_j

$$Z_J(M)\ Z_Y(1) = Z_J(1)\ Z_Y(M) \tag{A.5}$$

In addition to the eigenvalues, the application of the boundary conditions provides the relationship

$$a_1/a_2 = -Z_Y(1)/Z_J(1) \tag{A.6}$$

With (A.6), the solution for g_j becomes

$$g_j = a_2\{[-Z_Y(1)/Z_J(1)]Z_J(\eta)+Z_Y(\eta)\} \tag{A.7}$$

The scale factor a_2 may be fixed by the normalizing condition

$$\int_M^1 \eta\, g_j^2\, d\eta = 1 \tag{A.8}$$

It is also useful to note the following orthogonality properties of the eigenfunctions g_j

$$\int_M^1 g_j\, \eta\, d\eta = 0; \qquad \int_M^1 \eta\, g_i g_j\, d\eta = 0 \quad \text{for } i\neq j \tag{A.9}$$

With the g_j function thus fully determined, it remains to complete the $U^*(\chi^*,\eta)$ solution by finding the coefficient k_j in the series of (A.2). For this, the velocity condition at the duct entrance is used, namely, $u^*=\bar{u}^*$ at $x^*=0$. This yields

$$U^*(0,\eta) = \sum_{j=1}^{\infty} k_j g_j(\eta) = 1-U_{fd}(\eta) \tag{A.10}$$

If (A.10) is multiplied by ηg_j and integrated over the range $M\leq\eta\leq 1$ and if use is made of(A.7) and (A.9), it follows that

$$k_j = -\int_M^1 \eta\, U_{fd}\, g_j\, d\eta \tag{A.11a}$$

or

$$k_j = -\frac{2a_2}{1+M^2-2A}\int_M^1 \eta(1-\eta^2)\{-[Z_Y(1)/Z_J(1)]Z_J(\eta)+Z_Y(\eta)\}\,d\eta$$

$$-\frac{4a_2A}{1+M^2-2A}\int_M^1 \eta\,\ell n(\eta)\{-[Z_Y(1)/Z_J(1)]Z_J(\eta)+Z_Y(\eta)\}\,d\eta \qquad \text{(A.11b)}$$

Next, consider the identities (see, for example, the third and fourth equations of 9.1.29. on page 361 of Handbook of Mathematical Functions, National Bureau of Standards)

$$\eta f_\nu'(\eta) = \lambda q \eta^q f_{\nu-1}(\eta) + (p-\nu q) f_\nu(\eta) \qquad \text{(A.12a)}$$

$$\eta f_\nu'(\eta) = -\lambda q \eta^q f_{\nu+1}(\eta) + (p+\nu q) f_\nu(\eta) \qquad \text{(A.12b)}$$

where

$$f_\nu(\eta) = \eta^p J_\nu(\lambda\eta^q) \ , \quad f_\nu'(\eta) = df_\nu(\eta)/d\eta$$

Integrating (A.12a) and (A.12b) and rearranging, there results

$$\int \eta^{q-1+p} J_{\nu-1}(\lambda\eta^q)\,d\eta = -[(p-\nu q)/(\lambda q)]\int \eta^{p-1} J_\nu(\lambda\eta^{q-1})\,d\eta$$

$$+ [\eta^p/(\lambda q)]J_\nu(\lambda\eta^q) \qquad \text{(A.13a)}$$

$$\int \eta^{q-1+p} J_{\nu+1}(\lambda\eta^q)d\eta = +[(p+\nu q)/(\lambda q)]\int \eta^{p-1} J_\nu(\lambda\eta^q)d\eta$$

$$- [\eta^p/(\lambda q)]J_\nu(\lambda\eta^q) \qquad \text{(A.13b)}$$

With the use of (A.13a) and (A.13b), one obtains

$$\int \eta^3 J_0(\alpha_j\eta)d\eta = [\eta(\alpha_j^2\eta^2-4)/\alpha_j^3]J_1(\alpha_j\eta) + (2\eta^2/\alpha_j^2)J_0(\alpha_j\eta) \tag{A.14a}$$

$$\int \eta J_0(\alpha_j\eta)d\eta = (\eta/\alpha_j)J_1(\alpha_j\eta) \tag{A.14b}$$

Thus,

$$\int(\eta-\eta^3)J_0(\alpha_j\eta)d\eta = (\eta/\alpha_j)J_1(\alpha_j\eta) - [\eta(\alpha_j^2\eta^2-4)/\alpha_j^3]J_1(\alpha_j\eta) - (2\eta^2/\alpha_j^2)J_0(\alpha_j\eta) \tag{A.14c}$$

Also,

$$\int_M^1 (\eta-\eta^3)d\eta = (1-M^2)^2/4 \tag{A.14d}$$

Combining (A.14c) and (A.14d) and after rearranging, there results

$$\int_M^1 \eta(1-\eta^2)Z_J(\eta)d\eta = [(1+M^2)/(2\alpha_j)-(\alpha_j^2-4)/\alpha_j^3]J_1(\alpha_j)-(2/\alpha_j^2)J_0(\alpha_j) - [(1+M^2)M/(2\alpha_j)-(\alpha_j^2M^2-4)M/\alpha_j^3]J_1(M\alpha_j) + (2M^2/\alpha_j^2)J_0(M\alpha_j) \tag{A.15a}$$

Similarly, the following integral can be obtained

$$\int_M^1 \eta(1-\eta^2)Z_Y(\eta)d\eta=[(1+M^2)/(2\alpha_j)-(\alpha_j^2-4)/\alpha_j^3]Y_1(\alpha_j)-(2/\alpha_j^2)Y_0(\alpha_j) - [(1+M^2)M/(2\alpha_j)-(\alpha_j^2M^2-4)M/\alpha_j^3]Y_1(M\alpha_j) + (2M^2/\alpha_j^2)Y_0(M\alpha_j) \tag{A.15b}$$

The first term on the right-hand side of (A.11b) then becomes

$$-\frac{2a_2}{1+M^2-2A}\int_M^1 \eta(1-\eta^2)\{-[Z_Y(1)/Z_J(1)]Z_J(\eta)+Z_Y(\eta)\}\,d\eta$$

$$= +[Z_Y(1)/Z_J(1)]\{[(1+M^2)/(2\alpha_j)-(\alpha_j^2-4)/\alpha_j^3]J_1(\alpha_j)-(2/\alpha_j^2)J_0(\alpha_j)$$

$$- [(1+M^2)M/(2\alpha_j)-(\alpha_j^2M^2-4)M/\alpha_j^3]J_1(M\alpha_j) + (2M^2/\alpha_j^2)J_0(M\alpha_j)\}$$

$$- \{[(1+M^2)/(2\alpha_j)-(\alpha_j^2-4)/\alpha_j^3]Y_1(\alpha_j)-(2/\alpha_j^2)Y_0(\alpha_j)$$

$$- [(1+M^2)M/(2\alpha_j)-(\alpha_j^2M^2-4)M/\alpha_j^3]Y_1(M\alpha_j) + (2M^2/\alpha_j^2)Y_0(M\alpha_j)\} \qquad \text{(A.15c)}$$

After rearranging, (A.15c) reduces to

$$-\frac{2a_2}{1+M^2-2A}\int_M^1 \eta(1-\eta^2)\{-[Z_Y(1)/Z_J(1)]Z_J(\eta)+Z_Y(\eta)\}\,d\eta$$

$$= 2a_2F_1/(1+M^2-2A) \qquad \text{(A.15d)}$$

where

$$F_1 = -[Z_Y(1)/Z_J(1)]G_J + G_Y + 0.25(1-M^4)E \qquad \text{(A.15e)}$$

$$\alpha_j^3G_J = (\alpha_j^2-4)J_1(\alpha_j) - (\alpha_j^2M^2-4)MJ_1(M\alpha_j) + 2\alpha_jJ_0(\alpha_j)$$

$$- 2\alpha_jM^2J_0(M\alpha_j) \qquad \text{(A.15f)}$$

$$\alpha_j(1-M^2)E = 2\{-[Z_Y(1)/Z_J(1)][MJ_1(M\alpha_j)-J_1(\alpha_j)] + MY_1(M\alpha_j) - Y_1(\alpha_j)\} \quad \text{(A.15g)}$$

Next, the second term on the right-hand side of (A.11b) will be evaluated as follows.

Since

$$\int_M^1 \eta J_0(\alpha_j\eta)\ \ell n(\eta)\ d\eta = [-(M/\alpha_j)\ \ell n(M)]J_1(M\alpha_j) + [J_0(\alpha_j)-J_0(M\alpha_j)]/\alpha_j^2 \quad \text{(A.16a)}$$

and

$$\int_M^1 \eta\ \ell n(\eta)\ d\eta = -(M^2/2)\ \ell n(M) - (1-M^2)/4 \quad \text{(A.16b)}$$

it follows that

$$\int_M^1 \eta Z_J(\eta)\ \ell n(\eta)\ d\eta = -(M/\alpha_j)J_1(M\alpha_j)\ \ell n(M) + [J_0(\alpha_j)-J_0(M\alpha_j)]/\alpha_j^2 + [M^2-2M^2\ell n(M)-1][MJ_1(M\alpha_j)-J_1(\alpha_j)] / [2\alpha_j(1-M^2)] \quad \text{(A.16c)}$$

Similarly, one obtains the expression

$$\int_M^1 \eta Z_Y(\eta)\ \ell n(\eta)\ d\eta = -(M/\alpha_j)Y_1(M\alpha_j)\ \ell n(M) + [Y_0(\alpha_j)-Y_0(M\alpha_j)]/\alpha_j^2 + [M^2-2M^2\ell n(M)-1][MY_1(M\alpha_j)-Y_1(\alpha_j)] / [2\alpha_j(1-M^2)] \quad \text{(A.16d)}$$

Therefore, the second term on the right-hand side of

(A.11b) becomes

$$-\frac{4a_2A}{1+M^2-2A}\int_M^1 \eta\, \ell n(\eta)\{-[Z_Y(1)/Z_J(1)]Z_J(\eta)+Z_Y(\eta)\}\, d\eta$$

$$=-\frac{4a_2A}{1+M^2-2A}\, F_2 \qquad \text{(A.16e)}$$

where

$$F_2 = -[Z_Y(1)/Z_J(1)]H_J + H_Y + [M^2-2M^2\ell n(M)-1]E/4 \qquad \text{(A.16f)}$$

$$\alpha_j^2 H_J = -\alpha_j M J_1(M\alpha_j)\ell n(M) + J_0(\alpha_j) - J_0(M\alpha_j) \qquad \text{(A.16g)}$$

The scale factor a_2 is to be determined from (A.8) with the use of (A.7)

$$\int_M^1 \eta a_2^2\{-[Z_Y(1)/Z_J(1)]Z_J(\eta)+Z_Y(\eta)\}^2 d\eta = 1 \qquad \text{(A.17a)}$$

or

$$a_2^2 = \frac{1}{\int_M^1 \eta\{-[Z_Y(1)/Z_J(1)]Z_J(\eta)+Z_Y(\eta)\}^2 d\eta} \qquad \text{(A.17b)}$$

Let

$$B_J = 2[MJ_1(M\alpha_j)-J_1(\alpha_j)]/[\alpha_j(1-M^2)] \qquad \text{(A.18a)}$$

$$B_Y = 2[MY_1(M\alpha_j)-Y_1(\alpha_j)]/[\alpha_j(1-M^2)] \qquad \text{(A.18b)}$$

Since

$$2B_J \int \eta J_0(\alpha_j \eta)\, d\eta = \{4\eta J_1(\alpha_j \eta)/[\alpha_j^2(1-M^2)]\}[MJ_1(M\alpha_j)-J_1(\alpha_j)] \tag{A.18c}$$

$$B_J^2 \int \eta\, d\eta = \{2\eta^2/[\alpha_j^2(1-M^2)^2]\}[M^2 J_1^2(M\alpha_j)-2MJ_1(\alpha_j)J_1(M\alpha_j) + J_1^2(\alpha_j)] \tag{A.18d}$$

$$\int \eta J_0^2(\alpha_j \eta)\, d\eta = (\eta^2/2)[J_0^2(\alpha_j \eta)+J_1^2(\alpha_j \eta)] \tag{A.18e}$$

one obtains

$$\int \eta Z_J^2(\eta)\, d\eta = (\eta^2/2)[J_0^2(\alpha_j \eta)+J_1^2(\alpha_j \eta)] + \{2\eta^2/[\alpha_j^2(1-M^2)^2]\} [M^2 J_1^2(M\alpha_j)-2MJ_1(\alpha_j)J_1(M\alpha_j)+J_1^2(\alpha_j)] + \{4\eta J_1(\alpha_j \eta)/[\alpha_j^2(1-M^2)]\}[MJ_1(M\alpha_j)-J_1(\alpha_j)] \tag{A.19}$$

Similarly, the following expression can be obtained

$$\int \eta Z_Y^2(\eta)\, d\eta = (\eta^2/2)[Y_0^2(\alpha_j \eta)+Y_1^2(\alpha_j \eta)] + \{2\eta^2/[\alpha_j^2(1-M^2)^2]\} [M^2 Y_1^2(M\alpha_j)-2MY_1(\alpha_j)Y_1(M\alpha_j)+Y_1^2(\alpha_j)] + \{4\eta Y_1(\alpha_j \eta)/[\alpha_j^2(1-M^2)]\}[MY_1(M\alpha_j)-Y_1(\alpha_j)] \tag{A.20}$$

In addition, since

$$B_J \int \eta Y_0(\alpha_j \eta)\, d\eta + B_Y \int \eta J_0(\alpha_j \eta)\, d\eta = -\{2/[\alpha_j^2(1-M^2)]\} [\eta J_1(\alpha_j)Y_1(\alpha_j \eta)-M\eta J_1(M\alpha_j)Y_1(\alpha_j \eta) + \eta J_1(\alpha_j \eta)Y_1(\alpha_j)-M\eta J_1(\alpha_j \eta)Y_1(M\alpha_j)] \tag{A.21a}$$

$$B_J B_Y \int \eta d\eta = \{2\eta^2/[\alpha_j^2(1-M^2)^2]\}[M^2 J_1(M\alpha_j)Y_1(M\alpha_j) - MJ_1(\alpha_j)Y_1(M\alpha_j)$$

$$-MJ_1(M\alpha_j)Y_1(\alpha_j) + J_1(\alpha_j)Y_1(\alpha_j)] \qquad \text{(A.21b)}$$

$$\int \eta J_0(\alpha_j\eta)Y_0(\alpha_j\eta)d\eta = (\eta^2/2)[J_0(\alpha_j\eta)Y_0(\alpha_j\eta)$$

$$+ J_1(\alpha_j\eta)Y_1(\alpha_j\eta)] \qquad \text{(A.21c)}$$

it follows that

$$\int \eta Z_J(\eta)Z_Y(\eta)d\eta = \{2\eta^2/[\alpha_j^2(1-M^2)^2]\}[M^2 J_1(M\alpha_j)Y_1(M\alpha_j)$$

$$-MJ_1(\alpha_j)Y_1(M\alpha_j) - MJ_1(M\alpha_j)Y_1(\alpha_j) + J_1(\alpha_j)Y_1(\alpha_j)]$$

$$+(\eta^2/2)[J_0(\alpha_j\eta)Y_0(\alpha_j\eta) + J_1(\alpha_j\eta)Y_1(\alpha_j\eta)]$$

$$-\{2/[\alpha_j^2(1-M^2)]\}[\eta J_1(\alpha_j)Y_1(\alpha_j\eta) - M\eta J_1(M\alpha_j)Y_1(\alpha_j\eta)$$

$$+\eta J_1(\alpha_j\eta)Y_1(\alpha_j) - M\eta J_1(\alpha_j\eta)Y_1(M\alpha_j)] \qquad \text{(A.22)}$$

Substituting (A.19), (A.20), and (A.22) into (A.17b), yields

$$a_2^2 = \frac{1}{F_3(1) - F_3(M)} \qquad \text{(A.23a)}$$

where

$$F_3(\eta) = 0.5[Z_Y(1)/Z_J(1)]^2\eta^2[J_0^2(\alpha_j\eta) + J_1^2(\alpha_j\eta)] + 0.5\eta^2[Y_0^2(\alpha_j\eta)$$

$$+ Y_1^2(\alpha_j\eta)] + 0.5\eta^2E^2 - [Z_Y(1)/Z_J(1)]\eta^2[J_0(\alpha_j\eta)Y_0(\alpha_j\eta)$$

$$+ J_1(\alpha_j\eta)Y_1(\alpha_j\eta)] + (2E/\alpha_j)\{\eta^2 Y_1(\alpha_j\eta)$$

$$- [Z_Y(1)/Z_J(1)]\eta J_1(\alpha_j\eta)\} \qquad \text{(A.23b)}$$

Referring to (A.7) and (A.10), one can put

$$k_j a_2 = C_j \qquad \text{(A.24)}$$

With the use of (A.11b), (A.15d), (A.16e), and (A.23a), one finally obtains the desired expression for C_j

$$C_j = \frac{2(F_1 - 2AF_2)}{(1+M^2-2A)[F_3(1)-F_3(M)]} \qquad \text{(A.25)}$$

where F_1 , F_2 , F_3 , G_J , H_J , and E are expressed in equations (A.15e), (A.16f), (A.23b), (A.15f), (A.16g), and (A.15g), respectively. The terms G_Y and H_Y are obtained from G_J and H_J by replacing J by Y.

Appendix B

The Relationship Between the Stretched and Physical Axial Coordinates

Table B-1

The Relationship Among χ^*, ε, and χ for Annular Ducts

$$\chi^* = \frac{\xi^*/r^*_2}{\bar{u}^* r^*_2/\nu}, \quad \chi = \frac{x^*/r^*_2}{\bar{u}^* r^*_2/\nu}, \quad X^* = \{2K/(K-1)\}^2 \chi^*,$$

$$X = \{2K/(K-1)\}^2 \chi^*, \quad K = r^*_2/r^*_1$$

K=2.0

χ^*	X^*	ε	χ	X
0.0008	0.0128	0.58323	0.000387	0.006192
0.0010	0.0160	0.62079	0.000511	0.008176
0.0015	0.0240	0.70148	0.000842	0.013472
0.0020	0.0320	0.76936	0.001210	0.019360
0.0030	0.0480	0.87845	0.002033	0.032528
0.0040	0.0640	0.95875	0.002952	0.047232
0.0080	0.1280	1.09729	0.007064	0.113024
0.0160	0.2560	1.13044	0.015975	0.255600

K=3.33

χ^*	X^*	ε	χ	X
0.0010	0.008170	0.51948	0.000452	0.003693
0.0020	0.016341	0.62317	0.001024	0.008366
0.0025	0.020426	0.66559	0.001346	0.010997
0.0040	0.032681	0.77188	0.002424	0.019805
0.0080	0.065362	0.96001	0.005888	0.048107
0.0160	0.130724	1.09786	0.014120	0.115364

Table B-2

The Relationship Among X*, ε and X for Circular Tubes

(Huang, 1973)

$$X^* = \frac{\xi^*/r^*_0}{\bar{u}^* r^*_0/\nu}, \qquad X = \frac{x^*/r^*_0}{\bar{u}^* r^*_0/\nu}$$

X*	ε	X
0.002	0.50014	0.00087
0.003	0.55121	0.00140
0.005	0.63385	0.00258
0.006	0.66143	0.00323
0.007	0.70242	0.00392
0.009	0.76262	0.00539
0.010	0.79045	0.00616

Table B-3

The Relationship Among X*, ε and X for Parallel-Plate Channels

(Chen, 1966)

$$X^* = \frac{\xi^*/L^*}{\bar{u}^* L^*/\nu}, \qquad X = \frac{x^*/L^*}{\bar{u}^* L^*/\nu}$$

X*	ε	X
0.005	0.46627	0.00203
0.006	0.48465	0.00250
0.008	0.51755	0.00351
0.010	0.54682	0.00457
0.015	0.60998	0.00747
0.020	0.66390	0.01066
0.030	0.75465	0.01776
0.040	0.82960	0.02570
0.060	0.94345	0.04350
0.080	1.01789	0.06317
0.100	1.06384	0.08403
0.150	1.11426	0.13873
0.200	1.12945	0.19490
0.300	1.13624	0.30829

Appendix C

Neutral Stability Characteristics for Annular Duct Flow

$(c_i=0)$

$$R = \frac{\bar{u}^* r_2^* (K-1)}{\nu} \frac{(K-1)}{2K}, \quad \alpha = \alpha^* r_2^* \frac{(K-1)}{2K}, \quad c_r = c_r^*/\bar{u}^*, \quad K = r_2^*/r_1^*,$$

$$\chi^* = \frac{\xi^*/r_2^*}{\bar{u}^* r_2^*/\nu}, \quad \chi = \frac{x^*/r_2^*}{\bar{u}^* r_2^*/\nu}, \quad X^* = \{2K/(K-1)\}^2 \chi^*$$

$$X = \{2K/(K-1)\}^2 \chi$$

Table C-1

Neutral Stability Results for the Fully Developed Annular Duct Flow, $\chi^*=\infty$

K=2.0 N=100

α	R	c_r	α	R	c_r
0.57087	50000	0.18046	0.95000	9717	0.31534
0.61738	35000	0.20132	1.00000	10585	0.31659
0.68167	23079	0.22927	1.02866	14000	0.30285
0.72232	18494	0.24612	1.03099	16000	0.29515
0.78021	14219	0.26854	1.02667	21000	0.27903
0.82658	12040	0.28476	1.01107	30000	0.25793
0.90000	10103	0.30588	0.99477	40000	0.24125
0.94000	9725	0.31390	0.98188	50000	0.22853
0.94500	9716	0.31465			

K=3.33 N=150

α	R	c_r	α	R	c_r
0.67594	80000	0.17030	0.93000	40974	0.22287
0.73524	60000	0.18749	0.97375	45000	0.22215
0.81292	46000	0.20656	1.01482	60000	0.21185
0.90000	40554	0.22064	1.02606	80000	0.19962
0.90700	40529	0.22131	1.02661	100000	0.18985
0.91000	40540	0.22158	1.02236	140000	0.17505
0.92000	40675	0.22232			

Table C-2

Neutral Stability Results for the Developing Annular Duct Flow, $\chi^*=0.016$

K=2.0 N=150

Modified O-S Equation			Conventional O-S Equation		
α	R	c_r	α	R	c_r
0.9440	9920	0.31291	0.9440	9920.4	0.31268
0.9460	9919	0.31298	0.9460	9919.5	0.31296
0.9480	9920	0.31326	0.9480	9920.4	0.31323
			0.9520	9927	0.31373
			0.9560	9942	0.31418
			0.9600	9964	0.31458

K=3.33 N=150

Modified O-S Equation			Conventional O-S Equation		
α	R	c_r	α	R	c_r
0.93510	41040.8	0.21831	0.92000	41194	0.21693
0.93520	41040.7	0.21832	0.93400	41039	0.21823
0.93600	41040.8	0.21839	0.93500	41038.0	0.21831
			0.93650	41038.4	0.21842
			0.94000	41052	0.21868
			0.95000	41186	0.21930
			0.96000	41478	0.21973
			1.00000	44849	0.21892

Table C-3

Neutral Stability Results for the Developing Annular Duct Flow, $\chi^*=0.008$

K=2.0 N=150

Modified O-S Equation			Conventional O-S Equation		
α	R	c_r	α	R	c_r
0.96092	11170	0.30362	0.90000	12071	0.29110
0.96553	11150	0.30430	0.95000	11249	0.30178
0.97450	11134	0.30551	0.97440	11137	0.30545
0.97784	11136	0.30591	1.00000	11286	0.30776
0.98047	11140	0.30621	1.04852	13253	0.30350
			1.06122	15372	0.29600
			1.06205	22000	0.27579
			1.05115	28000	0.26201

K=3.33 N=200

Modified O-S Equation			Conventional O-S Equation		
α	R	c_r	α	R	c_r
0.77887	80000	0.17444	0.91927	50000	0.20471
0.83061	65000	0.18674	1.02000	42756	0.21900
0.91927	50000	0.20473	1.04000	42304	0.22083
1.05300	42226	0.22178	1.05300	42194	0.22179
1.05700	42223	0.22200	1.05400	42189	0.22187
1.05900	42228	0.22216	1.06000	42199	0.22223
1.15458	50000	0.21965	1.07000	42291	0.22275
1.18346	65000	0.20908	1.08000	42491	0.22314
1.18683	80000	0.20021	1.10000	43248	0.22348
1.18041	100000	0.19067	1.15483	50000	0.21965
1.15991	140000	0.17661			

Table C-4

Neutral Stability Results for the Developing Annular Duct Flow, $\chi^*=0.004$

K=2.0 N=150

Modified O-S Equation

α	R	c_r
0.72232	39301	0.20518
0.78021	29306	0.22488
0.82658	24019	0.23969
0.86273	21000	0.25061
0.99157	15000	0.28294
1.06812	13750	0.29583
1.07775	13700	0.29699
1.09100	13676	0.29837
1.10247	13700	0.29935
1.19000	16793	0.29489
1.20523	20000	0.28597
1.20334	28000	0.26738
1.18831	36000	0.25345

Conventional O-S Equation

α	R	c_r
0.90000	18626	0.26097
1.00000	14794	0.28452
1.06572	13771	0.29540
1.08500	13685	0.29766
1.09000	13680	0.29816
1.09500	13684	0.29862
1.10500	13717	0.29942
1.18171	16000	0.29700
1.20525	20000	0.28592

K=3.33 N=250

Modified O-S Equation

α	R	c_r
1.29400	43029	0.23171
1.29700	43025	0.23185
1.30000	43037	0.23197

Conventional O-S Equation

α	R	c_r
1.28600	42976	0.23133
1.29200	42959	0.23162
1.29800	41960	0.23189

Table C-5

Neutral Stability Results for the Developing Annular Duct Flow, $\chi^*=0.003$

K=2.0 N=150

Modified O-S Equation			Conventional O-S Equation		
α	R	c_r	α	R	c_r
1.15258	15050	0.29530	0.78021	39500	0.21020
1.16270	15020	0.29626	0.82656	31965	0.22451
1.16900	15015	0.29681	0.90000	24222	0.24546
1.17308	15017	0.29714	0.95000	20798	0.25834
1.17518	15020	0.29730	1.00000	18367	0.26993
			1.07825	16000	0.28504
			1.15000	15069	0.29486
			1.16000	15032	0.29585
			1.16500	15024	0.29630
			1.20000	15165	0.29859
			1.25088	16300	0.29817
			1.29437	20000	0.28922
			1.30344	28000	0.27113
			1.29058	36000	0.25725

Table C-6

Neutral Stability Results for the Developing Annular Duct Flow, $\chi^*=0.0025$

K=3.33 N=300

Modified O-S Equation			Conventional O-S Equation		
α	R	c_r	α	R	c_r
1.08581	80000	0.19310	1.33458	50000	0.22565
1.17380	65000	0.20637	1.52000	43797	0.23915
1.33617	50000	0.22585	1.54000	43680	0.23997
1.54200	43763	0.24007	1.54100	43670	0.24001
1.54700	43750	0.24025	1.71112	50000	0.23841
1.55200	43756	0.24041			
1.55700	43763	0.24056			
1.56200	43776	0.24071			
1.56700	43791	0.24086			
1.70942	50000	0.23846			
1.76327	65000	0.22727			
1.76369	80000	0.21793			
1.74488	100000	0.20796			
1.72087	120000	0.19994			
1.69562	140000	0.19336			

Table C-7

Neutral Stability Results for the Developing Annular Duct Flow, $\chi^*=0.002$

K=2.0 N=200

Modified O-S Equation			Conventional O-S Equation		
α	R	c_r	α	R	c_r
1.29534	17400	0.29412	0.95000	31842	0.23494
1.29861	17390	0.29437	1.00000	27366	0.24672
1.31300	17372	0.29534	1.05000	24057	0.25754
1.31350	17373	0.29537	1.15000	19816	0.27602
			1.25000	17755	0.28963
			1.30000	17401	0.29422
			1.31000	17387	0.29492
			1.35000	17553	0.29691
			1.40000	18235	0.29737

Table C-8

Neutral Stability Results for the Developing Annular Duct Flow, $\chi^*=0.0015$

K=2.0 N=200

Modified O-S Equation			Conventional O-S Equation		
α	R	c_r	α	R	c_r
0.95000	45228	0.21801	0.95000	45227	0.21786
1.15355	25985	0.26035	1.03006	35000	0.23601
1.30000	20867	0.28208	1.15352	26000	0.26007
1.40000	19463	0.29198	1.25000	22161	0.27525
1.45000	19314	0.29513	1.30000	20886	0.28176
1.45666	19325	0.29544	1.35000	20004	0.28725
1.46123	19337	0.29564	1.40000	19485	0.29164
1.55000	20506	0.29648	1.44500	19334	0.29454
1.62375	25000	0.28821	1.45000	19338	0.29479
1.64036	29000	0.28061	1.47000	19395	0.29566
1.62257	45000	0.25711	1.50000	19629	0.29614
			1.60357	23000	0.29196
			1.62356	25000	0.28804
			1.64031	29000	0.28047
			1.64035	36000	0.26897
			1.62268	45000	0.25704

Table C-9

Neutral Stability Results for the Developing Annular Duct Flow, $\chi^*=0.0010$

K=2.0 N=200

Modified O-S Equation			Conventional O-S Equation		
α	R	c_r	α	R	c_r
1.69000	22350	0.29501	1.35000	28738	0.26537
1.69200	22349	0.29508	1.40000	26887	0.27156
1.69500	22350	0.29519	1.45000	25422	0.27711
1.69800	22352	0.29530	1.50000	24282	0.28203
			1.55000	23427	0.28630
			1.60000	22831	0.28990
			1.65000	22486	0.29279
			1.68500	22396	0.29435
			1.70000	22399	0.29490
			1.75000	22607	0.29614

Table C-10

Axial Variation of Critical Stability Characteristics for Annular Duct Flow

K=2.0

Modified Orr-Sommerfeld Equation

χ	χ^*	X	X*	$(\alpha)_c$	$(R)_c$	$(c_r)_c$	N
∞	∞	∞	∞	0.9450	9716	0.31465	100
0.01598	0.016	0.255600	0.2560	0.9460	9920	0.31296	150
0.00706	0.008	0.113024	0.1280	0.9744	11137	0.30545	150
0.00295	0.004	0.047232	0.0640	1.0900	13680	0.29862	150
0.00203	0.003	0.032528	0.0480	1.1650	15024	0.29630	150
0.00121	0.002	0.019360	0.0320	1.3100	17387	0.29492	200
0.00084	0.0015	0.013472	0.0240	1.4450	19334	0.29454	200
0.00051	0.0010	0.008176	0.0160	1.6850	22396	0.29435	200

Table C-10 (continued)

K=2.0

Conventional Orr-Sommerfeld Equation

χ_∞	χ^*_∞	X_∞	X^*_∞	$(\alpha)_c$	$(R)_c$	$(c_r)_c$	N
				0.9450	9716	0.31465	100
0.01598	0.016	0.255600	0.2560	0.9460	9919	0.31298	150
0.00706	0.008	0.113024	0.1280	0.9745	11134	0.30551	150
0.00295	0.004	0.047232	0.0640	1.0910	13676	0.29837	150
0.00203	0.003	0.032528	0.0480	1.1690	15015	0.29681	150
0.00121	0.002	0.019360	0.0320	1.3130	17372	0.29534	200
0.00084	0.0015	0.013472	0.0240	1.4500	19314	0.29513	200
0.00051	0.0010	0.008176	0.0160	1.6920	22349	0.29508	200

K=3.33

Modified Orr-Sommerfeld Equation

χ_∞	χ^*_∞	X_∞	X^*_∞	$(\alpha)_c$	$(R)_c$	$(c_r)_c$	N
				0.9070	40529	0.22131	150
0.01412	0.016	0.115364	0.130724	0.9352	41041	0.21832	150
0.00589	0.008	0.048107	0.065362	1.0570	42223	0.22200	200
0.00242	0.004	0.019805	0.032681	1.2970	43025	0.23185	250
0.00135	0.0025	0.010997	0.021426	1.5470	43750	0.24025	300

Conventional Orr-Sommerfeld Equation

χ_∞	χ^*_∞	X_∞	X^*_∞	$(\alpha)_c$	$(R)_c$	$(c_r)_c$	N
				0.9070	40529	0.22131	150
0.01412	0.016	0.115364	0.130724	0.9350	41038	0.21831	150
0.00589	0.008	0.048107	0.065362	1.0540	42189	0.22187	200
0.00242	0.004	0.019805	0.032681	1.2920	42959	0.23169	250
0.00135	0.0025	0.010997	0.021426	1.5410	43670	0.24001	300

Appendix D

Neutral Stability Characteristics for Circular Tube Flow

$(c_i=0)$

$$R = \bar{u}^* r_0^*/\nu \ , \quad \alpha = \alpha^* r_0^* \ , \quad c_r = c_r^*/\bar{u}^* \ , \quad X^* = \frac{\xi^*/r_0^*}{\bar{u}^* r_0^*/\nu} \ ,$$

$$X = \frac{x^*/r_0^*}{\bar{u}^* r_0^*/\nu}$$

Table D-1

Neutral Stability Results at Various Axial Locations for Circular Tube Flow, Modified Orr-Sommerfeld Equation

$X^*=0.010$ $(X=0.00616)$ $N=100$

α	R	c_r
0.40616	54000	0.44894
0.52000	43466	0.44765
0.60630	38500	0.44624
0.75000	33799	0.44191
0.77500	33412	0.44062
0.80000	33180	0.43912
0.81500	33148	0.43800
0.82500	33167	0.43721
0.83000	33208	0.43672
0.85000	33487	0.43466
0.87500	34655	0.43040
0.88259	37500	0.42395
0.79257	52000	0.40694

$X^*=0.009$ $(X=0.00539)$ $N=150$

α	R	c_r
1.0700	24997	0.438343
1.1200	24809	0.436437
1.1300	24803	0.436006
1.1750	24970	0.433517

Table D-1 (continued)

X*=0.007 (X=0.00392) N=150

α	R	c_r
1.6300	20202	0.425184
1.6500	20174	0.424882
1.6700	20160	0.424576
1.7050	20182	0.423888

X*=0.006 (X=0.00323) N=150

α	R	c_r
0.71682	45000	0.40118
1.01447	32000	0.40608
1.32503	25000	0.41155
1.80000	20216	0.41708
1.96000	19785	0.41673
2.01000	19802	0.41618
2.07000	19946	0.41518
2.27517	23000	0.40370
2.29153	30000	0.38549
2.21718	38000	0.37051
2.12745	46000	0.35511

X*=0.005 (X=0.00258) N=150

α	R	c_r
2.3000	20245	0.40759
2.3300	20235	0.40755
2.3500	20242	0.40747
2.4000	20308	0.40711

Table D-1 (continued)

X*=0.003 (X=0.00140) N=200

α	R	c_r
1.52998	51717	0.34095
2.02995	36754	0.35747
2.52346	28964	0.37220
2.75000	26817	0.37787
3.30000	24174	0.38664
3.37500	24119	0.38711
3.38800	24118	0.38717
3.40000	24117	0.38722
3.42000	24129	0.38727
3.43000	24136	0.38729
3.50000	24236	0.38307
3.75000	25874	0.38355
3.96285	35302	0.36426
3.91191	44127	0.35011
3.82122	52953	0.33888

X*=0.002 (X=0.00087) N=200

α	R	c_r
4.190	29266	0.37368
4.360	29062	0.37517
4.500	29225	0.37536
4.700	29900	0.37506

Table D-2

Neutral Stability Results at Three Axial Locations for Circular Tube Flow, Conventional Orr-Sommerfeld Equation

$c_i=0$

X*=0.010 (X=0.00616) N=100

α	R	c_r
0.40000	54206	0.447563
0.50000	44580	0.446431
0.60000	38627	0.444637
0.70000	35066	0.441646
0.72500	34508	0.440575
0.75000	34102	0.439295
0.77500	33878	0.437720
0.80000	33909	0.435681
0.82500	34402	0.432739
0.84390	35751	0.428570
0.84850	37340	0.425103
0.82310	43696	0.415694
0.76870	52641	0.408043
0.78500	33840	0.431008

X*=0.006 (X=0.00323) N=150

α	R	c_r
0.7000	45030	0.37856
1.0000	31770	0.40341
1.3000	25004	0.40855
1.6000	21362	0.41270
1.7000	20640	0.41354
1.8000	20150	0.41393
1.9000	19914	0.41371
2.0000	19998	0.41257
2.1317	20935	0.40853
2.2272	23447	0.40031
2.2461	29309	0.38544
2.1750	37682	0.36981
2.0838	46056	0.35809
1.9300	19900	0.41349

Table D-2 (continued)

X*=0.003 (X=0.00140) N=200

α	R	c_r
1.5000	51717	0.336004
2.0000	36754	0.352190
2.5000	28964	0.366903
2.7500	26683	0.372937
3.0000	25248	0.377638
3.2500	24658	0.380504
3.2800	24620	0.380775
3.5000	25182	0.380550
3.7500	28424	0.374284
3.8456	35302	0.361132
3.8070	44127	0.306757
3.7259	52953	0.297178

Table D-3

Axial Variation of Critical Stability Characteristics for Circular Tube Flow

Modified Orr-Sommerfeld Equation

X*	X	$(\alpha)_c$	$(R)_c$	$(c_r)_c$	N
0.010	0.00616	0.815	33148	0.43800	100
0.009	0.00539	1.130	24803	0.43601	150
0.007	0.00392	1.670	20160	0.42458	150
0.006	0.00323	1.960	19785	0.41673	150
0.005	0.00258	2.330	20235	0.40755	150
0.003	0.00140	3.400	24117	0.38722	200
0.002	0.00087	4.360	29062	0.37517	200

Table D-3 (continued)

Conventional Orr-Sommerfeld Equation (Huang, 1973)

X*	X	$(\alpha)_c$	$(R)_c$	$(c_r)_c$	N
0.010	0.00616	0.785	33840	0.437008	100
0.009	0.00539	1.095	25006	0.434828	150
0.007	0.00392	1.635	20250	0.422166	150
0.006	0.00323	1.930	19900	0.413491	150
0.005	0.00258	2.260	20370	0.403830	150
0.003	0.00140	3.280	24621	0.380768	200
0.002	0.00087	4.190	30101	0.366564	200

Appendix E

Neutral Stability Characteristics for Parallel-Plate Channel Flow (c_i=0)

$$R = \bar{u}^*L^*/\nu \ , \quad \alpha = \alpha^*L^* \ , \quad c_r = c_r^*/\bar{u}^* \ , \quad X^* = \frac{\xi^*/L^*}{\bar{u}^*L^*/\nu} \ ,$$

$$X = \frac{x^*/L^*}{\bar{u}^*L^*/\nu}$$

Table E-1

Neutral Stability Results at Various Axial Locations for Parallel-Plate Channel Flow, Modified Orr-Sommerfeld Equation

$X^*=\infty$ ($X=\infty$) N=100

α	R	c_r
0.45977	83996	0.14936
0.60234	21166	0.22380
0.75050	8291	0.29769
0.99818	3883	0.39140
1.01000	3858	0.39397
1.02000	3850	0.39587
1.02841	3855	0.39724
1.04045	3884	0.39879
1.09416	6742	0.36895
0.95177	32840	0.26073
0.87743	62807	0.22389

$X^*=0.300$ ($X=0.30829$) N=100

α	R	c_r
1.0200	3883.77	0.39504
1.0215	3883.74	0.39530
1.0230	3884.06	0.39556

Table E-1 (continued)

X*=0.200 (X=0.19490) N=100

α	R	c_r
1.0230	4096.24	0.39047
1.0245	4096.18	0.39073
1.0260	4096.45	0.39098

X*=0.150 (X=0.13873) N=100

α	R	c_r
1.0320	4491.96	0.38303
1.0335	4491.92	0.38328
1.0350	4492.23	0.38351

X*=0.100 (X=0.08403) N=100

α	R	cr
1.0600	5434.30	0.36842
1.0660	5429.58	0.36933
1.0675	5429.236	0.36955
1.0690	5429.243	0.36976
1.0705	5429.60	0.36997

X*=0.080 (X=0.06317) N=100

α	R	c_r
0.600	41997	0.19186
0.700	21058	0.23571
0.800	12563	0.27642
0.900	8632	0.31247
1.050	6272	0.35378
1.090	6098	0.36099
1.100	6087	0.36242
1.103	6086	0.36282
1.110	6090	0.36368
1.120	6109	0.36474
1.130	6148	0.36558
1.200	7861	0.35741

Table E-1 (continued)

X*=0.060 (X=0.04350) N=100

α	R	c_r
1.1620	7059.88	0.35509
1.1635	7059.42	0.35527
1.1650	7059.27	0.35544
1.1660	7059.35	0.35555

X*=0.040 (X=0.02570) N=150

α	R	c_r
0.8000	27765.7	0.23228
1.1000	10471.1	0.31767
1.2830	8693.9	0.34724
1.2845	8693.6	0.34738
1.2860	8696.6	0.34751
1.3500	9016.0	0.35066

X*=0.030 (X=0.01776) N=150

α	R	c_r
1.3927	10092.7	0.34268
1.3942	10092.4	0.34279
1.3957	10092.3	0.34290
1.3975	10092.5	0.34304
1.4000	10093.4	0.34322

X*=0.020 (X=0.01066) N=150

α	R	c_r
0.7500	100765	0.17352
1.0000	32266	0.24269
1.2500	17155	0.29096
1.5920	12439.56	0.33761
1.5935	12439.33	0.33770
1.5945	12439.28	0.33775
1.5950	12439.29	0.33778
1.6000	12441	0.33805
1.7000	13054	0.34022
1.8000	19052	0.32187
1.7500	32089	0.29144
1.5000	98121	0.23117

Table E-1 (continued)

X*=0.015 (X=0.00747) N=200

α	R	c_r
1.7720	14369.1	0.33480
1.7735	14368.83	0.33487
1.7750	14368.72	0.33494
1.7770	14368.81	0.33502
1.7800	14369.5	0.33515

X*=0.010 (X=0.00457) N=200

α	R	c_r
1.7500	20450	0.30985
2.0990	17518.2	0.33156
2.1005	17518.1	0.33161
2.1500	17585	0.33284
2.3000	19017	0.33212

X*=0.008 (X=0.00351) N=200

α	R	c_r
2.3100	19469	0.32970
2.3150	19466	0.32984
2.3235	19464	0.33005
2.3335	19466	0.33030

X*=0.006 (X=0.00250) N=250

α	R	c_r
1.2500	99062	0.20811
1.5000	56587	0.24428
2.0000	29667	0.29546
2.5000	22633	0.32382
2.6750	22171	0.32858
2.6680	22170	0.32845
2.6610	22171	0.32831
3.0000	25654	0.32540
2.9900	53181	0.28591
2.7500	93360	0.25654

X*=0.005 (X=0.00203) N=250

α	R	c_r
2.9115	24061	0.32730
2.9195	24060	0.32744
2.9250	24061	0.32752

Table E-2

Axial Variation of Critical Stability Characteristics for Parallel-Plate Channel Flow

Modified Orr-Sommerfeld Equation

X*	X	$(\alpha)_c$	$(R)_c$	$(c_r)_c$	N
∞	∞	1.0200	3850	0.39587	100
0.300	0.30829	1.0215	3884	0.39530	100
0.200	0.19490	1.0245	4096	0.39073	100
0.150	0.13873	1.0335	4492	0.38328	100
0.100	0.08403	1.0675	5429	0.36955	100
0.080	0.06317	1.1030	6086	0.36282	100
0.060	0.04350	1.1650	7059	0.35544	100
0.040	0.02570	1.2845	8694	0.34738	150
0.030	0.01776	1.3957	10092	0.34290	150
0.020	0.01066	1.5945	12439	0.33775	150
0.015	0.00747	1.7750	14369	0.33494	200
0.010	0.00457	2.1005	17518	0.33161	200
0.008	0.00351	2.3235	19464	0.33005	200
0.006	0.00250	2.6680	22170	0.32850	250
0.005	0.00203	2.9195	24060	0.32744	250

Conventional Orr-Sommerfeld Equation (Chen, 1966)

X*	X	$(\alpha)_c$	$(R)_c$	$(c_r)_c$	N
∞	∞	1.0200	3850	0.39587	100
0.300	0.30829	1.0215	3884	0.39521	100
0.200	0.19490	1.0245	4098	0.39067	100
0.150	0.13873	1.0335	4497	0.38314	100
0.100	0.08403	1.0690	5442	0.36950	100
0.080	0.06317	1.1040	6103	0.36261	100
0.060	0.04350	1.1635	7085	0.35483	100
0.040	0.02570	1.2835	8736	0.34667	150
0.030	0.01776	1.3942	10152	0.34204	150
0.020	0.01066	1.5935	12533	0.33673	150
0.015	0.00747	1.7735	14495	0.33375	200
0.010	0.00457	2.0990	17705	0.33021	200
0.008	0.00351	2.3220	19694	0.32854	200
0.006	0.00250	2.6625	22465	0.32670	250
0.005	0.00203	2.9130	24402	0.32558	250

IX. VITA

The author, Francis Chung-ti Shen, was born on May 15, 1940 , in Shanghai, China. He received his primary and secondary education in the public schools of Taipei, Taiwan. He received a Bachelor of Science degree in Mechanical Engineering in June, 1963, from Cheng Kung University, Tainan, Taiwan and a Master of Science degree in Mechanical Engineering in May, 1968, from Polytechnic Institute of Brooklyn, Brooklyn, New York.

Since Feburary, 1968 he has been pursuing the Doctor of Philosphy degree in Mechanical Engineering at the Graduate School of the University of Missouri-Rolla.